A matter of timing

A modelling-based investigation of the dynamic behaviour of reproductive hormones in girls and women

Sophie Fischer-Holzhausen

Thesis for the degree of Philosophiae Doctor (PhD)
University of Bergen, Norway
2023

UNIVERSITY OF BERGEN

A matter of timing

A modelling-based investigation of the dynamic behaviour of reproductive hormones in girls and women

Sophie Fischer-Holzhausen

Thesis for the degree of Philosophiae Doctor (PhD)
at the University of Bergen

Date of defense: 05.05.2023

Year: 2023

Title: A matter of timing

Name: Sophie Fischer-Holzhausen

Print: Skipnes Kommunikasjon / University of Bergen

Scientific environment

The presented work was conducted at the Department of Informatics at University of Bergen. I was part of the Röblitz Group for Computational Systems Biology Group, which is associated with the Computational Biology Unit. The Trond Mohn Foundation funded my research position.

I was affiliated with the National Research School in Bioinformatics, Biostatistics and Systems Biology (NORBIS) and the Digital Life Norway Research School (DLN). I had the opportunity to attend several courses organized by DLN focusing on writing, communication and supervising skills. With the financial support of NORBIS I was able to work for three months at the Norwegian Institute for Public Health. Furthermore, I attended the 7th annual Joint Summer School in Computational Physiology 2021.

Acknowledgements

I wish that our perception of the menstrual cycle shifts. I do not believe that the menstrual cycle is a subject that purely concerns individuals who menstruate. On the contrary, I am convinced that it deserves closer attention because (i) it is of scientific interest due to the high number of open questions related to it, and (ii) it is of social interest due to its significant implications for the life quality of people worldwide. Therefore, I am grateful that I could dedicate the last three years to investigating the female menstrual cycle.

I want to thank the Department of Informatics, the University of Bergen, the Trond Mohn Foundation and Susanna Röblitz for giving me the opportunity to pursue this PhD.

A special thanks goes to Susanna for being extremely open-minded and understanding. Thank you for always listening.
My gratitude also goes to my co-advisors, Tom Michoel and Iain Johnston. Iain, thank you for offering your scientific advice. Your enthusiasm is inspiring!

I also want to thank everyone at CBU and the Department of Informatics for creating a friendly working environment. A special thanks to Neann – I learned to appreciate a cup of hot chocolate. A thank you to the folks from the Stochastic Biology Group. Without you, I would know so little about mitochondria and less prominent members of the tree of life. I also want to thank Noeska for mentoring me. You lent me more than once a sympathetic ear. Your compassionate nature offered needed comfort and encouraged me.

Lastly, I want to thank my family and friends. I want to thank my parents, who raised me to be a strong-minded and sensitive woman. Marek, I am thankful that you listened to me when I talked endlessly about my frustrations. Konstantin, you always believed I could finish my PhD - even when I did not. Thank you!

Abstract in English

The hypothalamic-pituitary-gonadal axis (HPG axis), a part of the human endocrine system, regulates the female reproductive function. Feedback interactions between hormones secreted from the glands forming the HPG axis are essential for establishing a regular menstrual cycle. Mathematical models predicting the time evolution of hormone concentrations and the maturation of ovarian follicles are useful tools for understanding the dynamic behaviour of the menstrual cycle. Such models can, for example, help us to investigate pathological conditions, such as endometriosis or Polycystic Ovary Syndrome. Furthermore, they can be used to systematically study the effects of drugs on the endocrine system. In doing so, menstrual cycle models could potentially be integrated into clinical routines as clinical decision support systems.

For the simulation-based investigation of hormonal treatments aiming to stimulate the growth of ovarian follicles (Controlled Ovarian Stimulation (COS)), we need models that predict hormone concentrations and the maturation of ovarian follicles in biological units throughout consecutive cycles. Here, I propose such a mechanistic menstrual cycle model. I also demonstrate its capability to predict the outcome of COS.

Individual time series data is usually used to calibrate mechanistic models having clinical implications. Collecting these data, however, is time-consuming and requires a high commitment from study participants. Therefore, integrating different data sets into the model calibration process is of interest. One type of data that is often more feasible to collect than individual time series is cross-sectional data. As part of my thesis, I developed a workflow based on Bayesian updating to integrate cross-sectional data into the model calibration process. I demonstrate the workflow using a mechanistic model describing the time evolution of reproductive hormones during puberty in girls. Exemplary, I show that a model calibrated with cross-sectional data can be used to predict individual dynamics after updating a subset of model parameters.

In addition to the scientific contributions of this thesis, I hope that it creates attention for the importance of research in the area of women's reproductive health and underpins the value of mathematical modelling for this field.

Abstract in Norwegian

Hypothalamus-hypofyse-gonade aksen er en del av det kvinnelige endokrine systemet, og regulerer evnen til reproduksjon. Hormoner produsert og utskilt fra tre kjertler (hypotalamus, hypofysen, eggstokkene) påvirker hverandre via tilbakemeldingsinteraksjoner, som er nødvendige for å etablere en regelmessig menstruasjonssyklus hos kvinner. Matematiske modeller som forutsier utviklingen av slike hormonkonsentrasjoner og modning av eggstokkfollikler er nyttige verktøy for å forstå menstruasjonssyklusens dynamiske oppførsel. Slike modeller kan for eksempel hjelpe oss med å undersøke patologiske tilstander som endometriose og polycystisk ovariesyndrom. Videre kan de brukes til systematiske undersøkelser av effekten av medikamenter på det kvinnelige endokrine systemet. Derfor kan vi potensielt bruke slike menstruasjonsyklusmodeller som kliniske beslutningsstøttessystemer.

Vi trenger modeller som forutsier hormonkonsentrasjoner sammen med modningen av eggstokkfollikler hos enkeltindivider gjennom påfølgende sykluser. Dette for å kunne simulere hormonelle behandlinger som stimulerer vekst av eggstokkfolliklene (eggstokkstimuleringsprotokoller). Her legger jeg fram et forslag til en matematisk menstruasjonsyklusmodell og viser modellens evne til å forutsi resultatet av eggstokkstimuleringsprotokoller.

For å kalibrere denne typen modell trenges individuelle tidsseriedata. Innsamling av slike data er tidskrevende, og forutsetter høy grad av engasjement fra deltakerne i studien. Det er derfor viktig å finne brukbare datatyper som er mindre tid- og ressurskrevende å samle inn, og som likevel kan brukes til modellkalibrering. En type data som er enklere å samle inn er tversnittdata. I denne avhandlingen har jeg utviklet en prosedyre for å bruke tversnittpopulasjonsdata i modellens kalibreringsprosess, og viser hvordan en modell kalibrert med tversnittdata kan brukes til å forutsi individuelle resultater ved oppdatering av en del av modellens parametere.

I tillegg til det vitenskapelige bidraget, håper jeg at avhandlingen min skaper oppmerksomhet rundt viktigheten av forskning på kvinners reproduktive helse, og at avhandlingen underbygger verdien av matematiske modeller i forskning på kvinnehelse.

List of publications

1. S. Fischer-Holzhausen and S. Röblitz. A workflow for incorporating cross-sectional data into the calibration of dynamic models. bioRxiv, 523407, 2023.

2. S. Fischer-Holzhausen and S. Röblitz. Hormonal regulation of ovarian follicle growth in humans: Model-based exploration of cycle variability and parameter sensitivities. Journal of Theoretical Biology, page 111150, 2022

3. S. Fischer-Holzhausen and S. Röblitz. Mathematical modelling of follicular growth and ovarian stimulation. Current Opinion in Endocrine and Metabolic Research, 26: 100385, 2022.

4. K. Yamamoto, S. Fischer-Holzhausen, M. P. Fjeldstad, and M. M. Maleckar. Ordinary Differential Equation-based Modeling of Cells in Human Cartilage. Computational Physiology, pages 25–39, 2022.

5. S. Fischer-Holzhausen, K. Yamamoto, M. P. Fjeldstad, and M. M. Maleckar. Probing the Putative Role of KATP Channels and Biological Variability in a Mathematical Model of Chondrocyte Electrophysiology. Bioelectricity, 3(4):272–281, 2021.

6. S. Fischer, R. Ehrig, S. Schäfer, E. Tronci, T. Mancini, M. Egli, F. Ille, T. H. Krüger, B. Leeners, and S. Röblitz. Mathematical Modeling and Simulation Provides Evidence for New Strategies of Ovarian Stimulation. Frontiers in Endocrinology, 12:613048, 2021.

List of acronyms

ODE Ordinary Differential Equation

HPG axis Hypothalamic-Pituitary-Gonadal axis

GnRH Gonadotropin-Releasing Hormone

LH Luteinising Hormone

FSH Follicle-Stimulating Hormone

E2 Estradiol

P4 Progesterone

MCL Menstrual Cycle Length

PCOS Polycystic Ovarian Syndrome

IVF In Vitro Fertilisation

COS Controlled Ovarian Stimulation

OHSS Ovarian Hyperstimulation Syndrome

CI Confidence Interval

ML Maximum Likelihood

MLE Maximum Likelihood Estimation

MAP Maximum A Posteriori

ABC Approximate Bayesian Computation

MCMC Markov Chain Monte Carlo

MH Metropolis–Hastings

PL Profile Likelihood

SA Sensitivity Analysis

PK Pharmacokinetic

PD Pharmacodynamic

PB Physiologically Based

Contents

Scientific environment i

Acknowledgements iii

Abstract in English v

Abstract in Norwegian vii

List of publications ix

List of acronyms xi

I Research overview 1

1 Introduction 3

1.1 Mathematical modelling of the hypothalamic-pituitary-gonadal axis . . . 4

1.2 Outline 9

2 Endocrinology of the female reproductive system 11

3 Mechanistic modelling in systems biology 21

3.1 Principles of model construction 25

3.2 Parameter estimation 27

3.2.1 Maximum likelihood estimation 28

3.2.2 Maximum a posteriori estimation 29

3.2.3 Approximate Bayesian Computation 30

3.3 Parameter identifiability 31

3.3.1 Profile likelihood 32

3.4 Uncertainty quantification 34

3.5 Sensitivity analysis 35

3.6 Modelling of pharmacokinetics and pharmacodynamics 37

4 Summary of scientific work **39**

4.1 Reproducibility and code reusability 39

4.2 Paper summaries 41

4.2.1 Paper A: Hormonal regulation of ovarian follicle growth in humans: Model-based exploration of cycle variability and parameter sensitivities 42

4.2.2 Paper B: Mathematical modelling and simulation provide evidence for new strategies of ovarian stimulation 43

4.2.3 Paper C: A workflow for incorporating cross-sectional data into the calibration of dynamic models 44

4.3 Concluding discussions 45

4.4 Future prospects 48

II Scientific articles **73**

Paper A: Hormonal regulation of ovarian follicle growth in humans: Model-based exploration of cycle variability and parameter sensitivities **75**

Paper B: Mathematical Modeling and Simulation Provides Evidence for New Strategies of Ovarian Stimulation **87**

Paper C: A workflow for incorporating cross-sectional data into the calibration of dynamic models **99**

Review: Mathematical modelling of follicular growth and ovarian stimulation **117**

Part I

Research overview

Chapter 1

Introduction

Biological systems, e.g. cells or organs, are built of many interacting components. Research in microbiology and biochemistry generates detailed insights into the structure and function of small units such as genes or proteins. However, studying the interactions and interconnections of these small functional units is vital to understand complex biological processes. Consequently, integrating the knowledge about the small units into a larger context can enable a new understanding of biological processes and diseases [Assmus et al., 2006; Kitano, 2002b; Klipp et al., 2016].

The field of complexity science is concerned with investigating systems where interacting components give rise to non-trivial functions (complex systems). Those systems exhibit properties such as nonlinearity, emergence and pattern formation [Kwapień and Drożdż, 2012; Mitchell, 2006, 2009]. In systems biology, we treat biological systems as complex systems aiming for a systematic understanding [Madhavan and Mustafa, 2022]. Central questions in systems biology are [Wolkenhauer and Mesarović, 2005]:

- How do the interactions between the components of a system contribute to the system's structure and function?
- How do systems give rise to higher-order functions and structure?

Scientists address these questions by combining computational and experimental tools [Klipp et al., 2016].

Mathematical models have a central role in systems biology [Klipp et al., 2005, 2016; Wolkenhauer and Mesarović, 2005]. Models provide us with abstract representations. Therefore, they can help to understand higher levels of complexity [Cartier et al., 2001; Epstein, 2008; Kohl et al., 2010] and the dynamic behaviour of a system, meaning its

development in time [Klipp et al., 2016; Strogatz, 2018; Wolkenhauer and Mesarović, 2005]. Furthermore, Kuepfer et al. [2016] claim that models can also function as knowledge management tools. Mechanistic models go beyond the data analysis – but on no account replace a thoughtful data analysis – and therefore help to understand causal relationships. Consequently, modelling can add a predictive component to the exploration of biological systems [Assmus et al., 2006; Wolkenhauer, 2014]. Finally, Kitano [2002a] promotes the value of computational systems biology for advancements in medicine and pharmacology because it can help us understand the system's interactions, robustness and emergent properties.

Applying ideas from systems biology in medical research allows for investigating the systematic nature of diseases [Ayers and Day, 2015]. In clinical research, patient-specific models have become popular because they pledge to improve treatment outcomes. Only one of many examples of a patient-specific model is the work by Maleckar et al. [2021]. Here, the authors assess the risk for dangerous arrhythmia in post-infarct patients by combining a patient-specific physiological heart model with a machine learning methodology. Patient-specific mathematical models can also be used for treatment planning and response prediction. For example, Jackson et al. [2015] utilise patient-specific tumour growth models to develop individualised treatment and surgery strategies. Maier et al. [2022] and Pedersen et al. [2021] are examples that give an idea of the application of patient-specific models to predict dosing regimes.

Overall, computational approaches and mathematical modelling have become integral to investigating living systems and diseases. Despite that, modelling-based explorations will never replace experimental work – rather, they provide additional approaches for generating understanding. Thus, a symbiotic relationship between experimental and computational work will allow us to study biological systems systematically.

1.1 Mathematical modelling of the hypothalamic-pituitary-gonadal axis

The endocrine system is a messenger system consisting of glands secreting hormones as messenger molecules. Those hormones regulate fundamental processes such as metabolism, reproduction and stress responses through feedback mechanisms. They have sensory and regulatory functions on multiple levels of organisation and different time scales. Consequently, exploring the endocrine system can benefit from mathematical modelling [Leng and MacGregor, 2008; Zavala et al., 2019].

The Hypothalamic-Pituitary-Gonadal axis (HPG axis) is part of the endocrine system and is central to regulating reproduction. In women, the hypothalamus, the pituitary gland, and the ovaries form the HPG axis. Those three organs communicate through feedback loops with hormones as messenger molecules, enabling the menstrual cycle. The major events within a menstrual cycle are the maturation of ovarian follicles (cellular unit that carries the oocytes in females), the release of oocytes and the preparation of the uterus lining for the implantation of a fertilised oocyte. In the absence of a fertilised oocyte, the shedding of the uterus lining – better known as menstrual bleeding – flags the beginning of a new menstrual cycle [Hawkins and Matzuk, 2008]. In a woman's lifetime, two significant changes in the endocrine regulation by the HPG axis are observed: (i) the reactivation of the HPG axis during puberty and (ii) menopause [Hoyt and Falconi, 2015]. Between those two events, a woman experiences about 451 menstrual cycles [Chavez-MacGregor et al., 2008].

Prior [2020] emphasises that we must view women's reproductive health as a multidimensional, interactive, dynamic, non-linear complex system to advance our understanding in this field. In this light, mathematical modelling of the HPG axis can contribute to investigating women's reproductive health, including diseases such as Polycystic Ovarian Syndrome (PCOS). Indeed, various aspects of the female reproductive axis have been subject to mathematical modelling-based studies [Fischer-Holzhausen and Röblitz, 2022b; Zavala et al., 2019]. Voliotis et al. [2018] present a mathematical model that underpins the role of neuronal control for the secretion of Gonadotropin-Releasing Hormone (GnRH) and Luteinising Hormone (LH) – both hormones are involved in regulating the menstrual cycle. With the higher-ranking aim of developing a model that can predict the effects of chemical compounds (e.g. drugs or toxins), J. Selgrade and P. Schlosser introduced the first mathematical model of the human menstrual cycle that is based on the knowledge of underlying mechanisms [Schlosser and Selgrade, 2000; Selgrade and Schlosser, 1999]. Their model describes the interactions between the five essential hormones that regulate the menstrual cycle. The simulation results display the time evolution of those hormones correctly. Harris [2002] and Clark et al. [2003] added an ovarian compartment to the model introduced by J. Selgrade and P. Schlosser. This newly introduced compartment describes the maturation of ovarian follicles and the production of ovarian hormones. Harris [2002] and Clark et al. [2003] observe two stable solutions for their model. One stable solution displays hormone profiles expected for a regular menstrual cycle, whereas the other shows characteristics of hormone profiles observed in PCOS patients. This second stable solution allows them to investigate whether a progesterone treatment could restore normal hormone profiles in PCOS patients. Hence, they were the first to demonstrate the model's applicability in simulating the effects of hormonal treatment on hormone profiles. Reinecke and Deuflhard [2007] and Reinecke [2009] used

the model from Harris [2002] as a starting point and increased the model complexity by adding a description of the GnRH pulse generator as well as receptor binding and recycling mechanisms. Reinecke [2009] applies the model in a pharmacological setting and simulates the administration of hormonal contraceptives, including the effects of intake errors. Wright et al. [2020] also test the effects of hormonal contraception on hormone dynamics. However, they use a less complex model version than Reinecke [2009]. The model published by Röblitz et al. [2013] is derived from the work by Reinecke [2009]; Reinecke and Deuflhard [2007]. The Röblitz et al. [2013] model focuses on describing the GnRH receptor. Thereby, they can predict shifts in the GnRH release pattern and the hormone profiles that result from hormonal treatments in Controlled Ovarian Stimulation (COS). Mancini et al. [2018] and Sinisi et al. [2020a,b] apply the model by Röblitz et al. [2013] in the context of precision medicine. Compared to Röblitz et al. [2013], they cover inter-individual variability by considering multiple model parametrisations (virtual phenotypes). In doing so, they can computationally optimise the treatment for a given virtual phenotype.

Besides the dynamics of reproductive hormones, the development of ovarian follicles (folliculogenesis) has also been subject to mathematical modelling-based studies. Clément [1998] introduces a description of folliculogenesis on a cellular level. The proposed model describes folliculogenesis by the time evolution of cell populations that form ovarian follicles. Clément [1998] investigates the relationship between the cellular composition of a follicle and its chances of ovulating. Recently, Clément et al. [2021] introduced a stochastic model (continuous-time Markov chain model) to describe the time evolution of follicle cell populations. Using this model, the authors study the sequence of events characterising follicle growth. Harris [2002] describes discrete developmental stages of follicles. This description does not reveal the number of follicles in each stage but the total follicular mass. However, this description is sufficient to describe the follicles' hormone production. Reinecke and Deuflhard [2007], Reinecke [2009] and Röblitz et al. [2013] adopted this description. Lacker [1981] proposes a maturation function for each follicle. This modelling approach allows for studying the dynamics of follicular growth in terms of follicle size. Chavez-Ross et al. [1997] refine the maturation function from Lacker [1981] to describe non-identical follicles. Considering non-identical follicles makes the model physiologically more plausible and allows for the observation of a follicle growth behaviour similar to what is described for PCOS patients. Lange et al. [2019] expanded this work further and introduced a maturation function that incorporates the competitive interactions between follicles. With this formulation, the authors can investigate the selection of a single follicle from a cohort of growing follicles in mono-ovulatory species. The basis for the maturation function in Lacker [1981], Chavez-Ross et al. [1997], and Lange et al. [2019] is semi-mechanistic. As an alternative, Shilo et al. [2022] introduce a matu-

ration function motivated by the knowledge about the physiological processes regulating folliculogenesis. This allows the authors to describe the relationship between hormonal unbalance observed in PCOS patients and disruptions in folliculogenesis.

Whereas there are several models published dealing with the HPG axis in women of reproductive age, very little modelling work addresses the immature and maturating HPG axis during childhood and puberty. So far, the modelling approaches aim to predict individual characteristics, such as puberty onset, or to find applicable puberty markers. Cole et al. [2014] use a mixed-effect model for estimating individuals' puberty timing and intensity. Bruserud et al. [2020] combine breast development stage with hormone levels to study the predictive value of endocrine profiles for breast development forecasts. Those models can potentially be used as clinical discussion support systems. However, they are not applicable to investigate fundamental questions such as (i) What regulates and triggers the reactivation of the HPG axis during puberty? or (ii) How is the oscillatory hormone release pattern established over time? Nevertheless, those questions are subjects of ongoing experimental research [Terasawa, 2022; Uenoyama et al., 2019], and a combination of experimental and computational approaches will help us to understand the multi-factorial activation process of the HPG axis during puberty [Ojeda et al., 2006]. A possible application of mathematical models is their integration into the investigation of the regulatory network controlling the inhibition of the GnRH pulse generator during childhood.

Compared to other fields in systems biology, women's reproductive health has received comparatively little attention. Therefore, this work, hopefully, will contribute to creating awareness that the menstrual cycle and related disorders need to be investigated further. Looking forward, our perception of the menstrual cycle should shift from a private matter to a subject that is (i) of scientific interest because there are many open questions and (ii) of social interest because it has significant implications for the health and life quality of people worldwide. For example, PCOS, an endocrinopathy where the ovaries produce pathologically high amounts of androgens, affects about 4%–20% of women of reproductive age worldwide. Since PCOS can cause irregular menstrual cycles and the absence of ovulation, it can lead to infertility. Hence, its consequences can significantly impact the life quality of patients. However, the underlying cause of PCOS is poorly understood, and the treatment strategies are mostly symptom-oriented [De Leo et al., 2016; Deswal et al., 2020].

The clinical investigation of the menstrual cycle and related disorders is challenging and time-consuming because (i) only a few species exhibit menstrual cycles, and (ii) the time scale of the process (an average menstrual cycle length is 28 days) is comparably long. Therefore, combining experimental with computational approaches will benefit its in-

vestigation. Mathematical modelling can be integrated in various ways into women's reproductive health studies. As it has been demonstrated in previously published research articles, e.g. Harris [2002], Reinecke [2009] and Röblitz et al. [2013], one great value of mechanistic menstrual cycle models is that they provide a tool to make a prediction about the effects of hormonal treatments on the hormone profiles. Also, it would be conceivable that those models become part of toxin risk assessment studies [Lipscomb et al., 2012; Schlosser and Selgrade, 2000]. Furthermore, modelling can support the investigation of pathological cases such as PCOS [Harris, 2002; Shilo et al., 2022]. PAEON [2017], Mancini et al. [2018] and Sinisi et al. [2020a,b] emphasise the potential of mechanistic menstrual cycle models as clinical decision support systems for personalised treatment planning. Finally, an industrial application of a menstrual cycle model is InSilicoENDO by InSilicoTrails [InSilicoTrials]. It is a tool to simulate treatment protocols of assisted reproduction medicine in virtual patients aiming to reduce, refine and replace animal tests and to improve clinical trials.

As previously published menstrual cycle models, the model presented in Fischer-Holzhausen and Röblitz [2022a] (Paper A) describes the hormone profiles of consecutive menstrual cycles correctly. The novelty of the presented model is its description of the ovarian follicles. This model describes each ovarian follicle with a maturation function. Consequently, simulation results display growth trajectories of the individual follicles. These simulation results can be compared to ultrasound measurements. This comparison to clinical data monitoring folliculogenesis was not feasible with previously published models, e.g. Schlosser and Selgrade [2000], Harris [2002], Reinecke [2009] and Röblitz et al. [2013]. Furthermore, this change in the model formulation enables the prediction of the growth of follicles under hormonal treatment (see Paper B [Fischer et al., 2021]), which offers the potential use of the model as a clinical decision support system in reproductive medicine.

1.2 Outline

My modelling work on aspects of the endocrinology of the female reproductive system, which I conducted as a PhD candidate at the University of Bergen, is summarised in three research articles. **Paper A** introduces a mathematical model of the HPG axis in women. **Paper B** presents a systems pharmacological study investigating the effects of different hormonal treatment strategies on hormone dynamics and ovarian follicle growth using the model from Paper A. **Paper C** shows how cross-sectional data can be integrated into the model calibration process of a mathematical model. The presented model aims to predict individuals' sex hormone dynamics during puberty. Furthermore, I have been a co-author of a **Review** article summarising modelling approaches developed to describe different aspects of the human menstrual cycle and follicular maturation. (Note that the review article does not count for the articles needed for an article-based thesis.)

This thesis is divided into two parts: "Research overview" and "Scientific articles". The chapters in "Research overview" provide the biological and methodological background for the work presented in Paper A, B and C. The last chapter of this part comprises short summaries of these articles, followed by a discussion and an outlook. The three complete scientific papers and the review can be found in "Scientific articles". They are listed as follows:

Paper A S. Fischer-Holzhausen and S. Röblitz. Hormonal regulation of ovarian follicle growth in humans: Model-based exploration of cycle variability and parameter sensitivities. Journal of Theoretical Biology, page 111150, 2022

Paper B S. Fischer, R. Ehrig, S. Schäfer, E. Tronci, T. Mancini, M. Egli, F. Ille, T. H. Krüger, B. Leeners, and S. Röblitz. Mathematical Modeling and Simulation Provides Evidence for New Strategies of Ovarian Stimulation. Frontiers in Endocrinology, 12:613048, 2021.

Paper C S. Fischer-Holzhausen and S. Röblitz. A workflow for incorporating cross-sectional data into the calibration of dynamic models. bioRxiv, 523407, 2023.

Review S. Fischer-Holzhausen and S. Röblitz. Mathematical modelling of follicular growth and ovarian stimulation. Current Opinion in Endocrine and Metabolic Research, page 100385, 2022

Chapter 2

Endocrinology of the female reproductive system

Hormones are essential signalling molecules that enable communication between tissues and organs in multi-cellular organisms. The positive and negative feedback interactions between hormones regulate physiological processes such as stress response, reproduction, and excretion [Hiller-Sturmhöfel and Bartke, 1998]. Glands are the organs that are responsible for the synthesis and release of hormones. Reproduction is primarily regulated by the interplay of hormones originating from three units: the hypothalamus, the pituitary gland, and the gonadal glands. These three glands form the so-called Hypothalamic-Pituitary-Gonadal axis [Hawkins and Matzuk, 2008].

Even though all mammals share the same reproductive system and regulatory units [Nowak, 2018; Yin and Ma, 2005], only a limited number of species (humans and other higher order primates [Emera et al., 2012], elephant shrews [van der Horst and Gillman, 1941], some bats, e.g. wild fulvous fruit bats [Emera et al., 2012], and spiny mice [Bellofiore et al., 2018]) exhibit menstrual cycles. More often, female mammals have estrous cycles. The most significant difference between an estrous and a menstrual cycle is the fate of the inner lining of the uterus (endometrium) in the absence of conceiving. Whereas species exhibiting an estrous cycle absorb the endometrium into the system (resorption), mammals with a menstrual cycle experience menstruation, which denotes the recurrent shedding of the endometrium [Nowak, 2018].

The human menstrual cycle comprises four key elements: menstruation, follicular phase, ovulation, and luteal phase. Fig 2.1 displays the two phases of the menstrual cycle (follicular and luteal phase) and the events that mark the transition from one phase to the other (ovulation and menstruation). Menstruation marks the first day of a menstrual

cycle and the beginning of the follicular phase. The maturation of ovarian follicles characterises this phase of the menstrual cycle. At the end of the follicular phase, one ovarian follicle (in rare cases, more than one) will release its mature oocyte in the process called ovulation. After ovulation, the remaining cellular material of the ovarian follicle forms the corpus luteum, and the luteal phase begins. During this phase, the released oocyte travels through the fallopian tube to the uterus; the endometrium is thickened and prepared for the possible implantation of a fertilised oocyte. If the oocyte is not fertilised, the corpus luteum will break down approximately ten days after its formation, and menstruation begins [Hawkins and Matzuk, 2008; Jabbour et al., 2006].

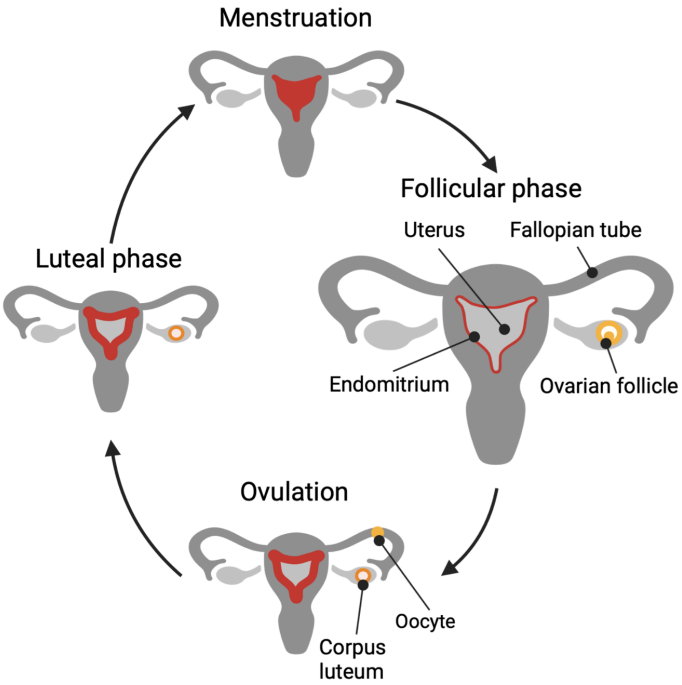

Figure 2.1: **Schematic representation of the key elements characterising a menstrual cycle.** The menstrual cycle starts with the first day of menstruation, which marks the beginning of the follicular phase. During the follicular phase, ovarian follicles maturate, and the endometrium thickens. Around mid-cycle, one ovarian follicle releases its oocyte during ovulation, and the remaining cellular components form the corpus luteum. Supposed the oocyte is not fertilised during the luteal phase, menstruation begins. [This figure is created with Biorender.com]

The menstrual cycle (Fig. 2.1) is governed by the endocrine control of the HPG axis (Fig. 2.2). The hypothalamus, the pituitary, and the ovaries are the three units building the HPG axis in women. During childhood, the secretion of GnRH is suppressed, and the HPG axis is inactive. Hence, there is a lack of reproductive function before puberty. With the onset of puberty, the HPG axis starts to mature, and the amounts of reproductive hormones in the system increase. That causes characteristic changes such as the transformation of body shape and sex organs, the growth of body hair and changes in social behaviour [Ellison et al., 2012; Oakley et al., 2009]. A milestone of girls' puberty is the first menstrual bleeding (menarche) occurring between the age of 10 to 16 [Eckert-Lind et al., 2020; Marques et al., 2022; Pinyerd and Zipf, 2005]. About 1-2 years after menarche, the endocrine control of a regular and ovulatory menstrual cycle is established [Carlson and Shaw, 2019].

The positive and negative feedback relationships between five hormones, secreted from the three glands of the HPG axis, are central to controlling the menstrual cycle (Fig. 2.2). The hypothalamus, located above the brainstem, synthesises and releases the Gonadotropin-Releasing Hormone. The role of GnRH is to stimulate the release of the Follicle-Stimulating Hormone (FSH) and the Luteinising Hormone from the pituitary gland. GnRH has a characteristic pulsatile release pattern controlled by the GnRH pulse generator, a functional unit of the hypothalamus formed by a subpopulation of neurons. This release pattern varies throughout a menstrual cycle, and its variation is mainly regulated by Estradiol (E2) and Progesterone (P4) [Bliss et al., 2010; Herbison, 2018; Nagae et al., 2021; Pohl and Knobil, 1982]. Having this release pattern provides the system with two beneficial properties: (i) it prevents the desensitisation of the pituitary gland to GnRH [Belchetz et al., 1978; Ulloa-Aguirre and Timossi, 2000], and (ii) variations in the release pattern allow for more complex signalling patterns [Haisenleder et al., 1991; Thompson and Kaiser, 2014; Ulloa-Aguirre and Timossi, 2000]. In particular, FSH signalling is favoured at low GnRH release pulse frequencies, whereas high GnRH release pulse frequencies promote LH synthesis. FSH and LH are synthesised and released from the pituitary gland, which is located underneath the brain behind the nose bridge. Both hormones reach the ovaries via the bloodstream, where they have regulatory functions in the process of folliculogenesis. The ovaries are the main location of E2 and P4 production and secretion [Christensen et al., 2012; Hawkins and Matzuk, 2008]. E2 and P4 form a feedback loop back to the hypothalamus and pituitary gland.

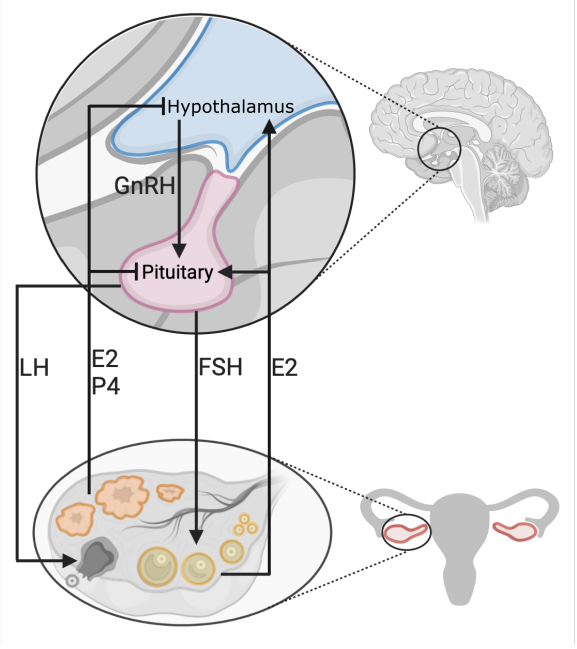

Figure 2.2: **Schematic representation of the endocrine regulation of the HPG axis.** The interplay between the hypothalamus (blue), pituitary (pink) and ovaries (red) has a central role in ensuring female reproduction. The hypothalamus secrets GnRH. It stimulates the synthesis and release of FSH and LH from the pituitary. Growing ovarian follicles (represented in yellow) are the primary source of E2 during the follicular phase. E2 secreted alone has positive feedback on the hypothalamus and the pituitary. LH triggers the release of a mature oocyte (ovulation). The corpus luteum (represented in orange), formed after ovulation, produces E2 and P4. The simultaneous secretion of these two ovarian hormones has an inhibitory effect on the hormone secretion from the hypothalamus and the pituitary. [This figure originates from [Fischer-Holzhausen and Röblitz, 2022b]]

At birth, the ovaries provide a large pool of resting follicles, which declines in size over a women's lifetime. Notable is that only a small fraction of those follicles will ovulate, whereas the majority of follicles undergo atresia [Faddy and Gosden, 1996; Faddy et al., 1992]. At puberty, the recruitment of follicles for further maturation begins. Baerwald et al. [2003a,b] provide experimental evidence supporting that maturation of ovarian follicles in humans is a synchronized process. The authors describe that groups of 4-14 ovarian follicles (called follicular cohorts or follicular waves) enter the maturation process together. Furthermore, the authors detect two to three of those follicular waves appearing per menstrual cycle. One wave is observed during the follicular phase, also called the major wave, and up to two minor waves emerge during the luteal phase. However, only one follicle – in rare cases, two follicles – selected from the major wave ovulates around mid-cycle. A follicle selected for ovulation is also called the dominant follicle.

Folliculogenesis and hormone dynamics interact as shown in Fig. 2.3. FSH stimulates the growth of ovarian follicles. At this, the concentration and duration of elevated FSH levels have an important regulatory function [Fauser and van Heusden, 1997; Schipper et al., 1998]. FSH needs to exceed a threshold (FSH threshold concept) to stimulate the growth of ovarian follicles. The limited duration of the elevation in the FSH concentration ensures the full maturation of a single follicle (FSH window concept) [Fauser, 1994; Schipper et al., 1998].

At the end of the luteal phase, FSH starts to rise. That increase in the FSH level triggers the growth of ovarian follicles of the major wave. During the early follicular phase, all follicles of that wave compete for dominance. Their secretion of E2 is critical for this competition. As a consequence of follicular growth, the E2 concentration increases and causes an inhibition of the FSH secretion from the pituitary gland. Hence, the FSH level decreases, falling under the threshold necessary to stimulate follicular growth. One follicle of the major wave has an advantageous precondition compared to other follicles of the same wave and continues growing without further FSH stimulation. Its secretion of E2 and inhibin promotes the growth suppression of the other follicles further [Ginther et al., 2001; Macklon and Fauser, 2001]. Eventually, one follicle becomes dominant and increases its E2 production. This increase in the E2 level stimulates the release of LH, which peaks around mid-cycle and stimulates the ovulation of the dominant follicle [Hawkins and Matzuk, 2008; Richards et al., 2010]. During ovulation, the dominant follicle releases its oocyte, and its cellular parts form the corpus luteum. Due to the disintegration of the dominant follicle, its E2 production stops [Buffet et al., 1998; Reed and Carr, 2015]. After ovulation, the corpus luteum becomes the primary source of E2 and P4. The simultaneous release of E2 and P4 from the corpus luteum suppresses the release of FSH [Devoto et al., 2009; Stocco et al., 2007], causing an endocrine environ-

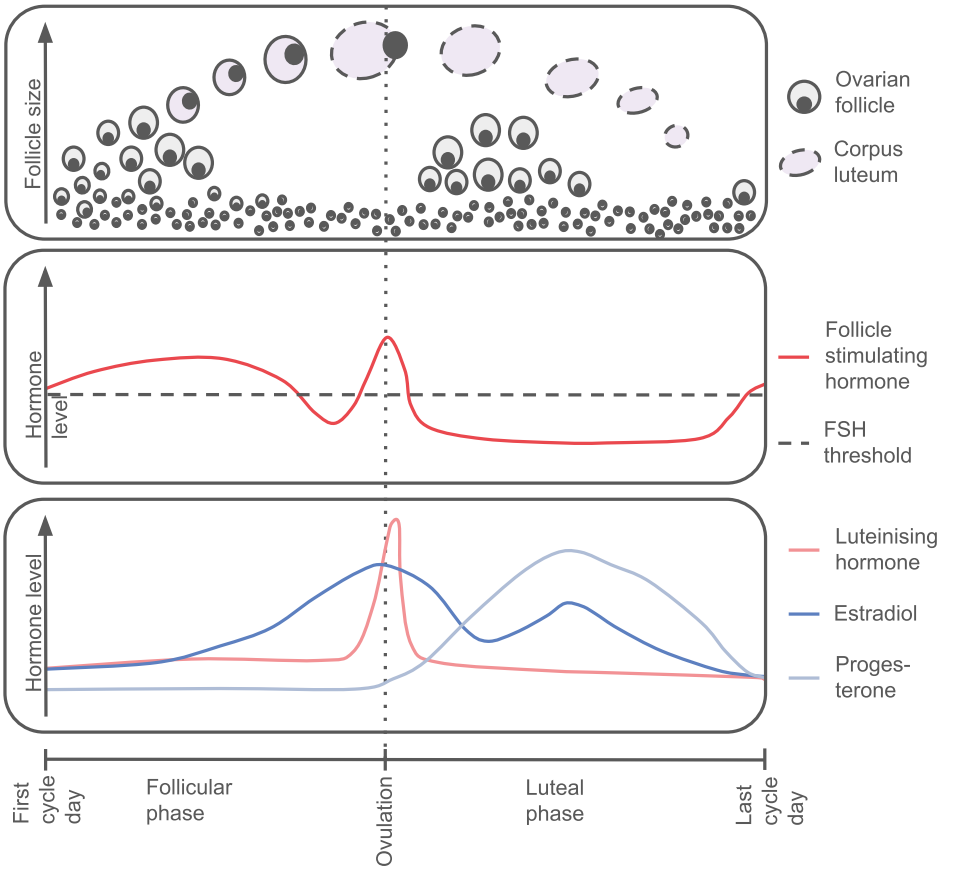

Figure 2.3: **Illustration of hormone and follicle dynamics throughout one menstrual cycle.** The upper panel shows the folliculogenesis, including the ovulation of a dominant follicle around mid-cycle. The middle panel shows the FSH profile. The dashed line indicates the FSH threshold. The lower panel shows the hormone dynamics of E2, P4 and LH. The vertical dotted line highlights the alignment of the LH peak with the ovulation.

ment that does not promote the competition between follicles [Baerwald et al., 2003a]. Consequently, follicle selection for dominance does not occur during the luteal phase. In cases where the oocyte, released during the last ovulation, did not get fertilised, the corpus luteum degrades. Consequently, E2 and P4 levels decrease towards the end of the luteal phase [Devoto et al., 2009; Stocco et al., 2007] and menstruation begins.

The feedback loops of the HPG axis result in oscillatory hormone dynamics (Fig. 2.3). The period of this oscillatory pattern is better known as Menstrual Cycle Length (MCL). On average, a menstrual cycle takes 28 days, and a healthy MCL ranges from 21 to 40 days [National Health Service, 2023]. Inter- and intra-individual variabilities are reported and can have various causes. The literature discusses the effect of intrinsic and extrinsic factors on MCL. Discussed intrinsic factors are: body weight, age, age at menarche, genetic factors and ovarian function. According to Campbell et al. [2021], the MCL's age-dependent shift is the best documented intrinsic factor. Several studies suggest longer MCL for obese women [Grieger and Norman, 2020; Lay et al., 2021; Tayebi et al., 2018], but the picture is not clear yet. Diseases such as endometriosis and PCOS impinge on MCL. Shift work is a possible extrinsic factor for MCL variability because it disrupts the circadian rhythm. Other extrinsic factors under investigation include exercise and consumption habits (dietary, alcohol, smoking, and drugs). Overall, it is essential to understand the causes of variability in MCL because it is an indicator for reproductive health [Campbell et al., 2021].

Infertility

Interruptions in the endocrine regulation of the human menstrual cycle (Fig. 2.2 and Fig. 2.3) impair reproductive function and can cause infertility. For example, the abnormal hormone secretion pattern observed in PCOS patients increases the probability of experiencing anovulatory cycles and developing ovarian cysts. Furthermore, it may impair the ability of the endometrium to prepare for a possible pregnancy. All those factors compromise conceiving.

In a clinical sense, a couple is categorised as infertile if they do not conceive within the first year of unprotected intercourse during the fertile phase of the menstrual cycles [Evers, 2002]. According to the WHO [World Health Organization, 2022], infertility affects approximately 15% of people of reproductive age. Since infertility prevents people from fulfilling their desired social role, it has significant implications for their lifes [Greil et al., 2010]. Consequently, those individuals suffer not only from unwanted childlessness and its underlying cause but also from the resulting psychological and psycho-social

burdens [Chow et al., 2016; Ho et al., 2020; Malina and Pooley, 2017]. Due to the high number of affected individuals and its drastic consequences, infertility can be seen as a global health issue [World Health Organization, 2022].

The causes of infertility are diverse. In about 85% of all cases, dysfunctions in the female or/and male reproductive system are the reason for infertility [Carson and Kallen, 2021]. In one-third of cases, a female factor is responsible for the experienced condition. Typical dysfunctions that cause the failure of the female reproductive system are disorders that cause anovulation/irregular ovulations (oligo-ovulation), such as PCOS and endometriosis, or abnormalities of the fallopian tubes [Unuane et al., 2011].

In many cases, In Vitro Fertilisation (IVF) can lead to a successful pregnancy by combining an oocyte and a sperm cell outside the human body (in vitro) and then reimplanting the fertilised oocyte into the uterus. It is a three-step procedure: (i) egg retrieval through Controlled Ovarian Stimulation, (ii) fertilisation of oocytes in the laboratory, and (iii) embryo transfer into the uterus [Anwar and Anwar, 2016]. In COS, the patient undergoes a hormone treatment to synchronise the maturation of multiple ovarian follicles, which are subsequently removed from the ovaries [Macklon et al., 2006].

There are several protocols established for COS. The most commonly applied protocols are the GnRH agonist protocol and the GnRH antagonist protocol [Karimzadeh et al., 2010]. Often, COS goes along with significant discomfort [Zech et al., 2015] and the risk of developing Ovarian Hyperstimulation Syndrome (OHSS) [Whelan III and Vlahos, 2000]. Enlarged ovaries are the most prominent characteristic of OHSS, but its symptoms range from abdominal pain, nausea and vomiting to severe complications such as acute renal failure [Kumar et al., 2011]. Another challenge in COS is patients showing only low numbers of maturating oocytes as treatment response (poor responder) [Polyzos and Sunkara, 2015]. Both the excessive and poor treatment response impair the success rate of COS. Consequently, there is an interest in developing new protocols that will increase the treatment's success and decrease its side effects [Polyzos and Sunkara, 2015; Zech et al., 2015].

Follicle growth in cohorts allows for new COS protocols [Sighinolfi et al., 2018]. One example is the stimulation during the luteal phase. This new stimulation strategy tries to prevent follicles of a minor wave from undergoing atresia. Therefore, FSH is administered to widen the FSH window [Kalra et al., 2008; Kuang et al., 2014b; Rombauts et al., 1998]. Another new strategy that takes advantage of the presence of multiple follicular waves within a menstrual cycle is the double stimulation protocol. Here, two consecutive stimulation cycles are performed, which increases the number of oocytes retrieved in the time span of one menstrual cycle [Kuang et al., 2014a; Vaiarelli et al., 2018]. Overall,

those new protocols hold promises. They are more flexible concerning treatment timing and, consequently, also applicable for patients where time is a limiting factor, e.g., cancer patients. Also, they might increase success rates of COS or decrease side effects [Sighinolfi et al., 2018]. Hence, various patient groups could benefit from new COS approaches.

In conclusion, infertility is a condition that various factors can cause but usually goes along with significant effects on the lives of individuals. IVF offers individuals suffering from infertility alternatives to natural conceiving. However, the treatment procedure, the side effects, and the not negligible failure rates are stressors for patients [Verhaak et al., 2007]. In addition, in many cases, more than one treatment cycle is needed [Wade et al., 2015]. Therefore it is crucial to investigate new approaches and protocols for COS that further increase success rates and reduce treatment time and side effects. Additionally, treatment protocols tailored to patients' needs are desirable [Sighinolfi et al., 2018].

For treatment testing and personalised treatment optimisation, mathematical models describing the human menstrual cycle hold the promise to be helpful. Models could be applied to predict the effects of drugs on the menstrual cycle. Such simulation-based studies could help us better understand the consequences of, for example, hormonal medication for the reproductive system. Furthermore, those models could be integrated into developing new drugs and treatment protocols because they provide us with a tool to reduce the experimental effort, making the drug development process safer and more efficient. A possible clinical application of menstrual cycle models is their use as clinical decision support systems in the context of IVF. A model that can predict individual IVF outcomes under different treatment conditions would be a valuable tool [Ehrig et al., 2016; Mancini et al., 2018; PAEON, 2017].

Chapter 3

Mechanistic modelling in systems biology

Lazebnik [2002] explains why systems approaches are needed to understand biological systems using the illustrative example of comparing a radio with a signalling pathway. He states that both are similar because they convert signals and are composed of small functional units. According to Lazebnik [2002], we need knowledge about the interactions of functional units and the consequences of those interactions to be able to understand how a radio works, i.e. more than an in-depth understanding of the functional units is required to grasp the functionality of a radio. The same applies to systems in biology, such as signalling pathways or endocrine regulation. We must understand the functional units and their interactions to understand their dynamic behaviour.

In science, models are used to understand, explain and predict the behaviour of real objects or systems. There are various ways to formulate scientific models, e.g. graphical representations such as diagrams, physical analogues or mathematical formulations and computer simulations. Mathematical modelling and simulation provide practical approaches and tools to gain a deeper understanding of the dynamic behaviour and higher-level functions we observe in biological systems. Often, the aim is to mimic and predict the system's behaviour, thereby gaining new insights [Gunawardena, 2014; Klipp et al., 2016; Wolkenhauer, 2014]. There are two main groups of mathematical models: (i) empirical models and (ii) mechanistic models [Smye and Clayton, 2002]. Observations, e.g. experimental data, mainly guide the construction of an empirical model. On the contrary, mechanistic models are based on a theory or prior knowledge we have about the system. Mechanistic models are a central element in the field of computational systems biology.

To formulate a mechanistic model, prior knowledge and assumptions about the biological system can be translated into a system of Ordinary Differential Equations (ODEs) in a step-wise process (Fig. 3.1) [Madhavan and Mustafa, 2022]. Such systems of ODEs allow us to study the time evolution of a set of interacting objects. However, systems of ODEs are only one possible formulation of mechanistic models. Other examples of model frameworks are systems of partial differential equations, agent-based models or Boolean models [Klipp et al., 2016].

During the modelling process, one aims for a "good" and "useful" model [Smye and Clayton, 2002; Wieland et al., 2021] with regard to:

- Accuracy: minimal error between model trajectories and measured data
- Predictive value: formulation of experimentally testable hypotheses based on simulation
- Complexity: model size tailored to the purpose
- Plausibility: mechanistic description and parameter ranges within the model context
- Usefulness: model serves its purpose.

At the beginning of the mechanistic modelling process (Fig. 3.1), the model's scope and purpose are set, and prior knowledge about the system is gathered. Prior knowledge may be found in the literature and in databases (KEGG [Kanehisa and Goto, 2000], Reactome [Fabregat et al., 2018], BioModels [Le Novere et al., 2006; Malik-Sheriff et al., 2020]). The amount of available prior knowledge and data limits the possible model complexity [Cvijovic et al., 2014].

In the "Design" step (Fig. 3.1), this systematically collected prior knowledge provides the foundation for a qualitative description of the system (conceptual model). The conceptual model represents all mechanisms and interactions presumably essential for the system and its behaviour; it is often realized as a cartoon-like schema. The conceptual model provides the basis for constructing a mechanistic model and, therefore, is an integral part of the model building process.

In the context of this thesis, the chosen modelling framework is the system of ODEs (Sec. 3.1). In this setting, model parameters (e.g. synthesis or clearance rates) must be specified. In some cases, these parameters are found in the literature or measured directly. However, it is prevalent that at least a subset of model parameters needs to

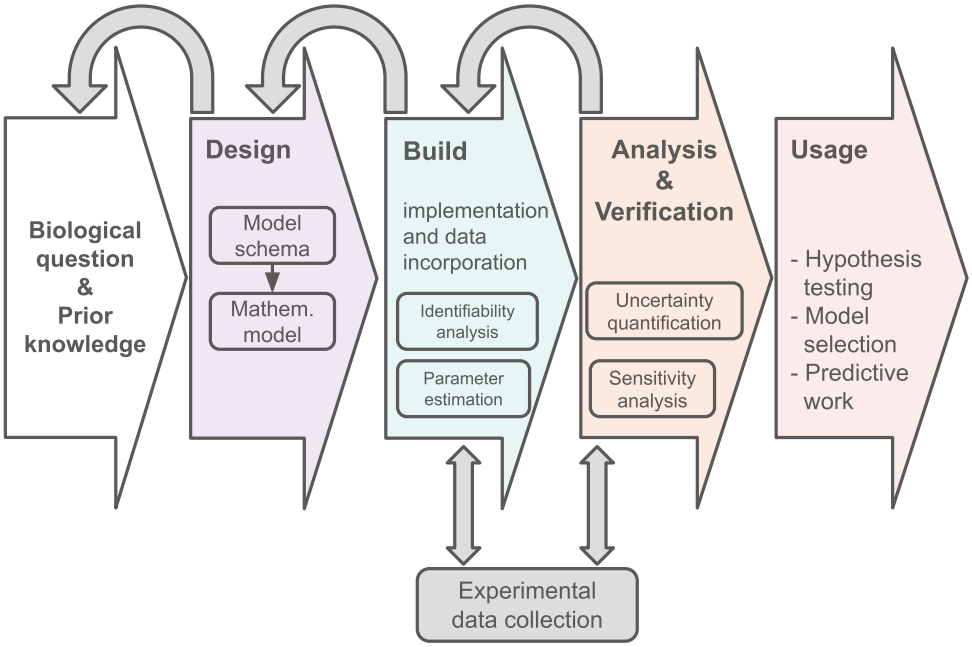

Figure 3.1: **Illustration of the ODE model construction, calibration and analysis workflow.** The presented workflow consists of five steps. (1) A model scope is defined, and knowledge about the system is gathered. (2) Design: Based on the knowledge of the system, a diagram of its components and their interactions is constructed and translated into a set of ODEs. (3) Model building: The mathematical model needs to be implemented in a programming language of choice to perform numerical simulations. Model parameters are either derived during model calibration or from literature research. Different approaches can be applied to assess parameter identifiability (see Wieland et al. [2021]) (4) Model analysis and verification: Various methods are available to analyse the model uncertainty and sensitivity (see Villaverde et al. [2022a]). (5) Usage. Curved grey arrows indicate that this workflow is an iterative and interdisciplinary process. Results from steps (3) and (4) can also be used to guide further experimental investigations.

be estimated based on experimental data (model calibration (Sec. 3.2)). The model calibration is vital to building a "good" model that can generate meaningful predictions.

Besides model calibration, model analysis and verification are also integral parts of the model building process. From an identifiability analysis, one gains knowledge about ambiguities in the model structure and tests whether the available data is sufficient to estimate parameter values with finite Confidence Intervals (CIs) (Sec. 3.3) [Wieland et al., 2021]. Both the model structure and the parameter values are subject to uncertainty [Mitra and Hlavacek, 2019; Schaber et al., 2009], which needs to be assessed (Sec. 3.4). Perturbations in the model input can propagate through the model, which can

be investigated by applying a Sensitivity Analysis (SA) (Sec. 3.5) [Sumner et al., 2012]. Identifiability analysis, uncertainty quantification and sensitivity analysis are essential to evaluate a model's robustness and predictive value and, thereby, its applicability [Eck et al., 2016].

As Fig. 3.1 shows, constructing an ODE model is an iterative process, where simulation results may guide experiments, and the modelling process integrates insights from experiments. Especially model building and analysis provide valuable information concerning the following two questions [Wolkenhauer and Mesarović, 2005]:

- Is the amount and quality of the available experimental data sufficient to construct a model that can serve its purpose?
- Is knowledge about the underlying mechanisms missing?

Mathematical models, in general, serve various purposes [O'Malley and Dupré, 2005]. In a so-called model-driven experimental setting, the model guides experimental decisions. A model can also be used to test different hypotheses – a special case of hypothesis testing being model selection. In model selection, the aim is to identify the most plausible model structure from a population of models [Kirk et al., 2013; Schaber et al., 2009]. In medical research, one important model purpose is the ability to make (patient-specific) predictions, e.g. a treatment outcome or a disease progression [Hastings et al., 2020; Kohl and Noble, 2009; Wierling et al., 2015]. One example of a predictive model that fits the context of this thesis is the work by Gavina et al. [2022]. Gavina et al. [2022] use a menstrual cycle model to estimate the minimum dosage for different contraceptive medications and to determine the optimal dosage timing to achieve contraception. Furthermore, mathematical models can also help to investigate drug effects, as Wright et al. [2020] demonstrate. The authors use a mechanistic model of the menstrual cycle to study how hormonal contraception might affect the hormone dynamics of the menstrual cycle and thereby prevent ovulation.

So far, I have based my discussion about modelling on the five criteria (see page 22) for a "good" model. Cho and Wolkenhauer [2003] and Wolkenhauer [2014] give an additional argument for the value of modelling. Both argue in favour of the value of the modelling process itself because it can be interpreted as a way to collect and integrate knowledge about the system in question. Thus, model construction enables systematic thinking about the system. Furthermore, the modelling process can reveal, for example, knowledge gaps and core dynamics/components of the system.

In conclusion, a mathematical model built thoroughly in terms of complexity and accuracy is a valuable addition to the experimental investigation of biological systems

[Aderem, 2005]. Such a model can be used for various tasks, such as predicting long-term dynamics or behaviour under perturbation. Furthermore, modelling allows for the investigation of features of the biological system that result from the interaction of its components (emergent properties) [Aderem, 2005]. Eventually, the modelling cycle (Fig. 3.1) enforces a systematic way of thinking that can help to deepen our understanding of a complex system.

This thesis presents a modelling-based investigation of the dynamic behaviour of reproductive hormones in girls and women. The known regulatory feedback loops between reproductive hormones are encoded in mechanistic models, formulated as systems of non-linear ODEs. In the following sections, I introduce the general principles that guided my model formulation and analysis.

3.1 Principles of model construction

Endocrine systems can be interpreted as non-linear dynamic systems, where the concentration of each hormone changes in time due to their regulatory interactions. One possible way to capture an endocrine system mathematically is to translate it into a set of ODEs. Solving those constitutes a way to investigate the system's dynamic behaviour computationally [Strogatz, 2018].

Generally, a system of ODEs is defined as

$$\frac{dx(t,\theta)}{dt} = f(x,t,\theta), \tag{3.1}$$

where $f(x,t,\theta)$ is a function that describes the derivative of the system's components (e.g. hormone concentrations) in time. To investigate the system's time evolution, Equation 3.1 is integrated for a given set of initial conditions x_0 and parameters θ. Solving this initial value problem yields $x(t,\theta)$, e.g. the hormone concentration at each time point. For most systems in biology, an analytical solution of the ODE can not be obtained. Consequently, the initial value problem has to be solved numerically.

The models considered in this thesis describe the time evolution of each reproductive hormone by its synthesis-clearance relationship, as illustrated in Fig 3.2. The respective ODE describing the rate of change of hormone S_1 reads:

$$\frac{dS_1}{dt} = k_{syn} \cdot \mathrm{stim}_{S_2} - k_{cl} S_1, \tag{3.2}$$

k_{syn} and k_{cl} are the rate constants for the synthesis and clearance of S_1, respectively. The variable stim_{S_2} denotes the stimulatory effect that the hormone S_2 has on the synthesis of S_1 (Fig. 3.2).

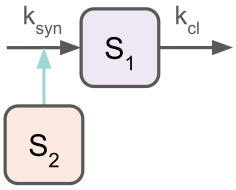

Figure 3.2: **Schematic representation of a synthesis-clearance relationship.** This example system consists of two components: S_1 and S_2. S_1 is synthesised with the rate constant k_{syn} and removed from the system with rate constant k_{cl}. S_2 has a stimulating effect on the synthesis of S_1.

Often, giving detailed mechanistic descriptions of feedback interactions is not possible. For stimulatory and inhibitory feedback mechanisms, Hill functions can be utilised as a heuristic/quantitative description. The positive Hill function for stimulatory interactions (H^+) and the negative Hill function for inhibitory interactions (H^-) are given by the following equations:

$$\begin{aligned} H^+(S_i, T_i^j, n_i^j) &= \frac{(S_i/T_i^j)^{n_i^j}}{1 + (S_i/T_i^j)^{n_i^j}} \\ H^-(S_i, T_i^j, n_i^j) &= \frac{1}{1 + (S_i/T_i^j)^{n_i^j}}. \end{aligned} \tag{3.3}$$

The regulatory effect of S_i on S_j is characterised by the Hill threshold $T_i^j > 0$ and the Hill exponent $n_i^j > 0$. If the concentration of S_i approaches T_i^j, its regulatory action establishes. The value of n_i^j determines the steepness of the switch-like behaviour that a Hill function exhibits, i.e. with higher n_i^j values, the switch is more rapid [Reinecke, 2009; Santillán, 2008].

Mathematical models in systems biology vary in complexity and abstraction. Consequently, the size of the system of ODEs and the dimension of the associated parameter space differ too. Several tools and techniques have been established to calibrate and analyse ODE models [Villaverde et al., 2022a]. The following sections give an overview of well-established methods, focusing on those used for the research conducted for this thesis.

3.2 Parameter estimation

Model calibration is one important step of the model building process. The model calibration aims to fit the model's prediction to experimental data [Banga, 2008; Raue et al., 2013b; Schmiester et al., 2020]. In the context of this thesis, fitting means finding a set of model parameters for which the error between the simulation trajectory (the solution of the corresponding initial value problem) and given data is minimised. Hereby, model parameters can be directly derived from experiments or inferred from the data using statistical estimators. Determining a model parameter directly from experiments/the literature is only possible if the parameter relates directly to a biological observable. Because of the level of abstraction we encounter in the mathematical model, this direct measurement is often not feasible. A direct measurement, for example, fails for the Hill threshold and exponent (Eq. 3.2) because the Hill function is a mechanistic simplification. Those parameters that can not be measured need to be estimated by applying statistical model fitting methods [Ashyraliyev et al., 2009; Jaqaman and Danuser, 2006; Schittkowski, 2002].

The estimation of parameters θ of a mathematical model as given in Eq. 3.1 with experimental data is called the inverse problem [Tarantola, 2006]. The inverse problem is the reverse of the forward problem, which is solving the initial value problem for a given set of parameters [Otten, 2003]. The inverse problem entails several challenges, such as parameter identifiability (Sec. 3.3), noise present in the data [Ashyraliyev et al., 2009; Aster et al., 2018], the shape of the error landscape and the uniqueness of optimal solutions.

The objective of parameter estimation is to find the set of model parameters that fits the data best. One way to solve such a parameter estimation problem is to consider it as a regression problem of a statistical model

$$y(t) = x(t, \theta) + \epsilon(t, \sigma), \tag{3.4}$$

with $y(t)$ presenting the measurements and $x(t, \theta)$ denoting the solution of Eq. 3.1. The random noise summarising all the effects resulting in a variance of the data around the model prediction $x(t, \theta)$ is given by $\epsilon(t, \sigma)$. Often it is assumed that $\epsilon(t, \sigma)$ is normally distributed [Schmiester et al., 2020]. However, alternative noise models are, for example, the Laplace or the Cauchy distribution [Maier et al., 2017].

Finding the parameters θ in Eq. 3.4 usually resembles an optimisation problem. One possible formulation of such an optimisation problem is minimising the func-

tion $J(\theta) = d(y(t), x(t, \theta))$, which describes the distance between the data $y(t)$ and the model's predictions $x(t, \theta)$. Minimizing the distance between the model prediction and the data yields an optimal parameter set $\hat{\theta}$ [Moles et al., 2003; Raue et al., 2013b; Sun et al., 2011].

In systems biology, a commonly used approach for parameter estimation is Maximum Likelihood Estimation (MLE) (Sec. 3.2.1). The resulting Maximum Likelihood (ML) estimate is the parameter set that maximises the probability of observing the data under the given model [Myung, 2003]. In some cases, however, it is preferable to choose a Bayesian estimator, for example, when dealing with noisy or sparse data. In a Bayesian setting, prior knowledge about the model parameters represented as prior parameter distributions gets updated by using additional information (e.g. experimental data), resulting in posterior parameter distributions. From these distributions, statistical measures such as the mode, which is of interest for Maximum A Posteriori (MAP) estimation (Sec. 3.2.2), can be computed [Kramer and Sorenson, 1988; Wilkinson, 2007]. MLE and MAP rely on the formulation of a parametric likelihood function that gives a measure for the probability of a certain parameter set resulting in the observation of the given data. For some models, it is not straightforward to formulate such a parametric likelihood function. In these cases, Approximate Bayesian Computation (ABC) [Csilléry et al., 2010; Liepe et al., 2014; Toni et al., 2009] provides a valuable alternative (Sec. 3.2.3). The ABC algorithm bypasses the likelihood function by simulation and comparison of the data $y(t)$ with the simulation trajectory $x(t, \theta)$ based on user-defined criteria. Overall, there is no general solution to all parameter estimation problems, which makes the task challenging.

3.2.1 Maximum likelihood estimation

In MLE, we search for the most likely model parameters given some observed data. With this, the likelihood function $L(\theta)$ is a joint probability, i.e. the product of the conditional probabilities of observing the data given the parameter set θ. For a data set with N_t independent observations for each of the N_{obs} observed species, the likelihood function reads [Fisher, 1922; Myung, 2003]:

$$L(\theta) = \prod_{i=1}^{N_t} \prod_{j=1}^{N_{obs}} p(y_{i,j}|\theta). \tag{3.5}$$

Here, $y_{i,j}$ denotes the data point of the j-th species observed at the i-th time point.

The ML estimate $\hat{\theta}_{ML}(y)$ is the parameter set for a given data set $y(t)$ that maximises $L(\theta)$. Because $L(\theta) > 0$ and *log* is monotone,

$$\hat{\theta}_{ML}(y) = \arg\max_{\theta \in \Theta} L(\theta) = \arg\min_{\theta \in \Theta}(-log(L(\theta))). \tag{3.6}$$

In other words, with $\hat{\theta}_{ML}(y)$, we have the highest probability of obtaining the data *y(t)*.

When estimating parameters in systems biology, we often assume that:

- the only source for a mismatch between the model trajectories $x(t, \theta)$ and the data *y(t)* is measurement noise
- the measurements are uncorrelated, and their noise is normally distributed.

Then $-log(L(\theta))$ can be written as weighted sum of squared residuals [Raue et al., 2013a; Schmiester et al., 2020]:

$$-log(L(\theta)) = \sum_{i}^{N_t} \sum_{j}^{N_{obs}} \frac{(y_{i,j} - x_j(\theta, t_i))^2}{2\sigma_{i,j}^2} + const. \tag{3.7}$$

Thus, the MLE is equivalent to the minimum in the objective function formulated as the mean squared error. The optimal parameter set $\hat{\theta}_{ML}(y)$, resulting from numerical optimisation, is a point estimate and, therefore, does not provide information about the uncertainty of the forecast. Combining MLE with an investigation of the uncertainty (Sec. 3.4) allows for gaining a more complete picture of the model parameters [Etz, 2018; Myung, 2003; Villaverde et al., 2022a].

3.2.2 Maximum a posteriori estimation

The aim of MAP estimation is to estimate the mode of the posterior distributions of the model parameters. The posterior distribution $p(\theta|y)$ can be expressed following Bayes theorem:

$$p(\theta|y) = \frac{p(y|\theta)p(\theta)}{p(y)}. \tag{3.8}$$

$p(\theta|y)$ denotes the conditional probability density of a parameter set given the data. $p(y|\theta)$ is the conditional probability of observing a data set given a set of parameters.

For a fixed data set *y(t)*, $p(y|\theta)$ is equal to the likelihood $L(\theta)$ (Sec. 3.2.1). $p(\theta)$ and *p(y)* are the probabilities of observing θ or y without any conditions. Because *p(y)* refers to the data and is therefore fixed, *p(y)* is a normalizing constant [Etz and Vandekerckhove, 2018; Mitra and Hlavacek, 2019; Villaverde et al., 2022b]. Consequently, the posterior in Eq. 3.8 can be phrased as proportional to the product of the likelihood and the prior:

$$p(\theta|y) \propto L(\theta)p(\theta). \tag{3.9}$$

The posterior $p(\theta|y)$ can be approximated numerically using a sampling strategy. Typically, Markov Chain Monte Carlo (MCMC) sampling algorithms are utilised to approximate the posterior distribution by creating a large number of samples [Andrieu et al., 2003]. The Metropolis–Hastings (MH) algorithm is a popular example of a MCMC algorithm. An acceptance-reject strategy forms its foundation. Here, the decision is based on comparing the values of $f(\theta)$, where $f(\theta)$ is chosen to be proportional to $p(\theta|y)$. Starting from an arbitrary set of parameters θ^0, the MH algorithm realises a Markov chain in the parameter space by executing repeatably the following two steps:

1. Proposing step: sampling a parameter set $\theta^{'}$ based on the current set of parameters θ^*
2. Accept-reject step: $\theta^{'}$ is tested against the Metropolis criterion $r = \frac{f(\theta^{'})}{f(\theta^*)}$
   - if $r \leq u$ with u being a random number from the uniform distribution $u \in [0, 1]$ then $\theta^{'}$ is accepted and replaces θ^*
   - else $r > u$ with u being a random number from the uniform distribution $u \in [0, 1]$ then $\theta^{'}$ is rejected

Over the sampling time, the Markov chain will converge towards a stationary distribution, approximating the desired parameter posterior distribution [Hastings, 1970; Metropolis et al., 1953]. The mean of this posterior distribution is the MAP estimate. Additional statistical measures, such as the median or percentiles, can be computed from the posterior distribution.

3.2.3 Approximate Bayesian Computation

The ABC method enables the estimation of parameter distributions without calculating a likelihood. The simplest ABC approach is an acceptance-reject sampling routine [Kirk et al., 2013; Liepe et al., 2014; Pritchard et al., 1999], as follows:

1. Create a parameter set θ^* by sampling each parameter θ_i from its proposal distribution $\pi_i(\theta_i)$

2. Calculate $x(\theta^*, t)$ by solving the forward problem

3. Compare $x(\theta^*, t)$ with the data set *y(t)*. If the difference between $x(\theta^*, t)$ and *y(t)* is sufficiently small, θ^* is accepted.

After a sufficiently larger number of sampling iterations, the posterior parameter distribution can be constructed from all accepted θ^*.

The comparison step in the ABC method allows model calibration using non-numeric measures. For example, in Fischer et al. [2021], the divergence between *y(t)* and $x(\theta^*, t)$ is evaluated based on a comparison of characteristic features of the hormone profile (e.g. an increase in FSH concentration 2 days before ovulation) and the physiological cycle length (see Fig. 2 in Paper A, Part II).

3.3 Parameter identifiability

The amount and quality of available data are a bottleneck for constructing mathematical models of biological systems. Often, systems are only partially observable - meaning experimental data are only available for a fraction of model components. Additionally, biological data are noisy. Whether the model parameters can be inferred with finite confidence intervals given the model's structure and the available data can be investigated by performing an identifiability analysis. The results from an identifiability analysis help to evaluate the model's applicability [Guillaume et al., 2019] and can guide further data collection and model reduction [Maiwald et al., 2016].

The literature defines two types of parameter identifiability: structural and practical identifiability. A structurally identifiable model has a unique parameterisation for each model prediction. Structural non-identifiability roots in the model's formulation. For example, redundancies in the model cause structural non-identifiability. Practical non-identifiability results from the amount and quality of available data. A parameter is practically non-identifiable if the information in the given data is insufficient to make a precise estimate [Lam et al., 2022; Wieland et al., 2021].

Identifiability analysis tools are divided into *a-priori* and *a-posteriori*/data-driven methods. *A priori* methods investigate the model structure and, therefore, do not require any data. Hence, the results do not provide information about practical non-identifiability.

A-priori methods have their theoretical origin in various mathematical concepts. One example is the investigation of the symmetry properties of the system by using Lie group theory [Wieland et al., 2021]. In contrast, *a-posteriori* methods need data. Consequently, their results will also indicate if the available data suits the model's complexity. In systems biology, the Profile Likelihood (PL) approach (Sec. 3.3.1) is a popular method to investigate identifiability [Kreutz et al., 2013; Raue et al., 2009]. This method covers the investigation of structural and practical identifiability locally. Furthermore, the literature provides us with Bayesian approaches to characterise model identifiability [Daly et al., 2018; Hines et al., 2014; Siekmann et al., 2012]. Here, the computed posterior distribution reveals the parameter ranges that agree with the data, and conclusions about parameter identifiability can be drawn based on how well the parameter ranges are constrained. Raue et al. [2013a] compare identifiability analysis results obtained through MCMC sampling and PLs. The authors conclude that both methods indicate non-identifiable model parameters, but the PL results are easier to interpret.

Parameter identifiability is one aspect to be considered when constructing mathematical models in biology. As outlined above, there are various methods to investigate identifiability. Even though a fully identifiable model is desirable, it is often not achievable due to the technical limitations of data collection. Rateitschak et al. [2012] demonstrate that a model can be valuable and applicable for predictive work, even though it is not fully identifiable.

3.3.1 Profile likelihood

Raue et al. [2009] introduce the idea of investigating the identifiability of model parameters in systems biology by using PLs [Murphy and Van der Vaart, 2000]. PLs project the likelihood function value onto each model parameter separately, i.e. for a parameter θ_i, all remaining parameters $\theta_{j\neq i}$ are reoptimised. The Profile Likelihood of a parameter θ_i reads:

$$PL(\theta_i) = \min_{\theta_{j\neq i}}(-log(L(\theta))) \tag{3.10}$$

Since this approach is optimisation-based, we can employ suitable methods from optimisation theory as long as it is possible to express a parametric form of $L(\theta)$.

Analysing the shape of the PL (Fig. 3.3) allows for distinguishing between identifiable and non-identifiable parameters. Identifiable parameters are characterised by a profile bounded towards positive and negative values of θ_i. Hence, they have an u-shaped like-

lihood profile (Fig. 3.3 left subfigure). Furthermore, the shape indicates structural and practical non-identifiability. Profiles of practically non-identifiable parameters (Fig. 3.3 middle subfigure) are bounded towards either positive or negative values, whereas structurally non-identifiable parameters have flat profiles (Fig. 3.3 right subfigure).

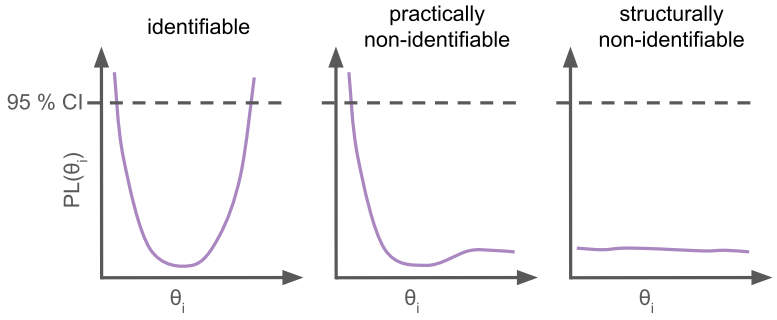

Figure 3.3: **Characteristic shapes of profile likelihoods.** The shape of the profile likelihood for a parameter θ_i reveals the parameter's identifiability type. An identifiable parameter reaches the confidence interval threshold on both sides, thus having a finite confidence interval. A practically non-identifiable parameter reaches the confidence interval threshold only on one side, here for the lower parameter ranges. A structurally non-identifiable parameter's profile is flat and never reaches the confidence interval threshold.

The confidence interval of a parameter θ_i gives the range of its likely values, i.e. for a 95% CI, in 5% of cases, the parameter lies outside the parameter range given by the 95% CI [Lele, 2020]. In the PL setting, the CI of a parameter θ_i can be defined as the parameter range where the PL-value fulfils the following condition [Raue et al., 2009; Venzon and Moolgavkar, 1988]:

$$CI_\alpha(\theta_i|y) = \{\theta_i|PL(\theta_i) \leq -log(L(\hat{\theta})) + \Delta_\alpha(\chi^2_1)\}. \tag{3.11}$$

Here, α denotes the desired significance level, and $-log(L(\theta))$ refers to the value of the likelihood function of the optimal parameter set (ML estimate or MAP estimate). The threshold $\Delta_\alpha(\chi^2_1)$ is the α-quantile of the χ^2-distribution with one degree of freedom. That means all values of θ_i which give a PL-value below the threshold are within the confidence interval [Kreutz et al., 2012; Tönsing et al., 2018].

Calculating PLs results in easily interpretable plots (similar to the illustration in Fig. 3.3), revealing the identifiability of parameters. Additionally, CIs can be derived to evaluate the uncertainty of the parameter estimate. The potential and applicability of the PL approach for analysing models in biology have been demonstrated in various pub-

lications [Kreutz et al., 2012, 2013; Merkle et al., 2016; Tönsing et al., 2018]. Tönsing et al. [2018], for example, compute the PLs for all model parameters of the proposed Zika virus disease spread model and uses this information about the model parameters to reduce the parameter space.

3.4 Uncertainty quantification

Mathematical models suffer from uncertainty. This uncertainty needs to be quantified to evaluate the model's usefulness and predictive value [Volodina and Challenor, 2021]. We distinguish between two sources of uncertainty: aleatoric uncertainty and epistemic uncertainty [Hoffman and Hammonds, 1994]. Aleatoric uncertainty results from randomness, which occurs in all processes, e.g. noise in gene expression. Consequently, we will observe some variation in the experimental outcome of individual runs under the same conditions. This source of uncertainty is unavoidable, but stochastic approaches can be used for its analysis. Epistemic uncertainty originates from incomplete knowledge, including a lack of mechanistic understanding, incomplete measurements and measurement errors. Therefore, model parameters derived from data will inherit uncertainty from the model formulation and the available data. This uncertainty can be characterised by applying methods such as Bootstrapping, Markov Chain Monte Carlo methods, and the calculation of Profile Likelihood [Kaltenbach et al., 2009; Lele, 2020].

Sampling from the posterior distribution using a MCMC algorithm gives a marginal posterior distribution for each model parameter. Hence, the sampling results provide each parameter's statistical measures, such as mean and median; corresponding CIs can be computed. In addition, by performing numerical simulations with parameter sets from the stationary sampling distribution, we gain insights into the mean prediction and the prediction uncertainty [Villaverde et al., 2019]. Consequently, this approach provides a comprehensive parameter study, yielding parameter estimates with uncertainty measures and information about parameter correlations. However, sampling routines, in particular, are computationally intensive [Mitra and Hlavacek, 2019], and convergence is only ensured for identifiable models [Bayarri and Berger, 2004; Raue et al., 2013a].

As an alternative, Profile Likelihoods can be exploited for uncertainty quantification. For each parameter, a CI can be computed from its PL (Eq. 3.11) [Raue et al., 2009].

Models in systems biology are affected by different sources of uncertainty, e.g. uncertainty of the parameter estimates. Quantifying this model uncertainty is vital for the model validation and underpins the model's credibility [Volodina and Challenor, 2021].

One central element is often the computation of CIs to perceive the uncertainty in the parameter estimate. However, due to the fluctuations in biological processes, even models with well-determined parameters are subject to uncertainty. This epistemic uncertainty can only be addressed by intense data collection and stochastic approaches.

3.5 Sensitivity analysis

ODE models are characterised by a deterministic input-output relationship. Therefore, uncertainty in the model input propagates to the model output [Turányi, 1990]. SA investigates this relationship between model input and output, i.e. it helps to identify model inputs that contribute the most to the variability in the model output (sensitive inputs). Vice-versa, SA also indicates parameters that do not contribute to the variance in the model output – this information can be utilised for reducing the parameter space [Saltelli et al., 2000; Zhang et al., 2015]. For model inputs limited to physiologically/biologically plausible ranges, SA can also be used to investigate model robustness [van Riel, 2006].

Local SA (one-factor-at-a-time method) is derivative-based and, therefore, provides information about the effect of small changes in the model input [Morio, 2011]. The effect of each parameter θ_i on each model output x_j is studied independently by evaluating the partial derivatives. Hence, the local sensitivity $LS_{i,j}$ of θ_i and x_j reads:

$$LS_{i,j} = \frac{\partial x_j}{\partial \theta_i}. \tag{3.12}$$

There are several examples [Omari et al., 2020; Schoeberl et al., 2002; Yue et al., 2006], where this technique has been used to analyse parameter sensitivity in models of biological systems.

Unlike local SA, global SA allows for varying model input over large input value ranges. One example of a global SA is the Sobol method. This method aims to decompose the model output's variance into inputs' contributions. Since the Sobol analysis allows for varying multiple inputs simultaneously, this method provides insights into the contribution of individual inputs and input combinations [Tosin et al., 2020; Zhang et al., 2015]. Thus, Sobol's analysis gives a more comprehensive picture than a local SA.

Sobol indices, computed as the ratio of a partial variance to the total variance in the model output, are derived as sensitivity measures from the Sobol analysis [Homma and Saltelli, 1996; Qian and Mahdi, 2020; Saltelli et al., 2010]. The first-order sensitivity

index

$$S_i = \frac{V_i}{V} \tag{3.13}$$

describes the contribution of the i-th model input, expressed as partial variance V_i, to the total output variance V. Hence, it gives a measure for the effect of varying only this i-th input. The second-order sensitivity index

$$S_{i,j} = \frac{V_{i,j}}{V} \tag{3.14}$$

is a measure of the contribution of a subset of two model inputs ($V_{i,j}$) to V. Consequently, it reveals information about the effect of the interactions within this input subset. The total-order sensitivity index for the *i-th* model input

$$S_{Ti} = \frac{V_i^{total}}{V} \tag{3.15}$$

is a combination of all contributions of the *i-th* input. The total variance of the *i-th* input

$$V_i^{total} = V_i + V_{i,\sim i}. \tag{3.16}$$

is the sum of the contribution of the *i-th* input alone (V_i) and in combination with all other inputs ($V_{i,j}$).

Various works across biological modelling disciplines have demonstrated the utility of the information provided by the Sobol analysis [Fieberg and Jenkins, 2005; Frank et al., 2021]. Lebedeva et al. [2012] emphasise the value of this technique for the analysis of models with uncertain parameters.

In conclusion, SA helps to better understand the relationship between model input and model output. Furthermore, identifying sensitive inputs can guide further experimentation and model/parameter space reduction.

3.6 Modelling of pharmacokinetics and pharmacodynamics

Pharmacokinetic (PK) and Pharmacodynamic (PD) modelling attempt to investigate drugs in silico. A PK model describes the time evolution of a drug concentration in different body compartments (e.g. blood or liver) from the drug's administration until its complete removal from the system. The central mission of PD modelling is to investigate the relationship between the drug concentration and its effect. Linking PK with PD modelling allows us to study the time delay between the drug administration and the drug's effect [Breimer and Danhof, 1997; Lippert et al., 2012]. Such models can, for example, be used to investigate dosing regimes, dosing schemes and routes of administration [Jones and Rowland-Yeo, 2013]. Thus, those models are integral to today's drug discovery and development.

When constructing a so-called Physiologically Based (PB) model, the biological system, e.g. the human body, is divided into units (compartments) [Andersen, 1991]. A compartment represents, for example, an organ or a tissue. The bloodstream (transport compartment) interconnects all compartments. Fig. 3.4 shows a two-compartment model, which is the simplest PB model structure [Jones and Rowland-Yeo, 2013; Nestorov, 2003]. In this example, a drug is administered to the central compartment (representation of the blood), distributed to the tissue compartment and eliminated from the central compartment. In a two-compartment model, only one tissue compartment is considered, which one can interpret as an abstract representation of the body, excluding the blood. Often at least a third compartment as the location for the drug elimination (e.g. liver) is included [Upton et al., 2016].

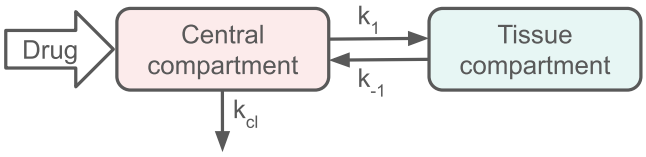

Figure 3.4: **Schematic representation of a two-compartment model.** In a two-compartment system, the drug is administered to a central compartment. The central compartment is linked to another compartment, representing the tissues where the drug takes effect. The drug travels between the two compartments. k_1 and k_{-1} denote the rate constants for the distribution between those two compartments. The drug is cleared from the central compartment with the clearance rate constant k_{cl}.

The number of compartments depends on the application of the model, the drug administration route, the location of drug action and the possible side effects. The number of

compartments directly affects the model complexity by increasing the number of model parameters (e.g. tissue volume) and, therefore, should be balanced with the amount of prior knowledge and data. PBPK models, which are reduced in complexity by "lumping" together compartments with similar properties, can be useful as Cao and Jusko [2012] demonstrate.

Further details that can be added to those pharmacological models are, for example, [Danhof et al., 2007]:

- Blood flow: affects the rate constant for the drug distribution [Stanski et al., 1979]
- Target binding and activation
- Drug-related feedback mechanisms
- Transport mechanisms into the cell (commonly, passive diffusion is assumed)

Two types of model parameters are described for PBPK/PD models: (i) drug-specific parameters and (ii) system-specific parameters. Drug-specific parameters cover a drug's chemical and biochemical properties, such as permeability, solubility and binding properties. They can be determined in in vitro experiments and are not subject to variability between individuals or species. Whereas system-specific parameters address physiological properties, e.g. organ volume and surface, blood pressure and tissue composition. Those parameters are assessed in in vivo experiments. They are subject to inter- and intra-individual variability [Danhof et al., 2007; Kuepfer et al., 2016].

Overall, PBPK/PD models provide a flexible framework for studying drugs in a mechanistic and physiologically plausible representation and have been proven useful [Kuepfer et al., 2016; Nestorov, 2003]. The model formulation allows for model scaling for individuals, subpopulations and across species [Upton et al., 2016]. In the context of this thesis, such a modelling approach is used to integrate the administration of hormonal medication into the menstrual cycle model. With this, we were able to run in silico studies investigating the effects of hormonal medication on hormone profiles and folliculogenesis ([Fischer et al., 2021]).

Chapter 4

Summary of scientific work

The endocrine regulation of the female reproductive system is complex and dynamic. Especially in humans, its clinical investigation is challenging because a high number of measurements (approximately every other day) over long time periods (at least one menstrual cycle) is needed to capture fluctuations in hormone concentrations. In three scientific articles and one review paper (for complete articles, see Part "Scientific articles"), I point out how mathematical modelling provides concepts that help us to understand the mechanisms regulating female fertility and how mechanistic models can contribute to developing new treatment strategies.

In Chapter 4, I briefly comment on the reproducibility of computational experiments and the accessibility of scripts. Subsequently, I will summarise the three scientific publications aggregating the research I conducted for this PhD thesis. Finally, I discuss the results, strengths and weaknesses of the work presented in those articles. The chapter ends with an outlook giving ideas on how the presented work could be extended.

4.1 Reproducibility and code reusability

Transparency and reproducibility of scientific results are central to their trustworthiness. To allow others to reproduce reported results, it becomes more common to make scripts that were used to generate computational results publicly available. Furthermore, making code available for the scientific community allows for its reuse, which bares the potential to speed up the scientific process and prevent people from repeating the same work [Bahaidarah et al., 2022; Editors at Nature Computational Science, 2021]. Thus, the accessibility of code is beneficial for the scientific community.

Regardless of the benefits of publicly available code, the primary purpose of scientific code is to answer a specific question rather than being used or reused by others. Consequently, those codes may be unstructured and poorly documented, and a lack of reproducibility is not uncommon. This lack of reproducibility is often caused by missing documentation, errors in the code or missing files [Trisovic et al., 2022]. To avoid this issue, authors can consult guidelines for good coding practices, such as Rivero and Chen [2020] or the author guidelines by Springer Nature. Furthermore, computational experiments, such as wetlab experiments, need thorough documentation to allow others to repeat them [Fehr et al., 2016; Schnell, 2015].

It is also important to point out that formal training teaching young scientists how to make code accessible and reusable is often missing [Bahaidarah et al., 2022; Trisovic et al., 2022]. This lack of formal education may result in a lack of confidence, hindering scientists from making their code publicly available [Barnes, 2010]. Despite that, Barnes [2010] encourages scientists to make their code publicly available regardless of the code quality because available code allows other scientists to engage.

I agree that making computational code publicly available is crucial to make scientific work transparent. Furthermore, I believe that the possibility of reusing code may benefit the scientific community. For this reason, I made my code publicly available on GitHub. In my repositories, you will find scripts that form the scientific foundation for all the articles discussed in this thesis. The repository of the model used for Paper A and Paper B includes all code files necessary to create the content presented in those papers. In principle, this allows for a complete reproduction of simulation results. However, I believe that it requires time to understand the code thoroughly. In the case of Paper C, I decided to publish a selection of scripts demonstrating the workflow, which is the paper's main contribution. These demos allow for generating most figures but not all of the results. Of course, my decision compromises reproducibility to the benefit of increasing the code's accessibility and readability.

All codes are published under the MIT license so that others can reuse and modify the codes free of charge. The links to the repositories are included in the publications. However, GitHub repositories can be changed. Therefore, it is a better practice to archive a GitHub repository using Zenodo (https://zenodo.org/) and refer to the archive using Digital Object Identifiers (DOI).

In addition to creating a GitHub repository, I could have considered uploading the mechanistic model presented in Paper A into the BioModels database [Malik-Sheriff et al., 2020]. The great benefit of BioModels is its independent model curation. With this, the platform ensures model correctness and increases the potential for model reuse. How-

ever, to publish code for methodological approaches (Paper B and Paper C), I believe that GitHub repositories provide a better solution to make the code publicly available.

Overall, I believe that the repositories I created allow others to engage, use and reuse the scripts underlying my work. However, I am aware that there is potential for me to improve my code readability, documentation and publishing practice.

4.2 Paper summaries

For this thesis, I worked on mechanistic models describing the endocrine regulation of the female reproductive system (HPG axis). The first two publications focus on the functionality of the mature HPG axis and folliculogenesis. Paper A introduces the first menstrual cycle model that couples hormone dynamics of the HPG axis with the maturation of ovarian follicles in a biologically interpretable fashion. Paper B expands on Paper A and demonstrates an application of the model in a pharmacological setting. Paper C introduces a model of the maturation process of the HPG axis during female puberty. The emphasis of Paper C lies on the proposed Bayesian updating workflow that allows the incorporation of cross-sectional data in the model calibration. In the following sections, I will summarise each scientific contribution and discuss them in this thesis's context.

4.2.1 Paper A: Hormonal regulation of ovarian follicle growth in humans: Model-based exploration of cycle variability and parameter sensitivities

Selgrade and Schlosser [1999] published the first mathematical model of the female menstrual cycle, which has been modified and expanded over the years, e.g. Harris [2002]; Harris and Selgrade [2014]; Reinecke and Deuflhard [2007]; Röblitz et al. [2013]. However, the description of ovarian follicles and their maturation remained heuristic throughout all model versions. Up to this point, follicles are not described as individual entities, but the models describe discrete follicle maturation stages. Consequently, none of those models predicts the size or count of ovarian follicles and the simulation results are not comparable to ultrasound data, despite ultrasound data being the most common way to monitor follicular growth. Thus, this heuristic description limits the model's applicability. For example, they can not be used to predict the effect of COS on the maturation of ovarian follicles, which is essential from a clinical perspective.

Paper A presents a modified version of the model published by Röblitz et al. [2013]. The main contribution of this work is replacing the heuristic description of folliculogenesis with a semi-mechanistic maturation function describing the growth trajectory of each ovarian follicle individually (one ODE per follicle). This description was derived from the work by Lange et al. [2019]. Differences in growth trajectories of follicles between simulation runs result from follicle-specific parameters sampled before each simulation run. The model introduced here is the first menstrual cycle model, which predicts ovarian follicles in a way that allows for a comparison to ultrasound data. In the model simulations, ovarian follicles grow in waves. This growth pattern is an emergent phenomenon. Hence, this modelling work supports the hypothesis that human ovarian follicles grow in waves.

During the model construction, we identified two aspects that made the model calibration challenging: (i) the limited availability of longitudinal data over multiple menstrual cycles and (ii) the variability in the length of simulated menstrual cycles resulting from random features in the follicle growth hinders an optimal alignment between measurements and simulation results. Consequently, a distance measure, such as the mean squared error, could not be defined, and classical optimisation approaches were not feasible. Instead, we bypassed the formulation of a likelihood function using ABC to investigate the model's parameters. Based on the ABC study, we conclude that the simulation output is sensitive to ensembles of parameters rather than single ones.

4.2.2 Paper B: Mathematical modelling and simulation provide evidence for new strategies of ovarian stimulation

In quantitative systems pharmacology, a model as presented in Paper A is useful for performing in silico studies of treatment protocols. One possible scenario is the simulation-based investigation of the effects of hormonal medications on hormone profiles, e.g. [Röblitz et al., 2013] and [Wright et al., 2020], and folliculogenesis. Here, we use the model proposed in Paper A for an in silico study of strategies for Controlled Ovarian Stimulation.

Newly developed COS strategies are often based on the hypotheses that (i) ovarian follicles grow in cohorts (follicle wave theory) and (ii) their growth is stimulated as long as the FSH concentration is above a certain threshold (FSH window concept). In contrast to previous models, our model exhibits (i) and (ii). Consequently, it is suitable for in silico investigations of the effect of COS on the growth of individual follicles.

In Paper B, we integrated the administration of recombinant FSH – a hormonal medication often used in COS – in the form typical for PBPK models. We investigated the effects of two COS protocols: ovarian stimulation during the luteal phase [Kuang et al., 2014b] and ovarian stimulation during the late follicular phase [Zhu and Fu, 2019] and compared simulation results with clinical data. Based on this comparison, we conclude that the model shows the expected behaviour. In particular, the model reflects the shifts in the hormone profiles caused by the treatment, e.g. the FSH level increases systematically. Due to an elevated FSH concentration, we expect the number of growing follicles to increase. In the simulations, this increase in the number of follicles in response to the drug (recombinant FSH) agrees with the clinical data. Since the clinical data used for the comparison have been taken into account during the model calibration, these results should be considered as a validation of the model rather than a prediction. Nevertheless, this work demonstrates a possible use case of mechanistic menstrual cycle models as tools for reproductive health care.

4.2.3 Paper C: A workflow for incorporating cross-sectional data into the calibration of dynamic models

The amount and quality of data available for model calibration often limit the complexity and accuracy of models in systems medicine. Individuals' longitudinal data are valuable for the calibration of dynamic models. However, they are particularly challenging to collect. In contrast, the collection of cross-sectional data is often more feasible. In Paper C, we propose a Bayesian updating workflow to incorporate cross-sectional data into the model calibration process.

The model we use in Paper C aims at predicting individuals' reproductive hormone levels during puberty, and biological knowledge motivates its formulation (system of ODEs). The interactions along the HPG axis are described in the same manner as presented in Paper A – but in less detail. For puberty, the reactivation of the GnRH pulse generator is central for developing the endocrine regulation of reproductive function. This reactivation process is described semi-mechanistically by using a sigmoidal input curve to describe the increase of GnRH release over time.

The Bayesian updating workflow proposed for the model calibration is a two-step procedure. In the first step, a population-average model describing the dynamics of the average hormone concentrations during puberty is calibrated using cross-sectional data. Characterising the uncertainty and sensitivity of this population-average model allows for (i) the reduction of the parameter space and (ii) the characterisation of the discrete marginal parameter distributions (used as prior parameter distributions in step two). In the second step, the population-average model is translated into an individual-specific model by updating the prior parameter distributions with individual data. To test the approach, we synthetically created longitudinal data. Indeed, after performing the parameter update, the individual-specific model predictions recover the complete synthetic hormone profiles, including correct future projections.

Since clinical data collection is time and resource intense, it is important to maximise the use of collected data. As demonstrated, Bayesian updating allows for incorporating cross-sectional data into the model calibration process. Hence, it is a valuable tool for assessing information from various data sets for calibrating dynamic models.

4.3 Concluding discussions

Ideas from systems biology play an important role in establishing predictive, preventive, personalised and participatory medicine (also called P4 medicine), which promises to improve healthcare, reduce costs, and inspire innovation. The diverse academic backgrounds of researchers in systems biology can be seen as an advantage to achieving this goal because this interdisciplinary nature increases the number of methods, approaches and perspectives involved in the scientific discussion. Finally, the highly interdisciplinary approach of systems biology helps us to deal with the complexity we encounter in life science [Hood, 2013].

As for modelling and simulation, combining different approaches will allow us to make use of their complementary strengths [Baker et al., 2018], which benefits clinical research, as shown, for example, in Hackenberg et al. [2022]. Here, the authors link ODEs to deep learning approaches to build a predictive model that can deal with the small data sets. In reproductive medicine, patient-tailored healthcare remains challenging [Tesarik and Mendoza-Tesarik, 2022]. However, the integration of modelling-based tools into clinical routines, for example, clinical decision support systems, holds the promise to improve the situation [Ehrig et al., 2016; PAEON, 2017].

The Avicenna Alliance, an association advocating for the regulation and deployment of in silico methods in healthcare, emphasises the benefits of including modelling and simulation in clinical trials. Modelling and simulation would make the drug development process more cost and time efficient and contribute to a decreased need for animal and human testing [Avicenna Alliance]. In the context of reproductive healthcare, the usefulness of menstrual cycle models for in silico studies of hormonal medication, e.g. for contraception [Wright et al., 2020] and COS [Röblitz et al., 2013], has been demonstrated. Creating a population of virtual patients [Sinisi et al., 2020a,b] allows for a description of subpopulations and corresponding treatment optimisation. Tailoring the treatment protocol to a patient's physiological condition and personal needs would optimise the treatment outcome in terms of pregnancy and live birth while simultaneously decreasing treatment-related risks such as Ovarian Hyperstimulation Syndrome [Sighinolfi et al., 2017].

Creating models that describe the periodic changes in reproductive hormones and folliculogenesis is the first step towards building clinical decision support systems for reproductive healthcare. The endocrine interactions of the menstrual cycle are complex in that hormones have different signalling effects depending on their concentration and the simultaneous secretion of other hormones. For example, E2 alone stimulates the secretion of pituitary hormones, whereas this stimulation is not observed if E2 and P4 are

secreted simultaneously. Because the signalling chains are complex, the model building process as a way of knowledge collection is valuable in itself [Kuepfer et al., 2016]. Following this argument, a mechanistic menstrual cycle model is valuable for representing and systematically understanding the complex regulatory system.

The simulation-based studies of hormonal medication for contraception [Wright et al., 2020] and COS [Röblitz et al., 2013] lack a biologically interpretable prediction of follicular growth. However, follicle maturation is a central aspect of both medications. Therefore, I argue that the model proposed in Paper A is better tailored for such studies and present a simulation-based investigation of COS protocols in Paper B. The simulations show the effects of hormonal treatment on hormone levels and predict the number of follicles that mature during the treatment. Since, COS aims at achieving a sufficient number of mature oocytes (at least three) without an unsafe elevation in hormone levels, predicting the number and size of maturating follicles besides the changes in hormone levels is of main interest for a clinical decision support system for COS protocols.

Unfortunately, the clinical data used for Paper B do not represent information about individuals. Therefore, repeating similar simulation studies with individuals' treatment data (treatment protocol, hormone levels, ultrasound data) would be a reasonable next step in moving towards a precision medicine tool.

Also, repeating the simulation-based study of the effects of hormonal contraception conducted by Wright et al. [2020] with the modified model (Paper A) would allow for investigating the effect of hormonal contraception on folliculogenesis. Such a study would be of interest because ovulation suppression is one possible mechanism of action for hormonal contraception.

Besides its clinical application, a mechanistic menstrual cycle model can also be useful to deepen our understanding of the consequences of the interactions in the system, e.g. by observing emergent properties. In Paper A and Paper B, we observe the growth of ovarian follicles in cohorts in the simulation results. This behaviour is such an emergent property. Therefore, this observation underlines that the interplay between hormones is essential for folliculogenesis and suggests that abnormal folliculogenesis, e.g. described in patients with PCOS or endometriosis, is likely related to endocrine disruptions.

As pointed out above, a mechanistic ODE model is a practical framework for menstrual cycle models. The model presented in Paper C is also biologically motivated, and formulated as a set of ODEs. Here, this formulation was necessary to demonstrate the proposed workflow. Indeed, whether a statistical or machine learning model would have a higher predictive value for individual predictions of the stage of pubertal development remains open. The drawback of a non-mechanistic modelling approach, however, is that

it is not biologically interpretable and motivated.

Inevitably, there is value to mechanistic menstrual cycle models. However, both a model reduction and recalibration of the model presented in Paper A and used in Paper B are needed to push the model towards becoming a tool for personalised medicine. The currently available data (daily hormone measurements throughout one menstrual cycle for individuals with a cycle length of 28 days) poses a bottleneck for the model's calibration because these data do not represent inter- and intra-individual variability in cycle length. Today those hormone concentrations are measured in blood samples. Consequently, collecting more comprehensive data sets, e.g. bi-daily hormone concentration measurements over multiple menstrual cycles, is time-consuming, resource-intense and requires a significant commitment from study participants. However, the new "Hormonix" method [Platt, 2020], which enables monitoring reproductive hormones in saliva samples, bares the potential to increase the availability of longitudinal hormone measurements. In addition to longitudinal hormone measurements, corresponding ultrasound data monitoring folliculogenesis would be valuable but are not publicly available yet.

A problem pointed out in Paper A is that the model complexity is not optimally aligned with the amount of available data. As a consequence, the menstrual cycle model is non-identifiable. Even though parameter identifiability is essential during model calibration, in our case, a fully identifiable model will probably not be obtained, even with an improvement in the amount of data available. Two important reasons for that are: (i) some species such as GnRH are not measurable, and (ii) model parameters, e.g. Hill coefficients, can not be directly linked to experimental observables. However, this does not necessarily mean that the model is not valuable, as Rateitschak et al. [2012] argue.

Beyond searching for additional data sources, I suggest a systematic reduction and reconstruction of the menstrual cycle model. The presented model can be seen as a "legacy model" that has been modified and improved over the last 20 years. Considering a modularisation of the model would allow for adjusting the model's complexity, making it straightforward to tailor the model to its purpose. I would suggest dividing the model into a core mechanistic model consisting of all hormonal interactions and "optional addons", such as detailed receptor binding mechanisms. The receptor binding mechanisms are of importance for pharmacological studies but could be neglected for the hormone regulation itself. Overall, this step is work-intense, but I believe it would benefit the model's accessibility and reuse.

For model calibration and analysis, there exists an established set of tools in systems biology, for example, summarised in Villaverde et al. [2022a]. As demonstrated in Paper A and Paper C, the literature provides more model calibration and analysis methods.

However, those are not yet well-established in the field of computational systems biology.

In Paper A, we use the ABC method for calibration of the model as an alternative to MLE or MAP. Here, the formulation of an objective function measuring the distance between model simulations and experimental data is not feasible because the variability in cycle length prevents an alignment between measured and simulated concentration profiles. Using ABC allows for comparing the concentration profiles based on their shape and, therefore, does not restrict the cycle length to 28 days.

With Paper C, we touch on the fact that longitudinal clinical data are often sparse or unavailable. Since clinical data collection is time and resource intense, it is vital to unleash the full potential of data sets. To address this challenge, we advocate for finding methods that allow for including additional information sources like cross-sectional data, symbolic data or covariates in the model calibration process. In Paper C, we demonstrate the value of Bayesian updating to integrate cross-sectional data in the model calibration process. Overall, there is room for improvement in how clinical data is shared and reused within the scientific community. I believe our obligation as scientists is to use the available resources to their full potential.

4.4 Future prospects

Looking forward, it would be valuable to modify the menstrual cycle model (Paper A) such that it describes the characteristic hormone imbalances observed in patients diagnosed with endometriosis. The most notable shift in the pathological endocrine profile is an elevated E2 level, which results from the endometriotic tissue being an additional location of E2 production [Bulun et al., 2012; Chantalat et al., 2020]. Reducing the E2 level and suppressing ovulation using endocrine agents are essential components of endometriosis management, besides the surgical removal of the endometriotic tissue [Andres et al., 2015; Chapron et al., 2019; Crosignani et al., 2006]. Progestins, synthetic steroid hormones with properties similar to P4, are a well-established group of endocrine agents for managing endometriosis symptoms. However, the administration of such progesterone-only pills can cause side effects such as mood changes, migraine and the formation of ovarian cysts. Here, mathematical modelling can inform the minimal dosage and the optimal dosing strategy. The model modification suggested above could be used to perform simulation-based studies of contraceptive medications used for endometriosis management, similar to the approaches presented in Gavina et al. [2022] and Riggs et al. [2012].

As for the open question about the type of model to be used in Paper C, the most exciting direction would be a combination of mechanistic and machine learning approaches. Guided by the example of the Lotka-Volterra systems presented in Rackauckas et al. [2020], I suggest formulating the model as a system of universal differential equations. Therein, the hormone interactions would be described mechanistically, as it has been established, and the input function, describing the reactivation of the GnRH pulse generator (described with a semi-mechanistic description in Paper C), would be represented as a neural network. A symbolic representation of the input function could be recovered after training the model described above. This recovered input function holds the potential to be biologically interpretable and could contribute to deepening our understanding of the reactivation of the HPG axis.

Bibliography

A. Aderem. Systems biology: Its practice and challenges. Cell, 121(4):511–513, 2005.

M. E. Andersen. Physiological modelling of organic compounds. The Annals of Occupational Hygiene, 35(3):309–321, 1991.

M. d. P. Andres, L. A. Lopes, E. C. Baracat, and S. Podgaec. Dienogest in the treatment of endometriosis: systematic review. Archives of Gynecology and Obstetrics, 292(3): 523–529, 2015.

C. Andrieu, N. De Freitas, A. Doucet, and M. I. Jordan. An introduction to MCMC for machine learning. Machine Learning, 50(1):5–43, 2003.

S. Anwar and A. Anwar. Infertility: A review on causes, treatment and management. Women's Health & Gynecology, 5:2, 2016.

M. Ashyraliyev, Y. Fomekong-Nanfack, J. A. Kaandorp, and J. G. Blom. Systems biology: parameter estimation for biochemical models. The FEBS Journal, 276(4): 886–902, 2009.

H. E. Assmus, R. Herwig, K.-H. Cho, and O. Wolkenhauer. Dynamics of biological systems: role of systems biology in medical research. Expert Review of Molecular Diagnostics, 6(6):891–902, 2006.

R. C. Aster, B. Borchers, and C. H. Thurber. Parameter Estimation and Inverse Problems. Elsevier, 2018.

Avicenna Alliance. in silico clinical trials: How computer simulation will transform the biomedical industry. URL `https://avicenna-alliance.com/files/user_upload/PDF/Avicenna_Roadmap.pdf`. [Accessed: 14.12.2022].

D. Ayers and P. J. Day. Systems medicine: the application of systems biology approaches for modern medical research and drug development. Molecular Biology International, 2015, 2015.

A. R. Baerwald, G. P. Adams, and R. A. Pierson. Characterization of Ovarian Follicular Wave Dynamics in Women. Biology of Reproduction, 69(3):1023–1031, 2003a.

A. R. Baerwald, G. P. Adams, and R. A. Pierson. A new model for ovarian follicular development during the human menstrual cycle. Fertility and Sterility, 80(1):116–122, 2003b.

L. Bahaidarah, E. Hung, A. F. D. M. Oliveira, J. Penumaka, L. Rosario, and A. Trisovic. Toward reusable science with readable code and reproducibility. 2022 IEEE 18th International Conference on e-Science (e-Science), pages 437–439, 2022.

R. E. Baker, J.-M. Pena, J. Jayamohan, and A. Jérusalem. Mechanistic models versus machine learning, a fight worth fighting for the biological community? Biology Letters, 14(5):20170660, 2018.

J. R. Banga. Optimization in computational systems biology. BMC systems biology, 2 (1):1–7, 2008.

N. Barnes. Publish your computer code: it is good enough. Nature, 467(7317):753–753, 2010.

M. J. Bayarri and J. O. Berger. The interplay of bayesian and frequentist analysis. Statistical Science, 19(1):58–80, 2004.

P. Belchetz, T. Plant, Y. Nakai, E. Keogh, and E. Knobil. Hypophysial responses to continuous and intermittent delivery of hypothalamic gonadotropin-releasing hormone. Science, 202(4368):631–633, 1978.

N. Bellofiore, F. Cousins, P. Temple-Smith, H. Dickinson, and J. Evans. A missing piece: the spiny mouse and the puzzle of menstruating species. Journal of Molecular Endocrinology, 61(1):R25–R41, 2018.

S. P. Bliss, A. M. Navratil, J. Xie, and M. S. Roberson. GnRH signaling, the gonadotrope and endocrine control of fertility. Frontiers in Neuroendocrinology, 31(3):322–340, 2010.

D. D. Breimer and M. Danhof. Relevance of the application of pharmacokinetic-pharmacodynamic modelling concepts in drug development. Clinical Pharmacokinetics, 32(4):259–267, 1997.

I. S. Bruserud, M. Roelants, N. H. B. Oehme, A. Madsen, G. E. Eide, R. Bjerknes, K. Rosendahl, and P. B. Juliusson. References for Ultrasound Staging of Breast Maturation, Tanner Breast Staging, Pubic Hair, and Menarche in Norwegian Girls. The Journal of Clinical Endocrinology & Metabolism, 105(5):1599–1607, 2020.

N. C. Buffet, C. Djakoure, S. C. Maitre, and P. Bouchard. Regulation of the Human Menstrual Cycle. Frontiers in Neuroendocrinology, 19(3):151–186, 1998.

S. E. Bulun, D. Monsavais, M. E. Pavone, M. Dyson, Q. Xue, E. Attar, H. Tokunaga, and E. J. Su. Role of Estrogen Receptor-β in Endometriosis. Reproductive Medicine, 30(01):39–45, 2012.

L. R. Campbell, A. L. Scalise, B. T. DiBenedictis, and S. Mahalingaiah. Menstrual cycle length and modern living: a review. Current Opinion in Endocrinology, Diabetes, and obesity, 28(6):566, 2021.

Y. Cao and W. J. Jusko. Applications of minimal physiologically-based pharmacokinetic models. Journal of Pharmacokinetics and Pharmacodynamics, 39(6):711–723, 2012.

L. J. Carlson and N. D. Shaw. Development of Ovulatory Menstrual Cycles in Adolescent Girls. Journal of Pediatric and Adolescent Gynecology, 32(3):249–253, 2019.

S. A. Carson and A. N. Kallen. Diagnosis and Management of Infertility: A Review. JAMA, 326(1):65–76, 2021.

J. Cartier, J. Rudolph, and J. Stewart. The Nature and Structure of Scientific Models. Working Paper. Education Resources Information Center, 2001.

E. Chantalat, M.-C. Valera, C. Vaysse, E. Noirrit, M. Rusidze, A. Weyl, K. Vergriete, E. Buscail, P. Lluel, C. Fontaine, et al. Estrogen Receptors and Endometriosis. International Journal of Molecular Sciences, 21(8):2815, 2020.

C. Chapron, L. Marcellin, B. Borghese, and P. Santulli. Rethinking mechanisms, diagnosis and management of endometriosis. Nature Reviews Endocrinology, 15(11): 666–682, 2019.

M. Chavez-MacGregor, C. H. Van Gils, Y. T. Van Der Schouw, E. Monninkhof, P. A. Van Noord, and P. H. Peeters. Lifetime cumulative number of menstrual cycles and serum sex hormone levels in postmenopausal women. Breast Cancer Research and Treatment, 108(1):101–112, 2008.

A. Chavez-Ross, S. Franks, H. Mason, K. Hardy, and J. Stark. Modelling the control of ovulation and polycystic ovary syndrome. Journal of Mathematical Biology, 36(1): 95–118, 1997.

K.-H. Cho and O. Wolkenhauer. Analysis and modelling of signal transduction pathways in systems biology. Biochemical Society Transactions, 31(6):1503–1506, 2003.

K.-M. Chow, M.-C. Cheung, and I. K. Cheung. Psychosocial interventions for infertile couples: a critical review. Journal of Clinical Nursing, 25(15-16):2101–2113, 2016.

A. Christensen, G. Bentley, R. Cabrera, H. H. Ortega, N. Perfito, T. Wu, and P. Micevych. Hormonal Regulation of Female Reproduction. Hormone and Metabolic Research, 44(8):587–591, 2012.

L. H. Clark, P. M. Schlosser, and J. F. Selgrade. Multiple stable periodic solutions in a model for hormonal control of the menstrual cycle. Bulletin of Mathematical Biology, 65(1):157–173, 2003.

F. Clément. Optimal control of the cell dynamics in the granulosa of ovulatory follicles. Mathematical Biosciences, 152(2):123–142, 1998.

F. Clément, F. Robin, and R. Yvinec. Stochastic nonlinear model for somatic cell population dynamics during ovarian follicle activation. Journal of Mathematical Biology, 82(3):1–52, 2021.

T. Cole, H. Pan, and G. Butler. A mixed effects model to estimate timing and intensity of pubertal growth from height and secondary sexual characteristics. Annals of Human Biology, 41(1):76–83, 2014.

P. Crosignani, D. Olive, A. Bergqvist, and A. Luciano. Advances in the management of endometriosis: an update for clinicians. Human Reproduction Update, 12(2):179–189, 2006.

K. Csilléry, M. G. Blum, O. E. Gaggiotti, and O. François. Approximate Bayesian computation (ABC) in practice. Trends in Ecology & Evolution, 25(7):410–418, 2010.

M. Cvijovic, J. Almquist, J. Hagmar, S. Hohmann, H.-M. Kaltenbach, E. Klipp, M. Krantz, P. Mendes, S. Nelander, J. Nielsen, et al. Bridging the gaps in systems biology. Molecular Genetics and Genomics, 289(5):727–734, 2014.

A. C. Daly, D. Gavaghan, J. Cooper, and S. Tavener. Inference-based assessment of parameter identifiability in nonlinear biological models. Journal of The Royal Society Interface, 15(144):20180318, 2018.

M. Danhof, J. de Jongh, E. De Lange, O. Della Pasqua, B. A. Ploeger, and R. A. Voskuyl. Mechanism-Based Pharmacokinetic-Pharmacodynamic Modeling: Biophase Distribution, Receptor Theory, and Dynamical Systems Analysis. Annual Review of Pharmacology and Toxicology, 47:21–21, 2007.

V. De Leo, M. Musacchio, V. Cappelli, M. Massaro, G. Morgante, and F. Petraglia. Genetic, hormonal and metabolic aspects of pcos: an update. Reproductive Biology and Endocrinology, 14(1):1–17, 2016.

R. Deswal, V. Narwal, A. Dang, and C. S. Pundir. The Prevalence of Polycystic Ovary Syndrome: A Brief Systematic Review. Journal of Human Reproductive Sciences, 13 (4):261, 2020.

L. Devoto, A. Fuentes, P. Kohen, P. Céspedes, A. Palomino, R. Pommer, A. Muñoz, and J. F. Strauss III. The human corpus luteum: life cycle and function in natural cycles. Fertility and Sterility, 92(3):1067–1079, 2009.

V. G. Eck, W. P. Donders, J. Sturdy, J. Feinberg, T. Delhaas, L. R. Hellevik, and W. Huberts. A guide to uncertainty quantification and sensitivity analysis for cardiovascular applications. International Journal for Numerical mMethods in Biomedical Engineering, 32(8):e02755, 2016.

C. Eckert-Lind, A. S. Busch, J. H. Petersen, F. M. Biro, G. Butler, E. V. Bräuner, and A. Juul. Worldwide Secular Trends in Age at Pubertal Onset Assessed by Breast Development Among Girls: A Systematic Review and Meta-analysis. JAMA Pediatrics, 174(4):e195881–e195881, 2020.

Editors at Nature Computational Science. But is the code (re)usable? Nature Computational Science, 449, 2021.

R. Ehrig, T. Dierkes, S. Schäfer, S. Röblitz, E. Tronci, T. Mancini, I. Salvo, V. Alimguzhin, F. Mari, I. Melatti, et al. An integrative approach for model driven computation of treatments in reproductive medicine. BIOMAT 2015: International Symposium on Mathematical and Computational Biology, pages 67–88, 2016.

P. T. Ellison, M. W. Reiches, H. Shattuck-Faegre, A. Breakey, M. Konecna, S. Urlacher, and V. Wobber. Puberty as a life history transition. Annals of Human Biology, 39 (5):352–360, 2012.

D. Emera, R. Romero, and G. Wagner. The evolution of menstruation: A new model for genetic assimilation. BioEssays, 34(1):26–35, 2012.

J. M. Epstein. Why model? Journal of Artificial Societies and Social Simulation, 11(4): 12, 2008.

A. Etz. Introduction to the Concept of Likelihood and Its Applications. Advances in Methods and Practices in Psychological Science, 1(1):60–69, 2018.

A. Etz and J. Vandekerckhove. Introduction to Bayesian Inference for Psychology. Psychonomic Bulletin & Review, 25(1):5–34, 2018.

J. L. H. Evers. Female subfertility. The Lancet, 360(9327):151–159, 2002.

A. Fabregat, S. Jupe, L. Matthews, K. Sidiropoulos, M. Gillespie, P. Garapati, R. Haw, B. Jassal, F. Korninger, B. May, et al. The reactome pathway knowledgebase. Nucleic Acids Research, 46(D1):D649–D655, 2018.

M. Faddy and R. Gosden. Ovary and ovulation: a model conforming the decline in follicle numbers to the age of menopause in women. Human Reproduction, 11(7): 1484–1486, 1996.

M. Faddy, R. Gosden, A. Gougeon, S. J. Richardson, and J. Nelson. Accelerated disappearance of ovarian follicles in mid-life: implications for forecasting menopause. Human Reproduction, 7(10):1342–1346, 1992.

B. Fauser. Step-down follicle-stimulating hormone regimens in polycystic ovary syndrome. Excerpta Medica International Congress Series, 1046(1):153–153, 1994.

B. Fauser and A. M. van Heusden. Manipulation of Human Ovarian Function: Physiological Concepts and Clinical Consequences. Endocrine Reviews, 18(1):71–106, 1997.

J. Fehr, J. Heiland, C. Himpe, and J. Saak. Best Practices for Replicability, Reproducibility and Reusability of Computer-Based Experiments Exemplified by Model Reduction Software. AIMS Mathematics, 1(3):261–281, 2016.

J. Fieberg and K. J. Jenkins. Assessing uncertainty in ecological systems using global sensitivity analyses: a case example of simulated wolf reintroduction effects on elk. Ecological Modelling, 187(2-3):259–280, 2005.

S. Fischer, R. Ehrig, S. Schäfer, E. Tronci, T. Mancini, M. Egli, F. Ille, T. H. Krüger, B. Leeners, and S. Röblitz. Mathematical Modeling and Simulation Provides Evidence for New Strategies of Ovarian Stimulation. Frontiers in Endocrinology, 12:613048, 2021.

S. Fischer-Holzhausen and S. Röblitz. Mathematical modelling of follicular growth and ovarian stimulation. Current Opinion in Endocrine and Metabolic Research, page 100385, 2022a.

S. Fischer-Holzhausen and S. Röblitz. Mathematical modelling of follicular growth and ovarian stimulation. Current Opinion in Endocrine and Metabolic Research, 26: 100385, 2022b.

R. A. Fisher. On the mathematical foundations of theoretical statistics. Philosophical transactions of the Royal Society of London. Series A, containing papers of a mathematical or physical character, 222(594-604):309–368, 1922.

A. S. Frank, K. Larripa, H. Ryu, R. G. Snodgrass, and S. Röblitz. Bifurcation and sensitivity analysis reveal key drivers of multistability in a model of macrophage polarization. Journal of Theoretical Biology, 509:110511, 2021.

B. L. A. Gavina, A. Aurelio, M. S. Olufsen, S. Lenhart, and J. T. Ottesen. Toward an optimal contraception dosing strategy. bioRxiv, 486926, 2022.

O. Ginther, M. Beg, D. Bergfelt, F. Donadeu, and K. Kot. Follicle Selection in Monovular Species. Biology of Reproduction, 65(3):638–647, 2001.

A. L. Greil, K. Slauson-Blevins, and J. McQuillan. The experience of infertility: a review of recent literature. Sociology of Health & Illness, 32(1):140–162, 2010.

J. A. Grieger and R. J. Norman. Menstrual Cycle Length and Patterns in a Global Cohort of Women Using a Mobile Phone App: Retrospective Cohort Study. Journal of Medical Internet Research, 22(6):e17109, 2020.

J. H. Guillaume, J. D. Jakeman, S. Marsili-Libelli, M. Asher, P. Brunner, B. Croke, M. C. Hill, A. J. Jakeman, K. J. Keesman, S. Razavi, et al. Introductory overview of identifiability analysis: A guide to evaluating whether you have the right type of data for your modeling purpose. Environmental Modelling & Software, 119:418–432, 2019.

J. Gunawardena. Models in biology:'accurate descriptions of our pathetic thinking'. BMC Biology, 12(1):1–11, 2014.

M. Hackenberg, P. Harms, M. Pfaffenlehner, A. Pechmann, J. Kirschner, T. Schmidt, and H. Binder. Deep dynamic modeling with just two time points: Can we still allow for individual trajectories? Biometrical Journal, 64:1426–1445, 2022.

D. J. Haisenleder, A. C. Dalkin, G. A. Ortolano, J. C. Marshall, and M. A. Shupnik. A Pulsatile Gonadotropin-Releasing Hormone Stimulus is Required to Increase Transcription of the Gonadotropin Subunit Genes: Evidence for Differential Regulation of Transcription by Pulse Frequency In Vivo. Endocrinology, 128(1):509–517, 1991.

L. A. Harris. Differential equation models for the hormonal regulation of the menstrual cycle. PhD thesis, North Carolina State University, 2002.

L. A. Harris and J. F. Selgrade. Modeling endocrine regulation of the menstrual cycle using delay differential equations. Mathematical Biosciences, 257:11–22, 2014.

J. F. Hastings, Y. E. O'Donnell, D. Fey, and D. R. Croucher. Applications of personalised signalling network models in precision oncology. Pharmacology & Therapeutics, 212: 107555, 2020.

W. K. Hastings. Monte Carlo sampling methods using Markov chains and their applications. Biometrika, 57(1):97–109, 1970.

S. M. Hawkins and M. M. Matzuk. The Menstrual Cycle: Basic Biology. Annals of the New York Academy of Sciences, 1135(1):10–18, 2008.

A. E. Herbison. The Gonadotropin-Releasing Hormone Pulse Generator. Endocrinology, 159(11):3723–3736, 2018.

S. Hiller-Sturmhöfel and A. Bartke. The Endocrine System: n overview. Alcohol Health and Research World, 22(3):153, 1998.

K. E. Hines, T. R. Middendorf, and R. W. Aldrich. Determination of parameter identifiability in nonlinear biophysical models: A Bayesian approach. Journal of General Physiology, 143(3):401–416, 2014.

T. T. T. Ho, M. T. Le, Q. V. Truong, V. Q. H. Nguyen, and N. T. Cao. Psychological Burden in Couples with Infertility and Its Association with Sexual Dysfunction. Sexuality and Disability, 38(1):123–133, 2020.

F. O. Hoffman and J. S. Hammonds. Propagation of Uncertainty in Uisk Assessments: The Need to Distinguish Between Uncertainty Due to Lack of Knowledge and Uncertainty Due to Variability. Risk Analysis, 14(5):707–712, 1994.

T. Homma and A. Saltelli. Importance measures in global sensitivity analysis of nonlinear models. Reliability Engineering & System Safety, 52(1):1–17, 1996.

L. Hood. Systems Biology and P4 Medicine: Past, Present, and Future. Rambam Maimonides Medical Journal, 4(2), 2013.

L. T. Hoyt and A. M. Falconi. Puberty and perimenopause: Reproductive transitions and their implications for women's health. Social Science & Medicine, 132:103–112, 2015.

InSilicoTrials. URL `https://insilicotrials.com/all-products/`. [Accessed 31.01.2023].

H. N. Jabbour, R. W. Kelly, H. M. Fraser, and H. O. Critchley. Endocrine Regulation of Menstruation. Endocrine Reviews, 27(1):17–46, 2006.

P. R. Jackson, J. Juliano, A. Hawkins-Daarud, R. C. Rockne, and K. R. Swanson. Patient-Specific Mathematical Neuro-Oncology: Using a Simple Proliferation and Invasion Tumor Model to Inform Clinical Practice. Bulletin of Mathematical Biology, 77(5):846–856, 2015.

K. Jaqaman and G. Danuser. Linking data to models: data regression. Nature Reviews Molecular Cell Biology, 7(11):813–819, 2006.

H. Jones and K. Rowland-Yeo. Basic Concepts in Physiologically Based Pharmacokinetic Modeling in Drug Discovery and Development. CPT: Pharmacometrics & Systems Pharmacology, 2(8):1–12, 2013.

S. K. Kalra, S. Ratcliffe, C. R. Gracia1, L. Martino, C. Coutifaris, and K. T. Barnhart. Randomized controlled pilot trial of luteal phase recombinant fsh stimulation in poor responders. Reproductive BioMedicine Online, 17(6):745–750, 2008.

H.-M. Kaltenbach, S. Dimopoulos, and J. Stelling. Systems analysis of cellular networks under uncertainty. FEBS Letters, 583(24):3923–3930, 2009.

M. Kanehisa and S. Goto. KEGG: Kyoto Encyclopedia of Genes and Genomes. Nucleic Acids Research, 28(1):27–30, 2000.

M. A. Karimzadeh, S. Ahmadi, H. Oskouian, and E. Rahmani. Comparison of mild stimulation and conventional stimulation in ART outcome. Archives of Gynecology and Obstetrics, 281(4):741–746, 2010.

P. Kirk, T. Thorne, and M. P. Stumpf. Model selection in systems and synthetic biology. Current Opinion in Biotechnology, 24(4):767–774, 2013.

H. Kitano. Computational systems biology. Nature, 420(6912):206–210, 2002a.

H. Kitano. Systems Biology: A Brief Overview. Science, 295(5560):1662–1664, 2002b.

E. Klipp, R. Herwig, A. Kowald, C. Wierling, and H. Lehrach. Systems biology in practice: concepts, implementation and application. John Wiley & Sons, 2005.

E. Klipp, W. Liebermeister, C. Wierling, and A. Kowald. Systems Biology: A Textbook. John Wiley & Sons, 2016.

P. Kohl and D. Noble. Systems biology and the virtual physiological human, 2009.

P. Kohl, E. J. Crampin, T. Quinn, and D. Noble. Systems Biology: An Approach. Clinical Pharmacology & Therapeutics, 88(1):25–33, 2010.

S. C. Kramer and H. W. Sorenson. Bayesian parameter estimation. IEEE Transactions on Automatic Control, 33(2):217–222, 1988.

C. Kreutz, A. Raue, and J. Timmer. Likelihood based observability analysis and confidence intervals for predictions of dynamic models. BMC Systems Biology, 6(1):1–9, 2012.

C. Kreutz, A. Raue, D. Kaschek, and J. Timmer. Profile likelihood in systems biology. The FEBS Journal, 280(11):2564–2571, 2013.

Y. Kuang, Q. Chen, Q. Hong, Q. Lyu, A. Ai, Y. Fu, and Z. Shoham. Double stimulations during the follicular and luteal phases of poor responders in IVF/ICSI programmes (Shanghai protocol). Reproductive Biomedicine Online, 29(6):684–691, 2014a.

Y. Kuang, Q. Hong, Q. Chen, Q. Lyu, A. Ai, Y. Fu, and Z. Shoham. Luteal-phase ovarian stimulation is feasible for producing competent oocytes in women undergoing in vitro fertilization/intracytoplasmic sperm injection treatment, with optimal pregnancy outcomes in frozen-thawed embryo transfer cycles. Fertility and Sterility, 101 (1):105–111, 2014b.

L. Kuepfer, C. Niederalt, T. Wendl, J.-F. Schlender, S. Willmann, J. Lippert, M. Block, T. Eissing, and D. Teutonico. Applied Concepts in PBPK Modeling: How to Build a PBPK/PD Model. CPT: Pharmacometrics & Systems Pharmacology, 5(10):516–531, 2016.

P. Kumar, S. F. Sait, A. Sharma, and M. Kumar. Ovarian hyperstimulation syndrome. Journal of Human Reproductive Sciences, 4(2):70, 2011.

J. Kwapień and S. Drożdż. Physical approach to complex systems. Physics Reports, 515 (3-4):115–226, 2012.

H. Lacker. Regulation of ovulation number in mammals. a follicle interaction law that controls maturation. Biophysical Journal, 35(2):433–454, 1981.

N. Lam, P. Docherty, and R. Murray. Practical identifiability of parametrised models: A review of benefits and limitations of various approaches. Mathematics and Computers in Simulation, 2022.

A. Lange, R. Schwieger, J. Plöntzke, S. Schäfer, and S. Röblitz. Follicular competition in cows: the selection of dominant follicles as a synergistic effect. Journal of Mathematical Biology, 78(3):579–606, 2019.

A. A. R. Lay, A. Pereira, and M. L. G. Miguel. Association between obesity with pattern and length of menstrual cycle: The role of metabolic and hormonal markers. European Journal of Obstetrics & Gynecology and Reproductive Biology, 260:225–231, 2021.

Y. Lazebnik. Can a biologist fix a radio? – Or, what I learned while studying apoptosis. Cancer Cell, 2(3):179–182, 2002.

N. Le Novere, B. Bornstein, A. Broicher, M. Courtot, M. Donizelli, H. Dharuri, L. Li, H. Sauro, M. Schilstra, B. Shapiro, et al. BioModels Database: a free, centralized

database of curated, published, quantitative kinetic models of biochemical and cellular systems. Nucleic Acids Research, 34(suppl_1):D689–D691, 2006.

G. Lebedeva, A. Sorokin, D. Faratian, P. Mullen, A. Goltsov, S. P. Langdon, D. J. Harrison, and I. Goryanin. Model-based global sensitivity analysis as applied to identification of anti-cancer drug targets and biomarkers of drug resistance in the ErbB2/3 network. European Journal of Pharmaceutical Sciences, 46(4):244–258, 2012.

S. R. Lele. How Should We Quantify Uncertainty in Statistical Inference? Frontiers in Ecology and Evolution, 8:35, 2020.

G. Leng and D. J. MacGregor. Mathematical Modelling in Neuroendocrinology. Journal of Neuroendocrinology, 20(6):713–718, 2008.

J. Liepe, P. Kirk, S. Filippi, T. Toni, C. P. Barnes, and M. P. Stumpf. A framework for parameter estimation and model selection from experimental data in systems biology using approximate Bayesian computation. Nature Protocols, 9(2):439–456, 2014.

J. Lippert, M. Brosch, O. Von Kampen, M. Meyer, H.-U. Siegmund, C. Schafmayer, T. Becker, B. Laffert, L. Görlitz, S. Schreiber, et al. A Mechanistic, Model-Based Approach to Safety Assessment in Clinical Development. CPT: Pharmacometrics & Systems Pharmacology, 1(11):1–8, 2012.

J. C. Lipscomb, S. Haddad, T. Poet, and K. Krishnan. Physiologically-Based Pharmacokinetic (PBPK) Models in Toxicity Testing and Risk Assessment. New Technologies for Toxicity Testing, pages 76–95, 2012.

N. S. Macklon and B. C. Fauser. Follicle-Stimulating Hormone and Advanced Follicle Development in the Human. Archives of Medical Research, 32(6):595–600, 2001.

N. S. Macklon, R. L. Stouffer, L. C. Giudice, and B. C. Fauser. The Science behind 25 years of Ovarian Stimulation for *in Vitro* Fertilization. Endocrine Reviews, 27(2): 170–207, 2006.

M. Madhavan and S. Mustafa. Systems biology – the transformative approach to integrate sciences across disciplines. Physical Sciences Reviews, 2022.

C. Maier, C. Loos, and J. Hasenauer. Robust parameter estimation for dynamical systems from outlier-corrupted data. Bioinformatics, 33(5):718–725, 2017.

C. Maier, J. de Wiljes, N. Hartung, C. Kloft, and W. Huisinga. A continued learning approach for model-informed precision dosing: Updating models in clinical practice. CPT: Pharmacometrics & Systems Pharmacology, 11(2):185–198, 2022.

T. Maiwald, H. Hass, B. Steiert, J. Vanlier, R. Engesser, A. Raue, F. Kipkeew, H. H. Bock, D. Kaschek, C. Kreutz, et al. Driving the Model to Its Limit: Profile Likelihood Based Model Reduction. PLoS ONE, 11(9):e0162366, 2016.

M. M. Maleckar, L. Myklebust, J. Uv, P. M. Florvaag, V. Strøm, C. Glinge, R. Jabbari, N. Vejlstrup, T. Engstrøm, K. Ahtarovski, et al. Combined *In-silico* and Machine Learning Approaches Toward Predicting Arrhythmic Risk in Post-infarction Patients. Frontiers in Physiology, 12:1745349, 2021.

R. S. Malik-Sheriff, M. Glont, T. V. N. Nguyen, K. Tiwari, M. G. Roberts, A. Xavier, M. T. Vu, J. Men, M. Maire, S. Kananathan, E. L. Fairbanks, J. P. Meyer, C. Arankalle, T. M. Varusai, V. Knight-Schrijver, L. Li, C. Dueñas-Roca, G. Dass, S. M. Keating, Y. M. Park, N. Buso, N. Rodriguez, M. Hucka, and H. Hermjakob. BioModels — 15 years of sharing computational models in life science. Nucleic Acids Research, 48(D1):D407–D415, 2020.

A. Malina and J. A. Pooley. Psychological consequences of IVF fertilization–Review of research. Annals of Agricultural and Environmental Medicine, 24(4):554–558, 2017.

T. Mancini, F. Mari, A. Massini, I. Melatti, I. Salvo, S. Sinisi, E. Tronci, R. Ehrig, S. Röblitz, and B. Leeners. Computing Personalised Treatments through In Silico Clinical Trials. A Case Study on Downregulation in Assisted Reproduction. Intelligenza Artificiale, pages 1–16, 2018.

P. Marques, T. Madeira, and A. Gama. Menstrual cycle among adolescents: girls' awareness and influence of age at menarche and overweight. Revista Paulista de Pediatria, 40, 2022.

R. Merkle, B. Steiert, F. Salopiata, S. Depner, A. Raue, N. Iwamoto, M. Schelker, H. Hass, M. Wäsch, M. E. Böhm, et al. Identification of Cell Type-Specific Differences in Erythropoietin Receptor Signaling in Primary Erythroid and Lung Cancer Cells. PLoS Computational Biology, 12(8):e1005049, 2016.

N. Metropolis, A. W. Rosenbluth, M. N. Rosenbluth, A. H. Teller, and E. Teller. Equation of State Calculations by Fast Computing Machines. The Journal of Chemical Physics, 21(6):1087–1092, 1953.

M. Mitchell. Complex systems: Network thinking. Artificial intelligence, 170(18):1194–1212, 2006.

M. Mitchell. Complexity: A guided tour. Oxford university press, 2009.

E. D. Mitra and W. S. Hlavacek. Parameter estimation and uncertainty quantification for systems biology models. Current Opinion in Systems Biology, 18:9–18, 2019.

C. G. Moles, P. Mendes, and J. R. Banga. Parameter Estimation in Biochemical Pathways: A Comparison of Global Optimization Methods. Genome Research, 13(11): 2467–2474, 2003.

J. Morio. Global and local sensitivity analysis methods for a physical system. European Journal of Physics, 32(6):1577, 2011.

S. A. Murphy and A. W. Van der Vaart. On Profile Likelihood. Journal of the American Statistical Association, 95(450):449–465, 2000.

I. J. Myung. Tutorial on maximum likelihood estimation. Journal of Mathematical Psychology, 47(1):90–100, 2003.

M. Nagae, Y. Uenoyama, S. Okamoto, H. Tsuchida, K. Ikegami, T. Goto, S. Majarune, S. Nakamura, M. Sanbo, M. Hirabayashi, et al. Direct evidence that KNDy neurons maintain gonadotropin pulses and folliculogenesis as the GnRH pulse generator. Proceedings of the National Academy of Sciences, 118(5):e2009156118, 2021.

National Health Service. Periods and fertility in the menstrual cycle, Jan 2023. URL `https://www.nhs.uk/conditions/periods/fertility-in-the-menstrual-cycle/`. [Accessed 14.01.2023].

I. Nestorov. Whole Body Pharmacokinetic Models. Clinical Pharmacokinetics, 42(10): 883–908, 2003.

R. A. Nowak. Estrous and menstrual cycles. Encyclopedia of Reproduction, Elsevier, 2018.

A. E. Oakley, D. K. Clifton, and R. A. Steiner. Kisspeptin Signaling in the Brain. Endocrine Reviews, 30(6):713–743, 2009.

S. R. Ojeda, A. Lomniczi, C. Mastronardi, S. Heger, C. Roth, A.-S. Parent, V. Matagne, and A. E. Mungenast. Minireview: The Neuroendocrine Regulation of Puberty: Is the Time Ripe for a Systems Biology Approach? Endocrinology, 147(3):1166–1174, 2006.

M. A. O'Malley and J. Dupré. Fundamental issues in systems biology. BioEssays, 27 (12):1270–1276, 2005.

M. Omari, A. Lange, J. Plöntzke, and S. Röblitz. Model-based exploration of the impact of glucose metabolism on the estrous cycle dynamics in dairy cows. Biology Direct, 15(1):1–22, 2020.

E. Otten. Inverse and forward dynamics: models of multi–body systems. Philosophical Transactions of the Royal Society of London. Series B: Biological Sciences, 358(1437): 1493–1500, 2003.

PAEON. Model driven computation of treatments for infertility related endocrinological diseases, April 2017. URL https://cordis.europa.eu/project/id/600773. [Accessed: 2022-12-14].

R. K. Pedersen, M. Andersen, T. A. Knudsen, V. Skov, L. Kjær, H. C. Hasselbalch, and J. T. Ottesen. Dose-dependent mathematical modeling of interferon-α-treatment for personalized treatment of myeloproliferative neoplasms. Computational and Systems Oncology, 1(4):e1030, 2021.

B. Pinyerd and W. B. Zipf. Puberty – Timing Is Everything! Journal of Pediatric Nursing, 20(2):75–82, 2005.

J. Platt. Eis & Mint Diagnostics develop ground-breaking new hormone monitoring technology, Aug 2020. URL https://eis2win.co.uk/article/eis-mint-diagnostics-develop-ground-breaking-new-hormone-monitoring\-technology/. [Accessed 20.12.2022].

C. Pohl and E. Knobil. The role of the central nervous system in the control of ovarian function in higher primates. Annual Review of Physiology, 44(1):583–593, 1982.

N. Polyzos and S. Sunkara. Sub-optimal responders following controlled ovarian stimulation: an overlooked group? Human Reproduction, 30(9):2005–2008, 2015.

J. C. Prior. Women's reproductive system as balanced estradiol and progesterone actions – a revolutionary, paradigm-shifting concept in women's health. Drug Discovery Today: Disease Models, 32:31–40, 2020.

J. K. Pritchard, M. T. Seielstad, A. Perez-Lezaun, and M. W. Feldman. Population growth of human Y chromosomes: a study of Y chromosome microsatellites. Molecular Biology and Evolution, 16(12):1791–1798, 1999.

G. Qian and A. Mahdi. Sensitivity analysis methods in the biomedical sciences. Mathematical Biosciences, 323:108306, 2020.

C. Rackauckas, Y. Ma, J. Martensen, C. Warner, K. Zubov, R. Supekar, D. Skinner, A. Ramadhan, and A. Edelman. Universal differential equations for scientific machine learning. arXiv, 2001.04385, 2020.

K. Rateitschak, F. Winter, F. Lange, R. Jaster, and O. Wolkenhauer. Parameter Identifiability and Sensitivity Analysis Predict Targets for Enhancement of STAT1 Activity in

Pancreatic Cancer and Stellate Cells. PLoS Computational Biology, 8(12):e1002815, 2012.

A. Raue, C. Kreutz, T. Maiwald, J. Bachmann, M. Schilling, U. Klingmüller, and J. Timmer. Structural and practical identifiability analysis of partially observed dynamical models by exploiting the profile likelihood. Bioinformatics, 25(15):1923–1929, 2009.

A. Raue, C. Kreutz, F. J. Theis, and J. Timmer. Joining forces of Bayesian and frequentist methodology: a study for inference in the presence of non-identifiability. Philosophical Transactions of the Royal Society A: Mathematical, Physical and Engineering Sciences, 371(1984):20110544, 2013a.

A. Raue, M. Schilling, J. Bachmann, A. Matteson, M. Schelke, D. Kaschek, S. Hug, C. Kreutz, B. D. Harms, F. J. Theis, et al. Lessons learned from quantitative dynamical modeling in systems biology. PloS one, 8(9):e74335, 2013b.

B. G. Reed and B. R. Carr. The Normal Menstrual Cycle and the Control of Ovulation. Endotext. South Dartmouth: MDText.com, 2015.

I. Reinecke. Mathematical Modeling and Simulation of the Female Menstrual Cycle. PhD thesis, Freie Universität Berlin, 2009.

I. Reinecke and P. Deuflhard. A complex mathematical model of the human menstrual cycle. Journal of Theoretical Biology, 247(2):303–330, 2007.

J. S. Richards, S. A. Pangas, et al. The ovary: basic biology and clinical implications. The Journal of Clinical Investigation, 120(4):963–972, 2010.

M. Riggs, M. Bennetts, P. Van Der Graaf, and S. Martin. Integrated Pharmacometrics and Systems Pharmacology Model-Based Analyses to Guide GnRH Receptor Modulator Development for Management of Endometriosis. CPT: Pharmacometrics & Systems Pharmacology, 1(10):1–9, 2012.

G. Rivero and J. K. Chen. Best coding practices to ensure reproducibility. 2020.

S. Röblitz, C. Stötzel, P. Deuflhard, H. M. Jones, D.-O. Azulay, P. H. van der Graaf, and S. W. Martin. A mathematical model of the human menstrual cycle for the administration of GnRH analogues. Journal of Theoretical Biology, 321:8–27, 2013.

L. Rombauts, Anne-MariaSuikkari, V. MacLachlan, A. O. Trounson, and D. L. Healy. Recruitment of Follicles by Recombinant Human Follicle-Stimulating Hormone Commencing in the Luteal Phase of the Ovarian Cycle. Fertility and Sterility, 69(4): 665–669, 1998.

A. Saltelli, S. Tarantola, and F. Campolongo. Sensitivity Analysis as an Ingredient of Modelling. Statistical Science, 15(4):377–395, 2000.

A. Saltelli, P. Annoni, I. Azzini, F. Campolongo, M. Ratto, and S. Tarantola. Variance based sensitivity analysis of model output. design and estimator for the total sensitivity index. Computer Physics Communications, 181(2):259–270, 2010.

M. Santillán. On the use of the Hill Functions in Mathematical Models of Gene Regulatory Networks. Mathematical Modelling of Natural Phenomena, 3(2):85–97, 2008.

J. Schaber, W. Liebermeister, and E. Klipp. Nested uncertainties in biochemical models. IET Systems Biology, 3(1):1–9, 2009.

I. Schipper, W. C. Hop, and B. C. Fauser. The Follicle-Stimulating Hormone (FSH) Threshold/Window Concept Examined by Different Interventions with Exogenous FSH during the Follicular Phase of the Normal Menstrual Cycle: Duration, Rather Than Magnitude, of FSH Increase Affects Follicle Development. The Journal of Clinical Endocrinology & Metabolism, 83(4):1292–1298, 1998.

K. Schittkowski. Numerical Data Fitting in Dynamical Systems: A Practical Introduction with Applications and Software, volume 77. Springer Science & Business Media, 2002.

P. M. Schlosser and J. F. Selgrade. A model of gonadotropin regulation during the menstrual cycle in women: Qualitative features. Environmental Health Perspectives, pages 873–881, 2000.

L. Schmiester, D. Weindl, and J. Hasenauer. Parameterization of mechanistic models from qualitative data using an efficient optimal scaling approach. Journal of Mathematical Biology, 81(2):603–623, 2020.

S. Schnell. Ten Simple Rules for a Computational Biologist's Laboratory Notebook. PLoS Computational Biology, 11(9):e1004385, 2015.

B. Schoeberl, C. Eichler-Jonsson, E. D. Gilles, and G. Müller. Computational modeling of the dynamics of the MAP kinase cascade activated by surface and internalized EGF receptors. Nature Biotechnology, 20(4):370–375, 2002.

J. F. Selgrade and P. M. Schlosser. A model for the production of ovarian hormones during the menstrual cycle. Fields Institute Communications, 21:429–446, 1999.

M. Shilo, A. Mayo, and U. Alon. A Mechanism for Ovulation Number Control. Frontiers in Endocrinology, 13, 2022.

I. Siekmann, J. Sneyd, and E. J. Crampin. MCMC Can Detect Nonidentifiable Models. Biophysical Journal, 103(11):2275–2286, 2012.

G. Sighinolfi, V. Grisendi, and A. La Marca. How to personalize ovarian stimulation in clinical practice. Journal of the Turkish German Gynecological Association, 18(3): 148, 2017.

G. Sighinolfi, S. K. Sunkara, and A. La Marca. New strategies of ovarian stimulation based on the concept of ovarian follicular waves: from conventional to random and double stimulation. Reproductive Biomedicine Online, 37(4):489–497, 2018.

S. Sinisi, V. Alimguzhin, T. Mancini, E. Tronci, and B. Leeners. Complete populations of virtual patients for in silico clinical trials. Bioinformatics, 36(22-23):5465–5472, 2020a.

S. Sinisi, V. Alimguzhin, T. Mancini, E. Tronci, F. Mari, and B. Leeners. Optimal Personalised Treatment Computation Through In Silico Clinical Trials on Patient Digital Twins. Fundamenta Informaticae, 174(3-4):283–310, 2020b.

S. W. Smye and R. H. Clayton. Mathematical modelling for the new millenium: medicine by numbers. Medical Engineering & Physics, 24(9):565–574, 2002.

Springer Nature. Guidelines for authors submitting code & software. URL `https://www.nature.com/documents/GuidelinesCodePublication.pdf`. [Accessed 23.01.2023].

D. R. Stanski, J. Ham, R. D. Miller, and L. B. Sheiner. Pharmacokinetics and Pharmacodynamics of d-Tubocurarine during Nitrous Oxide-Narcotic and Halothane Anesthesia in Man. The Journal of the American Society of Anesthesiologists, 51(3):235–241, 1979.

C. Stocco, C. Telleria, and G. Gibori. The Molecular Control of Corpus Luteum Formation, Function, and Regression. Endocrine Reviews, 28(1):117–149, 2007.

S. H. Strogatz. Nonlinear Dynamics and Chaos: With Applications to Physics, Biology, Chemistry, and Engineering. CRC Press, 2018.

T. Sumner, E. Shephard, and I. Bogle. A methodology for global-sensitivity analysis of time-dependent outputs in systems biology modelling. Journal of The Royal Society Interface, 9(74):2156–2166, 2012.

J. Sun, J. M. Garibaldi, and C. Hodgman. Parameter Estimation Using Metaheuristics in Systems Biology: A Comprehensive Review. IEEE/ACM Transactions on Computational Biology and Bioinformatics, 9(1):185–202, 2011.

A. Tarantola. Popper, Bayes and the inverse problem. Nature Physics, 2(8):492–494, 2006.

N. Tayebi, Z. Yazdanpanahi, S. Yektatalab, S. Pourahmad, and M. Akbarzadeh. The Relationship Between Body Mass Index (BMI) and Menstrual Disorders at Different Ages of Menarche and Sex Hormones. Journal of the National Medical Association, 110(5):440–447, 2018.

E. Terasawa. The mechanism underlying the pubertal increase in pulsatile gnrh release in primates. Journal of Neuroendocrinology, page e13119, 2022.

J. Tesarik and R. Mendoza-Tesarik. Patient-tailored reproductive health care. Frontiers in Reproductive Health, 4, 2022.

I. R. Thompson and U. B. Kaiser. GnRH pulse frequency-dependent differential regulation of LH and FSH gene expression. Molecular and Cellular Endocrinology, 385(1-2): 28–35, 2014.

T. Toni, D. Welch, N. Strelkowa, A. Ipsen, and M. P. Stumpf. Approximate Bayesian computation scheme for parameter inference and model selection in dynamical systems. Journal of the Royal Society Interface, 6(31):187–202, 2009.

C. Tönsing, J. Timmer, and C. Kreutz. Profile likelihood-based analyses of infectious disease models. Statistical Methods in Medical Research, 27(7):1979–1998, 2018.

M. Tosin, A. Côrtes, and A. Cunha. A Tutorial on Sobol' Global Sensitivity Analysis Applied to Biological Models. Networks in Systems Biology, pages 93–118, 2020.

A. Trisovic, M. K. Lau, T. Pasquier, and M. Crosas. A large-scale study on research code quality and execution. Scientific Data, 9(1):1–16, 2022.

T. Turányi. Sensitivity analysis of complex kinetic systems. Tools and applications. Journal of Mathematical Chemistry, 5(3):203–248, 1990.

Y. Uenoyama, N. Inoue, S. Nakamura, and H. Tsukamura. Central Mechanism Controlling Pubertal Onset in Mammals: A Triggering Role of Kisspeptin. Frontiers in Endocrinology, 10:312, 2019.

A. Ulloa-Aguirre and C. Timossi. Biochemical and functional aspects of gonadotrophin-releasing hormone and gonadotrophins. Reproductive BioMedicine Online, 1(2):48–62, 2000.

D. Unuane, H. Tournaye, B. Velkeniers, and K. Poppe. Endocrine disorders & female infertility. Best Practice & Research Clinical Endocrinology & Metabolism, 25(6): 861–873, 2011.

R. N. Upton, D. J. Foster, and A. Y. Abuhelwa. An introduction to physiologically-based pharmacokinetic models. Pediatric Anesthesia, 26(11):1036–1046, 2016.

A. Vaiarelli, D. Cimadomo, E. Trabucco, R. Vallefuoco, L. Buffo, L. Dusi, F. Fiorini, N. Barnocchi, F. M. Bulletti, L. Rienzi, and F. M. Ubaldi. Double stimulation in the same Ovarian cycle (DuoStim) to Maximize the Number of Oocytes retrieved From Poor Prognosis Patients: A Multicenter experience and SWOT Analysis. Frontiers in Endocrinology, 9:317, 2018.

C. van der Horst and J. Gillman. The menstrual cycle in elephantulus. South African Medical Journal, 6:27–42, 1941.

N. A. van Riel. Dynamic modelling and analysis of biochemical networks: mechanism-based models and model-based experiments. Briefings in Bioinformatics, 7(4):364–374, 2006.

D. Venzon and S. Moolgavkar. A Method for Computing Profile-Likelihood-Based Confidence Intervals. Journal of the Royal Statistical Society. Series C: Applied Statistics, 37(1):87–94, 1988.

C. M. Verhaak, J. Smeenk, A. a. Evers, J. A. Kremer, F. W. Kraaimaat, and D. Braat. Women's emotional adjustment to IVF: a systematic review of 25 years of research. Human Reproduction Update, 13(1):27–36, 2007.

A. F. Villaverde, E. Raimúndez, J. Hasenauer, and J. R. Banga. A comparison of methods for quantifying prediction uncertainty in systems biology. IFAC-PapersOnLine, 52(26): 45–51, 2019.

A. F. Villaverde, D. Pathirana, F. Fröhlich, J. Hasenauer, and J. R. Banga. A protocol for dynamic model calibration. Briefings in bioinformatics, 23(1):bbab387, 2022a.

A. F. Villaverde, E. Raimúndez, J. Hasenauer, and J. R. Banga. Assessment of Prediction Uncertainty Quantification Methods in Systems Biology. IEEE/ACM Transactions on Computational Biology and Bioinformatics, 2022b.

M. Voliotis, X. F. Li, R. De Burgh, G. Lass, S. L. Lightman, K. T. O'Byrne, and K. Tsaneva-Atanasova. Mathematical modelling elucidates core mechanisms underpinning GnRH pulse generation. bioRxiv, 245548, 2018.

V. Volodina and P. Challenor. The importance of uncertainty quantification in model reproducibility. Philosophical Transactions of the Royal Society. Series A: Mathematical, Physical and Engineering Science, 379(2197):20200071, 2021.

J. J. Wade, V. MacLachlan, and G. Kovacs. The success rate of IVF has significantly improved over the last decade. Australian and New Zealand Journal of Obstetrics and Gynaecology, 55(5):473–476, 2015.

J. G. Whelan III and N. F. Vlahos. The ovarian hyperstimulation syndrome. Fertility and Sterility, 73(5):883–896, 2000.

F.-G. Wieland, A. L. Hauber, M. Rosenblatt, C. Tönsing, and J. Timmer. On structural and practical identifiability. Current Opinion in Systems Biology, 25:60–69, 2021.

C. Wierling, T. Kessler, L. A. Ogilvie, B. M. Lange, M.-L. Yaspo, and H. Lehrach. Network and systems biology: essential steps in virtualising drug discovery and development. Drug Discovery Today: Technologies, 15:33–40, 2015.

D. J. Wilkinson. Bayesian methods in bioinformatics and computational systems biology. Briefings in Bioinformatics, 8(2):109–116, 2007.

O. Wolkenhauer. Why model? Frontiers in Physiology, 5:21, 2014.

O. Wolkenhauer and M. Mesarović. Feedback dynamics and cell function: Why systems biology is called systems biology. Molecular BioSystems, 1(1):14–16, 2005.

World Health Organization. Infertility, 2022. URL `https://www.who.int/health-topics/infertility#tab=tab_1`. [Accessed 04.02.2022].

A. A. Wright, G. N. Fayad, J. F. Selgrade, and M. S. Olufsen. Mechanistic model of hormonal contraception. PLoS Computational Biology, 16(6):e1007848, 2020.

Y. Yin and L. Ma. Development of the Mammalian Female Reproductive Tract. Journal of Biochemistry, 137(6):677–683, 2005.

H. Yue, M. Brown, J. Knowles, H. Wang, D. S. Broomhead, and D. B. Kell. Insights into the behaviour of systems biology models from dynamic sensitivity and identifiability analysis: a case study of an NF-κB signalling pathway. Molecular BioSystems, 2(12): 640–649, 2006.

E. Zavala, K. C. Wedgwood, M. Voliotis, J. Tabak, F. Spiga, S. L. Lightman, and K. Tsaneva-Atanasova. Mathematical Modelling of Endocrine Systems. Trends in Endocrinology & Metabolism, 30(4):244–257, 2019.

N. Zech, M. Zech, S. Baldauf, G. Comploj, M. Murtinger, D. Spitzer, L. Hradeckỳ, R. Ajayi, M. Schuff, and H. Zech. Ovarian stimulation in ART - Unwinding pressing issues. Minerva Ginecologica, 67(2):127–147, 2015.

X.-Y. Zhang, M. N. Trame, L. J. Lesko, and S. Schmidt. Sobol Sensitivity Analysis: A Tool to Guide the Development and Evaluation of Systems Pharmacology Models. CPT: Pharmacometrics & Systems Pharmacology, 4(2):69–79, 2015.

X. Zhu and Y. Fu. Evaluation of Ovarian Stimulation Initiated From the Late Follicular Phase Using Human Menopausal Gonadotropin Alone in Normal-Ovulatory Women for Treatment of Infertility: A Retrospective Cohort Study. Frontiers in Endocrinology, 10:448, 2019.

Part II

Scientific articles

Paper A

Hormonal regulation of ovarian follicle growth in humans: Model-based exploration of cycle variability and parameter sensitivities

Sophie Fischer-Holzhausen and Susanna Röblitz

Journal of Theoretical Biology (2022): 111150

Journal of Theoretical Biology 547 (2022) 111150

Contents lists available at ScienceDirect

Journal of Theoretical Biology

journal homepage: www.elsevier.com/locate/yjtbi

Hormonal regulation of ovarian follicle growth in humans: Model-based exploration of cycle variability and parameter sensitivities

Sophie Fischer-Holzhausen *, Susanna Röblitz

Computational Biology Unit, Department of Informatics, University of Bergen, Bergen, Norway

ARTICLE INFO

Article history:
Received 17 December 2021
Revised 23 March 2022
Accepted 28 April 2022
Available online 11 May 2022

Keywords:
HPG axis
Reproductive hormones
Mathematical modelling
Stochastic dynamical system

ABSTRACT

We present a modelling and simulation framework for the dynamics of ovarian follicles and key hormones along the hypothalamic-pituitary–gonadal axis throughout consecutive human menstrual cycles. All simulation results (hormone concentrations and ovarian follicle sizes) are in biological units and can easily be compared to clinical data. The model takes into account variability in follicles' response to stimulating hormones, which introduces variability between cycles. The growth of ovarian follicles in waves is an emergent property in our model simulations and further supports the hypothesis that follicular waves are also present in humans. We use Approximate Bayesian Computation and cluster analysis to construct a population of virtual subjects and to study parameter distributions and sensitivities. The model can be used to compare and optimize treatment protocols for ovarian hyperstimulation, thus potentially forming the integral part of a clinical decision support system in reproductive endocrinology.

1. Introduction

The interplay between the hypothalamus, the pituitary gland and the gonadal glands regulates and maintains the menstrual cycle. Gonadotropin-releasing hormone (GnRH) is responsible for the release of the two gonadotropins: follicle stimulating hormone (FSH) and luteinizing hormone (LH) from the pituitary gland. Gonadotropins have feedback actions on folliculogenesis, meaning the maturation of the ovarian follicle, and thereby the production of ovarian hormones. In turn, ovarian hormones such as estradiol (E2) and progesterone (P4) affect LH and FSH release both directly and indirectly via GnRH signalling (Speroff and Fritz, 2005).

In this work, we present a nonlinear differential–algebraic system of equations (DAEs) to model the time-evolution of these five key hormones and the growth dynamics of ovarian follicles. The mechanistic model adopts the interplay of these five hormones from previously published models of the menstrual cycle (Clark et al., 2003; Reinecke and Deuflhard, 2007; Röblitz et al., 2013). As a novelty, our model connects the hormone dynamics to the time evolution of the diameter of ovarian follicles. Since the unit of the follicular diameter is given in units of millimeter, our simulation results can be compared to ultrasound measurements. Every emerging follicle is described by an ordinary differential equation (ODE) with follicle specific parameters. The work of Lange et al. (2019) inspired the mathematical formulation of the follicular growth. The coupling of the follicle model to a hormone dynamics model makes it possible to perform in silico studies of the interplay between sex hormones and follicular growth behaviour during normal menstrual cycles, as well as under ovarian hyperstimulation treatment conditions (Fischer et al., 2021).

In a series of articles Schlosser, Selgrade, and Harris-Clark introduced a mathematical model of the hormone control system (Selgrade, 2001; Clark et al., 2003). Their model combines pituitary hormone dynamics of LH and FSH with the dynamics of the ovarian hormones P4, E2, and inhibin. Reinecke and Deuflhard (2007) expanded and modified the model from Clark et al. (2003). Major changes were the incorporation of a GnRH pulse generator responsible for the release of GnRH, equations for the GnRH concentration, receptor binding mechanisms and addition of further feedback interactions to LH, FSH, and ovarian hormone dynamics. Röblitz et al. (2013) added further mechanistic details and re-parameterized the model from Reinecke and Deuflhard (2007) in order to simulate treatments with GnRH analogues. Mathematical models and numerical simulations have proven themselves useful to get a better understanding of various aspects of the menstrual cycle, for example to study the polycystic ovary syndrome (PCOS) (Chavez-Ross et al., 1997), to create virtual patient cohorts for in silico clinical trials (Sinisi et al., 2020; Sinisi et al., 2020), or to simulate ovarian stimulation protocols (Reinecke and Deuflhard, 2007; Fischer et al., 2021).

* Corresponding author at: Institute of Informatics, University of Bergen, Bergen, Norway.
E-mail address: sophie.fischer@uib.no (S. Fischer-Holzhausen).

https://doi.org/10.1016/j.jtbi.2022.111150
0022-5193/

Ovarian hormone dynamics and the growth behaviour of ovarian follicles are closely associated. Their interactions are crucial to enable female fertility. The literature contains different approaches for modelling follicle growth. The work by Selgrade (2001) and Clark et al. (2003) used the description of follicular masses in discrete stages to simulate folliculogenesis. As a result, the discrete number of active follicles is unknown in the model. Another approach focused on the cellular activity of theca and granulosa cells (Clément et al., 1997). Both cell types play an essential role in ovarian hormone production. The authors in Reinecke and Deuflhard (2007) proposed combining the first two approaches by describing a granulosa- and a theca-cell mass instead of a follicluar mass, thereby focusing on the location of ovarian hormone production. An entirely different approach is modeling the dynamics of single follicles instead of follicular or cellular masses (Lacker and Akin, 1988; Chavez-Ross et al., 1997; Lange et al., 2019). The simulation of individual follicles allows for the comparison to ultrasound measurements (Lange et al., 2019) and for observing pathological behaviour such as PCOS (Chavez-Ross et al., 1997).

In this paper, we combine the approaches from Röblitz et al. (2013) and Lange et al. (2019) into a model that couples hormone dynamics with the growth dynamics of individual follicles. Compared to already existing approaches, our model is the first model that can be used to simulate both hormone concentrations and follicle sizes throughout consecutive menstrual cycles, with or without ovarian stimulation treatment. The two key questions we want to answer with our model are the following. Does follicular competition combined with hormone dynamics result in follicular waves? Are there single parameters that are particularly sensitive for cycle length, follicular count, or abnormal hormone profiles? In this paper, we address these two questions by running simulations and by combining a search in parameter space with model-checking techniques for parameter space exploration. The model is evaluated quantitatively by using hormone profile data. Its predictive power has been tested previously in Fischer et al. (2021), where we showcased the use of the coupled model to perform a simulation based study of ovarian hyper-stimulation protocols. In the following, we introduce this modelling and simulation framework for the menstrual cycle in more detail.

2. Model construction and biological background

The flowchart in Fig. 1 gives an abstract representation of the interaction network governing the menstrual cycle. The hypothalamus releases GnRH in a pulse fashion. GnRH stimulates the synthesis and release of pituitary hormones LH and FSH (Marshall and Griffin, 1993). In the ovaries, LH and FSH regulate folliculogenesis. Each growing follicle faces one of two fates: either apoptosis or becoming the dominant follicle, which releases its egg cell during ovulation. The remaining parts of the dominant follicle transform into the corpus luteum. Follicles are recruited in cohorts and the majority of recruited follicles undergo apoptosis (Fortune, 1994). Growing follicles are the main source of E2, while the corpus luteum produces both E2 and P4. Through the blood stream, E2 and P4 arrive at the hypothalamus and the pituitary gland, where their feedback interactions modulate the GnRH, LH and FSH dynamics. This process results in quasi-periodic hormone profiles with a cycle length of 25 to 35 days (Bakos et al., 1994; Harlow, 2000; Bull et al., 2019). However, the average cycle length shows a high variability between women and is age-dependent. One cycle consists of two characteristic phases: the follicular phase and the luteal phase. The ovulation of one follicle, in rare events also multiple follicles, separates the two phases. The timing of ovulation mainly determines the cycle length. Therefore, the observed fluctuations in the length of the follicular phase are larger than those in the luteal phase (Bull et al., 2019).

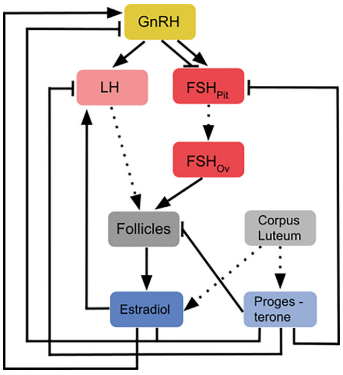

Fig. 1. Flowchart of key mechanisms of the menstrual cycle. Solid lines indicated feedback interactions encoded in the model. Positive feedback is encoded by arrows and negative feedback is presented by bars. Dotted lines represent the following other types of interactions: FSH release from the pituitary to the blood, the LH concentration dependent ovulation of dominant follicles, and the production of E2 and P4 by the corpus luteum. Reading the figure from top to bottom, the endocrine signalling that runs the menstrual cycle can be summed up as follows. GnRH stimulates LH. FSH is both stimulated and inhibited by GnRH. LH and FSH effect follicular maturation. Growing follicles produce E2, which stimulates the release of LH. A sufficiently high LH concentration triggers the ovulation of a follicle which then transitions into the corpus luteum. The simultaneous release of E2 and P4 by the corpus luteum inhibits the release of GnRH. Additionally, P4 has an inhibitory effect on LH and FSH. E2 stimulates or inhibits GnRH concentration dependent on the E2 concentration.

Our model is formulated as a semi-explicit differential–algebraic system of the form:

$$\begin{aligned} \tfrac{dx}{dt} &= f(t, x(t,\theta), y(t,\theta)) \\ 0 &= g(t, x(t,\theta), y(t,\theta)), \end{aligned} \tag{1}$$

with a pair of state variables $(x(t,\theta), y(t,\theta))$ depending on the time t and parameters θ. The dynamics of $x(t,\theta)$ are described by ODEs, whereas the dynamics of $y(t,\theta)$ are described by algebraic equations.

Since feedback interactions are often unknown or too complex to be modeled in detail, Hill functions are a common tool to describe feedback interactions in a qualitative manner. Stimulatory functions (H^+) and inhibitory functions (H^-) are given by the following equations:

$$\begin{aligned} H^+\left(S_i, T_i^j, n_i^j\right) &= \frac{\left(S_i/T_i^j\right)^{n_i^j}}{1+\left(S_i/T_i^j\right)^{n_i^j}} \\ H^-\left(S_i, T_i^j, n_i^j\right) &= \frac{1}{1+\left(S_i/T_i^j\right)^{n_i^j}}. \end{aligned} \tag{2}$$

When the regulator species S_i approaches a threshold $T_i^j > 0$, it regulates species S_j. The Hill exponent $n_i^j > 0$ influences the rapidity of the regulatory process. A menstrual cycle includes both fast and slow processes. This is reflected by different exponents in the Hill functions, that is by a different steepness of the sigmoidal response curves. If the Hill exponent is high enough, the qualitative response changes rapidly within a small range of values in the independent variable, whereas for low Hill exponents ($n < 2$) the Hill function effectively behaves closer to a Michaelis–Menten type response.

Parameters and their units are given in the list of parameters in Appendix A.1. Hill thresholds and other parameters were explored

with the ABC method (Section 3), whereas the Hill exponents were adopted from previous models. Units for hormone concentrations are adopted from clinical data to enable the comparison between experimental data and simulation results. The time scale of reaction rates is 'per day'. Characteristics of the simulation results such as cycle length are on a time scale of four weeks. The model is initiated in the early follicular phase of the menstrual cycle. This phase is characterized by low concentrations of all four hormones. The initial conditions are chosen accordingly (available from the code in the GitHub repository).

Our model of the menstrual cycle can be divided into two parts. The first part describes the hormone dynamics in the hypothalamus and the pituitary. These equations are mainly based on the work of Röblitz et al. (2013) and partially overlap with other previously published models (Clark et al., 2003; Reinecke and Deuflhard, 2007; Lange et al., 2019). The second part covers follicular growth (Lange et al., 2019) and ovarian hormone dynamics. Both parts are connected through feedback interactions, which closes the loop.

2.1. Hypothalamus and pituitary model

GnRH is released from the hypothalamus in a pulse pattern (Carmel et al., 1976; Knobil et al., 1980; Martin et al., 1998). To account for pulsatile release, a release frequency, $freq(t)$, and amount of released GnRH, $mass(t)$, are included in the equation for the GnRH concentration, $G(t)$:

$$freq(t) = f_0 \cdot H^-\left(P4(t), T_{P4}^{freq}, n_{P4}^{freq}\right) \cdot \left(1 + H^+\left(E2(t), T_{E2}^{freq}, n_{E2}^{freq}\right)\right) \tag{3}$$

$$mass(t) = m_0 \cdot \left(H^+\left(E2(t), T_{E2}^{mass,1}, n_{E2}^{mass,1}\right) + H^-\left(E2(t), T_{E2}^{mass,2}, n_{E2}^{mass,2}\right)\right) \tag{4}$$

$$\frac{d}{dt}G(t) = mass(t) \cdot freq(t) - k_{on}^{G} \cdot G(t) \cdot R_{G,a}(t) + k_{off}^{G} \cdot GR_a(t) - k_{degr}^{G} \cdot G(t). \tag{5}$$

Hereby, f_0 is the basal frequency and m_0 the basal mass. Both are modulated by Hill functions due to the feedback actions of steroids. While P4 only has an inhibitory effect on GnRH dynamics, E2 can exhibit both positive and negative feedback actions (Nakai et al., 1978). During the luteal phase, E2 and P4 cooperatively inhibit the GnRH frequency (Goodman et al., 1981). During the period leading up to the preovulatory LH surge, E2 suppresses GnRH pulse size and thereby reduces the amount of released GnRH (Evans et al., 1994). Estradiol's feedback action on the GnRH release switches prior to ovulation from negative to positive, and thereby induces a GnRH surge in the late follicular phase (Christian and Moenter, 2010).

GnRH signalling in the pituitary is receptor mediated. The GnRH receptor belongs to the class of G-protein coupled receptors (GPCR). It is important to include the receptor binding mechanism in the model to enable simulation of drug administration. The works by Shankaran et al. (2007) and Riccobene et al. (1999) provide the basis for the receptor binding model used here. Four different receptor states are considered: (i) active GnRH receptors, $R_{G,a}$, with the ability for GnRH binding, (ii) inactive GnRH receptors, $R_{G,i}$, which are not able to bind GnRH, (iii) active GnRH-receptor complexes, GR_a, which mediate downstream feedback actions, and (iv) inactive GnRH-receptor complexes, GR_i. Table 1 lists all processes. The corresponding set of ODEs reads:

Table 1
Summary of all GnRH receptor binding mechanisms that are included in the model equations.

Process	Rate
Binding of GnRH to active GnRH receptors	$k_{on}^{G} \cdot G(t) \cdot R_{G,a}(t)$
Dissociation of active receptor complex	$k_{off}^{G} \cdot GR_a(t)$
Recycling of inactive to active receptors	$k_{recy}^{R_{G,i}} \cdot R_{G,i}(t)$
Deactivation of active to inactive receptors	$k_{inter}^{R_{G,a}} \cdot R_{G,a}(t)$
Synthesis of inactive receptors	$k_{syn}^{R_{G,i}}$
Degradation of inactive receptors	$k_{degr}^{R_{G,i}} \cdot R_{G,i}(t)$
Inactivation of active receptor complex	$k_{inact}^{GR_a} \cdot GR_a(t)$
Activation of inactive receptor complex	$k_{act}^{GR_i} \cdot GR_i(t)$
Degradation of inactive GnRH receptor complexes	$k_{degr}^{GR_i} \cdot GR_i(t)$
Dissociation of inactive receptor complex	$k_{diss}^{GR_i} \cdot GR_i(t)$

$$\frac{d}{dt}R_{G,a}(t) = k_{off}^{G} \cdot GR_a(t) - k_{on}^{G} \cdot G(t) \cdot R_{G,a}(t) - k_{inter}^{R_{G,a}} \cdot R_{G,a}(t) + k_{recy}^{R_{G,i}} R_{G,i} \tag{6}$$

$$\frac{d}{dt}R_{G,i}(t) = k_{diss}^{GR_i} \cdot GR_i(t) + k_{inter}^{R_{G,a}} \cdot R_{G,a}(t) - k_{recy}^{R_{G,i}} \cdot R_{G,i}(t) + k_{syn}^{R_{G,i}} - k_{degr}^{R_{G,i}} \cdot R_{G,i}(t) \tag{7}$$

$$\frac{d}{dt}GR_a(t) = k_{on}^{G} \cdot G(t) \cdot R_{G,a}(t) - k_{off}^{G} \cdot GR_a(t) - k_{inact}^{GR_a} \cdot GR_a(t) + k_{act}^{GR_i} \cdot GR_i(t) \tag{8}$$

$$\frac{d}{dt}GR_i(t) = k_{inact}^{GR_a} \cdot GR_a(t) - k_{act}^{GR_i} \cdot GR_i(t) - k_{degr}^{GR_i} \cdot GR_i(t) - k_{diss}^{GR_i} \cdot GR_i(t) \tag{9}$$

As suggested by Schlosser and Selgrade (2000), equations for LH and FSH are based on synthesis–release–clearance relationships. The basal LH-synthesis rate, b_{syn}^{LH}, is stimulated by E2 and the active GnRH-receptor complex and inhibited by P4. Eqs. (12) and (13) account for the release of LH from the pituitary into the blood stream and the related volume change. LH is cleared from the blood with a clearance rate constant k_{cl}^{LH}. LH dynamics are formulated as follows:

$$Syn_{LH}(t) = \frac{b_{syn}^{LH} + k_{E2}^{LH} \cdot H^+\left(E2(t), T_{E2}^{LH}, n_{E2}^{LH}\right)}{1 + k_{P4}^{LH} \cdot \left(\frac{P4(t)}{T_{P4}^{LH}}\right)^{n_{P4}^{LH}}} \cdot \left(1 + H^-\left(freq(t), T_{freq}^{LH}, n_{freq}^{LH}\right)\right) \tag{10}$$

$$Rel_{LH}(t) = \left(b_{rel}^{LH} + k_{GR_a}^{LH} \cdot H^+\left(GR_a(t), T_{GR_a}^{LH}, n_{GR_a}^{LH}\right)\right) \cdot LH_{Pit}(t) \tag{11}$$

$$\frac{d}{dt}LH_{Pit}(t) = Syn_{LH}(t) - Rel_{LH}(t) \tag{12}$$

$$\frac{d}{dt}LH_{Blood}(t) = \frac{1}{V_{Blood}} \cdot Rel_{LH}(t) - k_{cl}^{LH} \cdot LH_{Blood}(t). \tag{13}$$

FSH in the pituitary, FSH_{Pit}, has a synthesis rate constant b_{syn}^{FSH}, which is inhibited by P4 and high GnRH frequencies (Marshall and Griffin, 1993). The release of FSH from the pituitary, $Rel_{FSH}(t)$, is stimulated by the active GnRH receptor complex, $GR_a(t)$ and inhibited by the amount of E2 (Shaw et al., 2010). The transition between compartments with different sizes (pituitary to blood, blood to ovaries) is related to a change in concentration, which is included in the equations through different compartment volumes. In the ovaries, FSH

binds its receptor located at the follicles' surfaces with the binding rate $k_{on}^{FSH} \cdot R_{FSH}(t) \cdot FSH_{Ov}(t)$. FSH is cleared from the blood with clearance rate constant $k_{cl_{Blood}}^{FSH}$ and the ovaries with clearance rate constant $k_{cl_{Ov}}^{FSH}$. The ODEs describing the FSH concentrations in the system read:

$$Syn_{FSH}(t) = \frac{b_{syn}^{FSH}}{1 + \left(\frac{P4(t)}{T_{P4}^{FSH}}\right)^{n_{P4}^{FSH}}} \cdot H^{-}\left(freq, T_{freq}^{FSH}, n_{freq}^{FSH}\right) \tag{14}$$

$$Rel_{FSH}(t) = \left(b_{rel}^{FSH} + k_{GR_a}^{FSH} \cdot H^{+}\left(GR_a(t), T_{GR_a}^{FSH}, n_{GR_a}^{FSH}\right) \cdot H^{-}\left(E2(t), T_{E2}^{FSH}, n_{E2}^{FSH}\right)\right) \cdot FSH_{Pit}(t) \tag{15}$$

$$\frac{d}{dt}FSH_{Pit}(t) = Syn_{FSH}(t) - Rel_{FSH}(t) \tag{16}$$

$$\frac{d}{dt}FSH_{Blood}(t) = \frac{1}{V_{Blood}} \cdot Rel_{FSH}(t) - \left(k_{Blood}^{FSH} + k_{cl_{Blood}}^{FSH}\right) \cdot FSH_{Blood}(t) \tag{17}$$

$$\frac{d}{dt}FSH_{Ov}(t) = \frac{V_{Blood}}{V_{Ov}} \cdot k_{Blood}^{FSH} \cdot FSH_{Blood}(t) - \left(k_{on}^{FSH} \cdot R_{FSH}(t) - k_{cl_{Ov}}^{FSH_{Ov}}\right) \cdot FSH_{Ov}(t) \tag{18}$$

The dynamics of the FSH receptor on the surface of follicles is modeled as follows: FSH binds to free receptors, R_{FSH}, with a binding rate constant k_{on}^{FSH}, forming a FSH-receptor complex $FSHR$ that dissociates with rate constant k_{dis}^{FSH}. The inactive receptors $R_{FSH,dis}$ get reactivated with rate constant k_{recy}^{FSH}.

$$\frac{d}{dt}R_{FSH}(t) = k_{recy}^{FSH} \cdot R_{FSH,dis}(t) - k_{on}^{FSH} \cdot FSH_{foll}(t) \cdot R_{FSH}(t) \tag{19}$$

$$\frac{d}{dt}FSHR(t) = k_{on}^{FSH} \cdot FSH_{foll}(t) \cdot R_{FSH}(t) - k_{dis}^{FSH} \cdot FSHR(t) \tag{20}$$

$$\frac{d}{dt}R_{FSH,dis}(t) = k_{dis}^{FSH} \cdot FSHR(t) - k_{recy}^{FSH} \cdot R_{FSH,dis}(t). \tag{21}$$

2.2. Ovarian model

The authors in Lange et al. (2019) propose an ODE that describes the growth behaviour of a single follicle. We adjusted the equation and integrated hormone dependencies. Here, the size of each follicle x_i which is recruited during the simulation time, is described as follows:

$$\frac{d}{dt}x_i = H^{+}(FSHR, T_{FSHR}(i), n_{FSHR}) \cdot (\xi - x_i)x_i\left(\gamma - \kappa\left(\sum_j x_j^{\nu} - \mu x_i^{\nu}\right)\right). \tag{22}$$

This equation includes follicle specific parameters as well as parameters which are shared among all follicles. The following five parameters are common for all follicles: (i) maximum size of each follicle, ξ, (ii) growth rate γ, (iii) strength of competition, κ, (iv) fractal dimension ν, and (v) proportion of self-harm μ. μ relates to the role of androgen in follicular maturation and atresia during the late follicular phase. The source of androgen are the follicles themselves, and the inhibitory effect of androgen on follicular maturation appears to be important to ensure mono-ovulation (Hillier and Tetsuka, 1997; Franks and Hardy, 2018). The parameter ν has been fixed to $\nu = 2$ in all simulations, meaning that the strength of competition is proportional to the follicular surface area. The positive Hill term in front of the equation contains a follicle specific threshold, $T_{FSHR}(i)$, which we refer to as FSH sensitivity threshold value. This follicle-specific threshold causes individual growth behaviour. Follicular growth is stimulated if the FSH-receptor complex concentration approaches and exceeds this threshold. This formulation is related to the biological finding that follicle growth does not occur below a certain level of FSH and that follicles respond differently to FSH (Brown, 1978). In our simulation, the threshold values are sampled from a normal distribution. Overall, whether a follicle starts growing depends on various factors, such as the current hormone levels, its FSH sensitivity threshold value, and the number and size of competing follicles.

We model the time points at which follicles are recruited as a Poisson point process with parameter λ being equal to the expected number of follicles that start growing within a time interval of certain length. The Poisson parameter λ is modulated by the FSH concentration because the number of recruited follicles is affected by the FSH level:

$$\lambda = \lambda_0 \cdot \left(1 + s_{FSH}^{Pois} \cdot H^{+}\left(FSH(T), T_{FSH}^{Pois}, n_{FSH}^{Pois}\right)\right)$$

The FSH window concept stresses the importance of elevated FSH levels for the selection of a dominant follicle (Baerwald et al., 2011; Fauser et al., 1997; Adams et al., 1993). The time period during which FSH is above a certain threshold effects the number of follicles reaching the dominant follicle's size (Schipper et al., 1998; Baird, 1990). This concept is incorporated in our model. Coupling κ, which is the parameter addressing the competition for dominance between follicles, to a negative Hill term causes an FSH-dependant decrease in follicular competition.

$$\kappa = \kappa_0 \cdot H^{-}\left(FSH, T_{FSH}^{\kappa}, n_{FSH}^{\kappa}\right). \tag{23}$$

Follicle growth is stimulated by FSH and inhibted by P4 (Baird et al., 1984). Therefore, two Hill functions modulate the growth rate γ:

$$\gamma = \gamma_0 \cdot H^{-}\left(P4, T_{P4}^{\gamma}, n_{P4}^{\gamma}\right) \cdot H^{+}\left(FSHR, T_{FSHR}^{\gamma}, n_{FSHR}^{\gamma}\right). \tag{24}$$

A major source of E2 are growing follicles and the dominant follicle produces the most E2 (Baird and Fraser, 1975; McNatty et al., 1976; Hiller et al., 1981), considered by the model with a size-dependant E2 production. We assume the E2 production by growing follicles to be proportional to the follicular surface term FS,

$$FS = \pi \cdot \sum H^{+}(x_i, T_{FS}, n_{FS}) \cdot (x_i)^2. \tag{25}$$

The positive Hill function with $T_{FS} = 15$ accounts for the fact that larger follicles have a higher contribution to the E2 production. The overall E2 production is the sum of basal production, b_{syn}^{E2}, the E2 production by follicles (first addend in Eq. 26), and the E2 production of the corpus luteum after the ovulation of a dominant follicle (second addend in Eq. 26):

$$E2(t) = b_{syn}^{E2} + s_{FS} \cdot FS + h_{E2} \cdot \exp\left(-w_{E2}(t - (T_{Ovu} + \tau))^2\right) \tag{26}$$

Similarly, P4 is produced by the corpus luteum:

$$P4(t) = b_{syn}^{P4} + h_{P4} \cdot \exp\left(-w_{P4}(t - (T_{Ovu} + \tau))^2\right) \tag{27}$$

The parameters for steroid production during the luteal phase, i.e., peak heights h_{E2}, h_{P4}, and inverse peak width w_{P4}, were estimated by fitting Gaussian curves to the data from 12 healthy patients (Fischer et al., 2021; Röblitz et al., 2013). The peaks' center position $(T_{Ovu} + \tau)$ is set with respect to the last time point of ovulation, T_{ovu}.

Overall, we were able to decrease the number of parameters from 119 (114 parameters in Röblitz et al. (2013) and 5 parameters in Lange et al. (2019)) to 82, mainly by replacing the heuristic description of the follicular growth dynamics used in Röblitz

et al. (2013) by the equation from Lange et al. (2019). A detailed parameter list can be found in Appendix A.1.

2.3. Model simulation

In the presented model, 13 ODEs and 2 algebraic equations describe the hormone dynamics. The number of ODEs describing follicular growth increases with simulation time because a new ODE is created for each follicle that is initialized at a given time point. Moreover, the model exhibits a stochastic behaviour because the initial times of follicles and the FSH sensitivity of follicles follow random processes. This causes variability within a simulation and between simulations.

Prior to the simulation, parameter values and initial conditions are loaded from files and the simulation time interval $[t_b, t_e]$ is set (Algorithm 1). In addition, the entries of an array with follicle-specific FSH sensitivity threshold values, $T_{FSHR}(i)$, are sampled from a normal distribution.

During the simulation, the global simulation time $[t_b, t_e]$ is divided into sequential time intervals $[t, t_n]$, whereby t_n are either the time points at which new follicles emerge or the time points of ovulation. In any case, the simulation has to stop at these intermediate time points. This results in a more complex code structure, which is represented in Algorithm 1.

Algorithm 1: Model simulation

Input: begin time t_b, end time t_e, initial system state $x(t_b), y(t_b)$
Output: system state $x(t_e), y(t_e)$
  Initialize
  $t = t_b, x(t) = x(t_b), y(t) = y(t_b), startNewFollicle = 1$;
  while $t \leqslant t_e$ **do**
    if $startNewFollicle == 1$ **then**
      sample time τ at which the next follicle emerges;
      $t_{nextStart} = t + \tau$;
    end if
    if $t_{nextStart} < t_e$ **then**
      $t_n = t_{nextStart}$;
    else if
      $t_n = t_e$;
    end if
    $tspan = [t, t_n]$;
    $(x(t_f), y(t_f)), t \leqslant t_f \leqslant t_n \leftarrow$ DAE solver with event detection
    if $t_f < t_n$ **then**
    $startNewFollicle = 0$; ▷ovulation occurd in *tspan*
    else if $t_f == t_n$ **then**
      $startNewFollicle = 1$;
      if the right hand side of the ODE for a new follicle is positive **then**
        initiate a new follicle;
      end if
    end if
    update the destinies of all follicles;
  $t = t_f$;
end while

The starting time of a new follicle, $t_{nextStart}$, is determined from an exponential distribution with parameter $1/\lambda$, the inverse Poisson parameter. At each time point $t_{nextStart}$, a new follicle is initialized with size y_0^{foll} and specific FSH sensitivity value $T_{FSHR}(i)$. Then the right hand side of the ODE, which can be interpreted as a growth rate corresponding to this new follicle, is evaluated. A negative right hand side means a decrease in size, i.e., the new follicle cannot start growing under the conditions at this specific time point and is hence rejected. In case of a positive growth rate, the new follicle is added to the list of active follicles and the ODE system is extended by one equation.

The time integration is evaluated by an event function that checks at every time step if an ovulation occurred. An ovulation is detected if the following two criteria are met:

- the largest follicle is at least 18 mm in size
- the value of LH is greater than the threshold parameter $T_{LH} = 25 \frac{mIU}{mL}$

Whenever the integration stops, either because ovulation occurred or because a new follicle is initiated, the destinies of all follicles are updated. For this purpose, the state of maturation for each follicle is evaluated based on the right hand side of the ODE system. Four possible follicular destinies are defined: (i) ovulation, (ii) growth, (iii) decreasing, and (iv) large but no ovulation because of too low LH concentrations.

The simulation output covers time courses of hormone concentrations and follicles' diameters. In addition to that, there is a readout of the number and time points of ovulation and cycle lengths. The model and the simulation algorithm have been implemented in *MATLAB* and are accessible on *GitHub* (https://github.com/SoFiwork/GynCycle_newVersion). Numerical simulations have been performed using the ODE solver *ode15s*.

3. Methods

We used Approximate Bayesian Computation (ABC) with summary statistics to investigate the parameter space. The goal is to find parameters that have narrow value ranges and that can therefore be interpreted as sensitive, and to find parameter clusters.

3.1. Population of models, model checking, and sensitivity analysis

Sensitivity analysis methods help to understand how uncertainty and noise in the model input effect the model output and its ambiguity. Classical sensitivity analysis algorithms evaluate model outputs at specific time points. However, these methods are not applicable to the presented model because of variation in simulation results, such as cycle length and composition of follicular cohorts, prevent the specification of a set of evaluation time points. Alternatively, ABC can be used to study parameter spaces and sensitivities and to estimate parameters. The overall idea of all ABC-based approaches is to bypass the evaluation of a likelihood function by performing high numbers of simulations which are compared to observed data (Toni et al., 2009). Our ABC algorithm is based on the ABC rejection sampler introduced by Pritchard et al. (1999) and consists of the following four steps:

1. A parameter vector $\hat{\theta}$ is sampled from a prior distribution $\pi(\theta)$.
2. Using $\hat{\theta}$ as model parameters, a data set $\widehat{D}$ is generated by simulation.
3. $\widehat{D}$ is evaluated with respect to a set of defined criteria and will either be accepted or rejected.
4. Return to step 1.

We defined two sets of prior distributions: (i) $\pi(\theta)_{Hormones}$ for parameters associated with hormone dynamics, and (ii) $\pi(\theta)_{Follicles}$ for parameters used in the follicular growth equation. Parameters that were used to create the two model populations are marked (*) in the parameter list given in Appendix A.1. In all cases, model parameters were sampled from uni-variate log normal prior distributions with mean $\mu = \theta_0$, where θ_0 denotes the original parameter value (Appendix A.1), and standard deviation $\sigma = 0.15$.

The comparison between simulations is challenging because of the stochastic elements included in the model. The composition of follicle cohorts varies between simulations because the time points of follicle initialization and the follicle-specific sensitivities to FSH are sampled prior to each simulation run. Differences in the follicular cohort composition influence the hormone dynamics and the selection of the dominant follicle. To study the effects of variation in the model parameters on the simulation results, we needed to ensure that the effects we observe are not caused by differences in follicular cohort composition. Therefore, the initialization time points and FSH sensitivity values of the follicles were fixed for all simulations performed for the ABC analysis. However, we still observe variations in cycle length and offset between simulations with different parametrizations. Therefore, a distance function to evaluate the difference between $\widehat{D}$ and D is not applicable. Instead, the following three characteristics (Fig. 2) were assessed as summary statistics for each simulation run and were used for the comparison.

- At least 75% of the FSH profiles of consecutive cycles have to follow a characteristic profile as it is illustrated in Fig. 2.
- The mean cycle length has to be between 21 and 40 days (Rosenfield, 2013 and National Health Service, 2021 state that most cycles are within this range.)
- The variability in cycle length needs to be smaller than 4 days.

The simulation time was set to 300 days, which ensures that about 13 consecutive menstrual cycles can be evaluated (Fig. 2a). The FSH profile of each simulated cycle was evaluated automatically by checking three properties which give the profile its characteristic shape (Fig. 2b):

- decrease of the FSH concentration between 5 and 3 days before ovulation
- increase of the FSH concentration right before ovulation
- decrease of the FSH concentration after ovulation

Each cycle within a simulation run was marked by the ovulation of the dominant follicle. This characteristic time point was used as a reference time point to calculate the average rate of change of the FSH profile within a defined time interval. The cycle length of all menstrual cycles within one simulation was also evaluated automatically by measuring the time difference from one ovulation to the next one (Fig. 2a).

We observed that in simulations with a regular FSH profile, also the remaining hormone profiles are physiologically reasonable.We therefore only analysed FSH profiles for the summary statistics. This observation can certainly be attributed to the fact that the model represents a fully closed feedback loop.

Based on the summary statistics, simulation runs were classified as successful or unsuccessful, whereby successful simulations constitute a virtual patient population. A simulation was classified as successful if all of the above criteria were satisfied. For each parameter we thus obtained one distribution from successful simulations and one distribution from unsuccessful ones. The similarity between these two discrete distributions was evaluated using the Jensen–Shannon divergence, which is a symmetric and smoothed formulation of the Kullback–Leibler divergence (Lin, 1991).

3.2. Parameter clustering

For each of the two model populations, created by variation in either the follicle or the hormone parameters, the parameter spaces of the two subgroups (accepted and rejected simulations) were analysed with the aim to find parameter dependencies and clusters. By comparing the individual parameter distributions of successful and unsuccessful simulations, we explore differences in the parameter ranges between these two groups.

For this purpose, we applied a spectral clustering method, the robust Perron cluster analysis (PCCA+) (Röblitz and Weber, 2013), to a pairwise similarity matrix. The similarity between two parameter vectors i and j, s_{ij}, was derived from the pairwise distance d_{ij} as $s_{ij} = 1 - d_{ij}$, whereby pairwise distances were normalized such that $\max_{i,j} d_{ij} = 1$. For the distance measure d_{ij}, we used a path-based distance measure based on connectedness rather than compactness (Fischer et al., 2001). This criterion captures data sources that are spread out on a low-dimensional manifold which is embedded in a high dimensional data space. The connectedness criterion considers two objects as similar if there exists a mediating path without an edge with large cost, whereby we used the Euclidian distance as cost function. This distance can be computed by solving the minimax path problem (also called bottleneck shortest path problem) on the complete undirected graph, which asks for the path between two points that minimizes the maximum edge capacity. We used the minimax variant of the Floyd-Warshall algorithm to solve this problem.

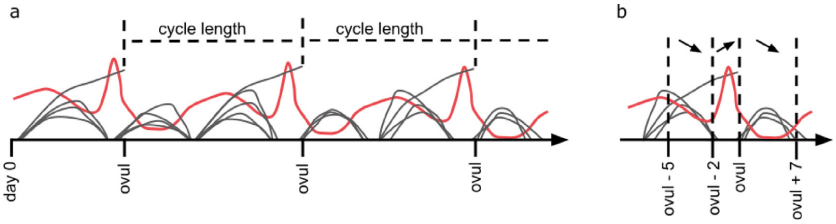

Fig. 2. Sketch of simulation results to illustrate the assessment of summary statistics. Grey lines are individual ovarian follicles. The FSH profile is given in red. Ovulations (ovul) of a dominant follicle are marked by terminating growth trajectories. a) Within each simulation multiple consecutive menstrual cycles are observed. A cycle is defined from one ovulation of a follicle to the next one. b) The shape of each FSH profile is evaluated based on three characteristic slopes: i) a decrease during the late follicular phase (five to two days prior to ovulation), (ii) an increase during the two days before ovulation, and (iii) a decrease during the luteal phase (during seven days after ovulation).

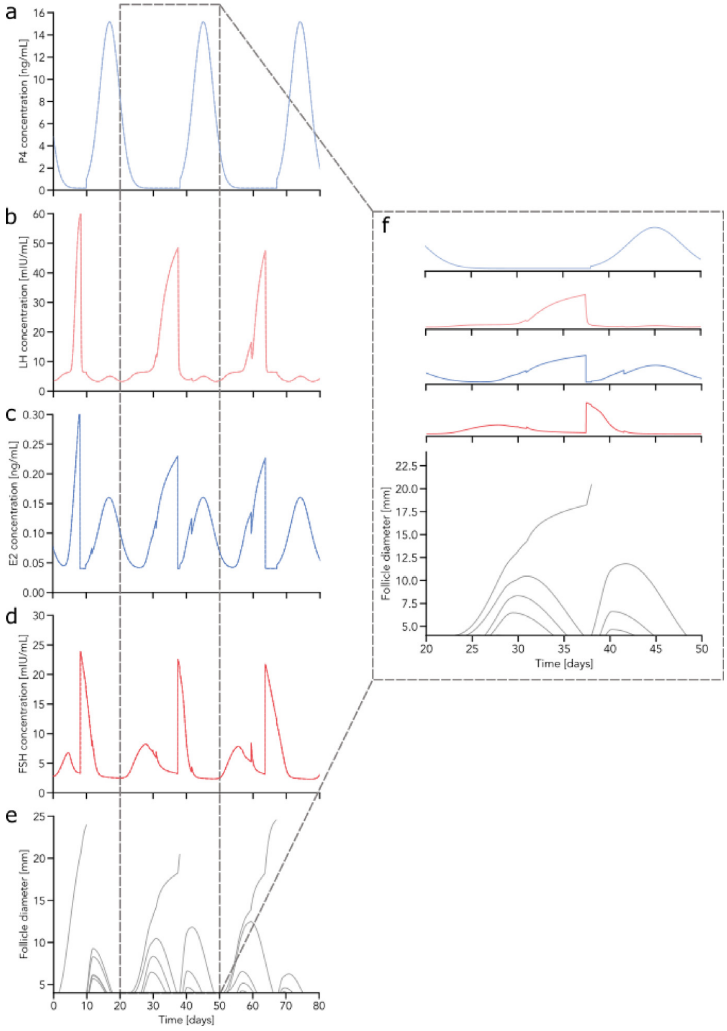

Fig. 3. Example simulation of three consecutive cycles. Panels a-d) show the time-evolution of the four hormones P4, LH, E2, and FSH. Panel e) illustrates the growth trajectories of follicles within this time frame. Panel f) is a zoom into the second cycle represented on the left.

4. Results

4.1. Model simulation

The model enables simulations of consecutive cycles as represented in Fig. 3, which displays simulated follicular growth trajectories (Fig. 3e) and hormone profiles (Fig. 3a-d) of three menstrual cycles originating from the same simulation. The zoom in panel (3f) showcases the interplay between follicular growth and hormone dynamics. Fundamental features of the interaction are apparent. Follicles grow under elevated FSH levels and the peak in LH concentration triggers the ovulation of the largest active follicle. Increased P4 concentrations during the luteal phase prevent the growth of any large follicles.

Furthermore, follicles grow in cohorts/waves consisting of about five follicles. The property that follicles grow in distinct cohorts (one cohort during the follicular phase and one during the luteal phase) is not implemented in the model itself. This emergent behaviour is rather a result of the interplay between hormones and follicles covered by the model. The elevated P4 levels during the luteal phase prevent ovulation. Hence, there is no dominant follicle when the P4 level is high. The ovulation of the dominant follicle, which is visible as a terminated growth trajectory around day 15, is aligned with the LH peak.

Fig. 4 shows the hormone profiles (LH, FSH, E2, and P4) of three consecutive cycles and pooled hormone data for one menstrual cycle from 12 healthy women (data set from Röblitz et al., 2013). The three consecutive cycles originating from one simulation and were overlaid by shifting them along the time axis. All curves are aligned on the day of ovulation. Simulated peak concentrations and concentration ranges agree with the data set. The overall shape of simulated hormone profiles are also comparable to the data. The

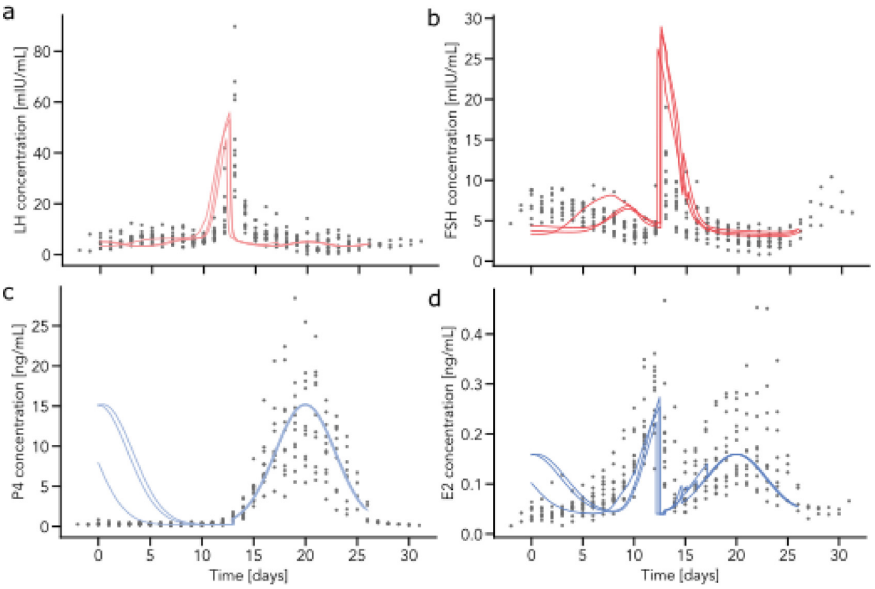

Fig. 4. Comparison of simulated hormone profiles for LH, FSH, P4 and E2 and pooled hormone data from 12 healthy women. Simulated hormone profiles and measurement data are aligned with the ovulation at day 13. Grey dots represent the pooled data set. For each hormone, three consecutive cycles are overlaid.

simulated cycle lengths range from 22.7 to 27.8 days. A detailed overview of the cycle length distribution is presented in Appendix A.2.

However, there are notable discrepancies between the data and the simulation results. The measured FSH profiles show a longer rise of FSH during the follicular phase from day 1 to day 10 (Fig. 4b). The simulated LH peak is shifted to the left compared to the peak in the data (Fig. 4 a). There is also a mismatch between the data and the simulated hormone profile for E2 during the early follicular phase up to day 5 (Fig. 4a).

4.2. Model Analysis

To investigate the parameter space, we created two populations of models, one focusing on hormone dynamics and one focusing on follicular growth behaviour. Each population is composed of 1000 parameter realizations. Follicles were initialized with the same follicle-specific properties (FSH sensitivity and start times) to ensure that variability is not caused by changes in the initial composition of the cohort of follicles. Each simulation was checked automatically according to the shape of the FSH profile, the cycle length and its variability (Fig. 2). A simulation that meets all three criteria was categorized as successful. Since the duration of a cycle is measured from one ovulation to the next one, ovulations of two follicles shorty after each other cause an incorrect cycle length. Hence, successful simulations contain only mono-ovulatory cycles. This bias is negligible, because we rarely observed the ovulation of multiple follicles around mid-cycle in our simulation results.

Figs. 5a) and b) show the numbers of successful and unsuccessful simulations in the two populations of models. For both populations about 1/3 of the parameter realizations give successful simulations. The event plots in Figs. 5c) and d) illustrate the criteria on which 100 randomly selected unsuccessful simulations failed. In all of these 100 simulations, it is the FSH profile that does not satisfy the criteria, whereas in both model populations abnormal cycle length or cycle length variability are less often the reason for failure.

Fig. 5e) shows the distribution for the model parameter μ, which is one of the parameters varied to create the follicle specific model population. The distribution of μ differs between successful simulations (green histogram) and unsuccessful simulations (red histogram), with a Jensen-Shannon divergence of 0.13. For all other parameters striking differences are not present (Figs. A.7 and A.8). Using Pearson correlation, we investigated the relationship between μ and the average cycle length as well as between μ and the variance of the cycle length. A negative linear correlation was found between μ and the average cycle length (Pearson correlation coefficient = -0.71, see Fig. 5f). The analysis was repeated for an alternative follicle initialization, which gave comparable results (A.4).

By applying a clustering method on the multivariate parameter distributions, we aimed at finding parameter clusters to classify simulations. Our hypothesis was that parameters that lead to successful and unsuccessful simulations, respectively, will fall into different clusters. We applied PCCA+, which did not indicate any clusters in the parameter space.

5. Discussion

This work presents and explores a novel mathematical model of the menstrual cycle, which combines hormone dynamics and follicular growth in a mechanistic manner. None of the previously published models allowed for simultaneously simulating hormone dynamics and follicular maturation throughout consecutive menstrual cycles. The applicability of our model in a medical setting is demonstrated in Fischer et al. (2021), which can be considered as a validation for the presented model.

The growth of ovarian follicles in cohorts of about five follicles can be observed as an emerging property in our simulation results. While the growth of ovarian follicles in cohorts is a well-described

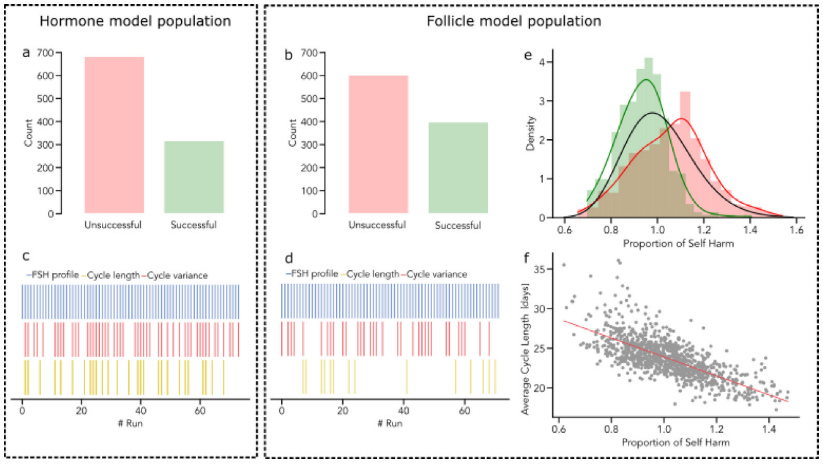

Fig. 5. Summary of the model analysis. The left box sums up results for the population of models that resulted from variation of parameters important for hormone dynamics, whereas the right box shows results for the model population based on variation of follicle parameters. Each population consists of 1000 randomly drawn parameter realizations. Histograms in Figures a) and b) present the count of successful (green) and unsuccessful (red) simulations for each population of models. The event plots in Figures c) and d) illustrate the cause of failure for 100 failed simulations from each population (top/blue: failure due to irregular FSH profile, middle/red: failure due to abnormal cycle length, bottom/yellow: failure due to abnormal cycle length variability). Figure e) shows the distribution of parameter μ, which is the proportion of self harm included in the follicle growth equation. The solid black line shows the prior distribution of μ used for sampling. The green and red distributions are the parameter distributions for successful and unsuccessful simulations, respectively (Jensen-Shannon divergence = 0.13). Figure f) demonstrates the negative linear correlation between μ and the average cycle length (Pearson correlation coefficient = −0.71).

phenomenon in some mono-ovulatory species such as cattle, it counts as hypothesis in human. Our model can be considered as further evidence that follicular waves also occur in human.

Differeences between patients' data and simulation trajectories are visible in Fig. 4. We argue that the difference in cycle length contributes to the mismatches. The simulated average cycle length ranges from 22.7 to 27.8 days (Fig. A.6), which is within the physiological range (Bull et al., 2019). The cycle length is unfortunately not specified in the data set, but we estimated it to be about 28 days. Therefore, simulated cycles can be about five days shorter than in the data set. In line with the literature (Bull et al., 2019), we implemented the model in a way that little variation occurs in the length of the luteal phase. It is therefore the follicular phase that causes variation in cycle length and that is responsible for shorter simulated cycles (compared to the duration of the follicular phase in the patients' data). A shorter follicular phase in the simulations compared to the data explains the shift of the LH peak as well as the shorter period of the FSH rise.

It is also important to note that neither the parameters in the follicle model nor in the equations for E2 and P4 were optimized using these data, in contrast to the parameters in the hormone model, which had previously been estimated from these data (Röblitz et al., 2013). Therefore, a re-parameterization of the model could improve the difference between data and simulation curves, but parameter estimation for the given model is challenging. Most of the parameters included in the current model version are non-identifiable given the available data. One reason is that there is simply not enough data available given the complexity of the model.

The balance between available data and model parameters could be improved with a systematic model reduction. However, this would result in losing parts of the model for which no measurement data are available at the moment, e.g., the GnRH receptor binding model. By removing that part of the model, treatments with GnRH analogues could not be simulated any more.

Moreover, the data we could access only covers hormone profiles for one cycle, and does not provide any information about individuals' cycle lengths or variability. Since our model simulates consecutive cycles, data sets covering multiple menstrual cycles would be preferable.

We used an ABC-based approach to investigate model parameters in more depth. Our hypothesis was that parameters for successful/unsuccessful simulations would form clusters. However, PCCA + cluster analysis did not reveal clusters in the parameter space. We conclude that there is no particular subset of parameters that leads to non-biological simulation results. Instead, our analysis indicates that the composition of the complete parameter set determines the fate of a simulation.

By comparing the parameter distributions or each parameter with respect to the simulation fate of successful and unsuccessful simulations, we did not find parameters that are restricted to narrow ranges of values. This leads us to the conclusion that non of the selected parameters is particularly sensitive. A clear limitation of our approach is that the parameter distributions were not derived from data.

Based on the Jensen–Shannon divergence, the distribution of μ differs between successful and unsuccessful simulations. The correlation between μ and the cycle length is in line with biological knowledge. μ encodes a process that results in follicle atresia. Hence, if μ is higher, more follicles undergo atresia, which reduces competition and results in earlier emergence of a dominant follicle.

As demonstrated in Fischer et al. (2021), the model can be used to simulate controlled ovarian stimulation protocols. However, the model formulation does not allow for an application to all pathological cases. The mathematical formulation of the follicular growth adopted from Lange et al. (2019) does not allow for the arrest of multiple premature follicles as it is described for the Polycystic Ovary Syndrome (PCOS). Therefore, this model is not eligible to describe PCOS or to simulate ovarian stimulation protocols in PCOS patients. Cell-based models of follicular morphogenesis such as the one proposed in Monniaux et al. (2016) could allow for a simulation-based exploration of PCOS. Note that the model could potentially also be used to further investigate the relationship between follicles in mono-ovulatory species compared to poly-

ovulatory species, since these mechanisms are still poorly understood (Sirotkin et al., 2017).

To conclude, our presented modelling approach is the first one that allows for simulation-based studies of the interplay between hormones and ovarian follicles throughout consecutive menstrual cycles. Therefore, it can be used to test new treatment strategies for ovarian hyper stimulation in silico. Our simulation results display variability in the cycle dynamics as a result of stochasticity in the recruitment process of follicles. To our knowledge, none of the previously published models contains stochastic elements resulting in variability between cycles, which resembles intra-individual variability. The growth of follicles in cohorts is an emergent property of the implemented mechanistic interactions between hormones and follicles, which supports the follicular wave theory in humans. Re-parameterization of the model could increase its predictive values, but this would require longitudinal ultrasound measurements of follicles as well as hormone profiles throughout consecutive cycles from several individuals.

CRediT authorship contribution statement

Sophie Fischer-Holzhausen: Methodology, Validation, Visualization, Writing - original draft, Writing - review & editing. **Susanna Röblitz:** Conceptualization, Supervision, Methodology, Writing - original draft, Writing - review & editing.

Declaration of Competing Interest

The authors declare that they have no known competing financial interests or personal relationships that could have appeared to influence the work reported in this paper.

Acknowledgments

The work of SF and SR was supported by the Trond Mohn Foundation (BSF, https://www.mohnfoundation.no/), Grant No. BFS2017TMT01. The funder had no role in study design, data collection and analysis, decision to publish, or preparation of the manuscript.

Appendix A. Supplementary data

Supplementary data associated with this article can be found, in the online version, at https://doi.org/10.1016/j.jtbi.2022.111150.

References

Adams, G., Kot, K., Smith, C., Ginther, O., 1993. Selection of a dominant follicle and suppression of follicular growth in heifers. Animal Reproduction Science 30 (4), 259–271.
Baerwald, A., Adams, G., Pierson, R., 2011. Ovarian antral folliculogenesis during the human menstrual cycle: A review. Human Reproduction Update 18 (1), 73–91.
Baird, D., 1990. The selection of the follicle of the month, in: From Ovulation to Implantation Proceedings of the VII Regnier de Graaf Symposium. Maastricht, the Netherlands: Excerpta Medica, 384, 1990..
Baird, D., Fraser, I., 1975. Concentration of oestrone and oestradiol in follicular fluid and ovarian venous blood of women. Clin. Endocrinol. 4 (3), 259–266.
Baird, D.T., Bäckström, T., McNeilly, A.S., Smith, S.K., Wathen, C.G., 1984. Effect of enucleation of the corpus luteum at different stages of the luteal phase of the human menstrual cycle on subsequent follicular development. J. Reprod. Fertil. 70 (2), 615–624.
Bakos, O., Lundkvist, Ö., Wide, L., Bergh, T., 1994. Ultrasonographical and hormonal description of the normal ovulatory menstrual cycle. Acta obstetricia et gynecologica Scandinavica 73 (10), 790–796.
Brown, J., 1978. Pituitary control of ovarian function–concepts derived from gonadotrophin therapy. Aust. N. Z. J. Obstet. Gynaecol. 18 (1), 47–54.
Bull, J.R., Rowland, S.P., Scherwitzl, E.B., Scherwitzl, R., Danielsson, K.G., Harper, J., 2019. Real-world menstrual cycle characteristics of more than 600,000 menstrual cycles. NPJ Digital Med. 2 (1), 1–8.
Carmel, P., Araki, S., Ferin, M., 1976. Pituitary stalk portal blood collection in rhesus monkeys: evidence for pulsatile release of gonadotropin-releasing hormone (GnRH). Endocrinology 99 (1), 243–248.
Chavez-Ross, A., Franks, S., Mason, H., Hardy, K., Stark, J., 1997. Modelling the control of ovulation and polycystic ovary syndrome. J. Math. Biol. 36 (1), 95–118.
Christian, C.A., Moenter, S.M., 2010. The neurobiology of preovulatory and estradiol-induced gonadotropin-releasing hormone surges. Endocrine Rev. 31 (4), 544–577.
Clark, L.H., Schlosser, P.M., Selgrade, J.F., 2003. Multiple stable periodic solutions in a model for hormonal control of the menstrual cycle. Bull. Math. Biol. 65 (1), 157–173.
Clément, F., Gruet, M., Monget, P., Terqui, M., Jolivet, E., Monniaux, D., 1997. Growth kinetics of the granulosa cell population in ovarian follicles: an approach by mathematical modelling. Cell proliferation 30 (6–7), 255–270.
Evans, N., Dahl, G., Glover, B., Karsch, F., 1994. Central regulation of pulsatile gonadotropin-releasing hormone (GnRH) secretion by estradiol during the period leading up to the preovulatory GnRH surge in the ewe. Endocrinology 134 (4), 1806–1811.
Fauser, B.B., van Heusden, A.M., 1997. Manipulation of human ovarian function: physiological concepts and clinical consequences, Endocrine Reviews..
Fischer, B., Zoller, T., Buhmann, J.M., 2001. Path Based Pairwise Data Clustering with Application to Texture Segmentation, in: International Workshop on Energy Minimization Methods in Computer Vision and Pattern Recognition (EMMCVPR) 2001, Lecture Notes in Computer Science, Springer-Verlag, Berlin Heidelberg, 235–250..
Fischer, S., Ehrig, R., Schäfer, S., Tronci, E., Mancini, T., Egli, M., Ille, F., Krüger, T.H., Leeners, B., Röblitz, S., 2021. Mathematical Modeling and Simulation Provides Evidence for New Strategies of Ovarian Stimulation. Front. Endocrinol. 12, 117.
Fortune, J., 1994. Ovarian follicular growth and development in mammals. Biol. Reproduction 50 (2), 225–232.
Franks, S., Hardy, K., 2018. Androgen action in the ovary. Front. Endocrinol. 9, 452.
Speroff, L., Fritz, M.A., 2005. Clinical gynecologic endocrinology and infertility. Lippincott Williams & wilkins.
Goodman, R.L., Bittman, E.L., Foster, D.L., Karsch, F.J., 1981. The endocrine basis of the synergistic suppression of luteinizing hormone by estradiol and progesterone. Endocrinology 109 (5), 1414–1417.
Harlow, S.D., 2000. 9 – Menstruation and Menstrual Disorders: The Epidemiology of Menstruation and Menstrual Dysfunction, in: M.B. Goldman, M.C. Hatch (Eds.), Women and Health, Academic Press, San Diego, 99–113, ISBN 978-0-12-288145-9, 2000..
Hiller, S.G., Reichert, L.E., Van Hall, E.V., 1981. Control of preovulatory follicular estrogen biosynthesis in the human ovary. J. Clinical Endocrinol. Metabolism 52 (5), 847–856.
Hillier, S.G., Tetsuka, M., 1997. 3 Role of androgens in follicle maturation and atresia. Bailliere's Clinical Obstetrics Gynaecology 11 (2), 249–260.
Knobil, E., Plant, T., Wildt, L., Belchetz, P., Marshall, G., 1980. Control of the rhesus monkey menstrual cycle: permissive role of hypothalamic gonadotropin-releasing hormone. Science 207 (4437), 1371–1373.
Lacker, H.M., Akin, E., 1988. How do the ovaries count? Math. Biosci. 90 (1–2), 305–332.
Lange, A., Schwieger, R., Plöntzke, J., Schäfer, S., Röblitz, S., 2019. Follicular competition in cows: the selection of dominant follicles as a synergistic effect. J. Math. Biol. 78 (3), 579–606.
Lin, J., 1991. Divergence measures based on the Shannon entropy. IEEE Trans. Inform. Theory 37 (1), 145–151.
Marshall, J., Griffin, M., 1993. The role of changing pulse frequency in the regulation of ovulation. Human Reproduction 8 (suppl_2), 57–61.
Martin, K.A., Welt, C.K., Taylor, A.E., Smith, J.A., Crowley Jr, W.F., Hall, J.E., 1998. Is GnRH Reduced at the Midcycle Surge in the Human? Neuroendocrinology 67 (6), 363–369.
McNatty, K., Baird, D., Bolton, A., Chambers, P., Corker, C., McLean, H., 1976. Concentration of oestrogens and androgens in human ovarian venous plasma and follicular fluid throughout the menstrual cycle. J. Endocrinol. 71 (1), 77–85.
Monniaux, D., Michel, P., Postel, M., Clément, F., 2016. Multi-scale modelling of ovarian follicular development: From follicular morphogenesis to selection for ovulation. Biol. Cell 108 (6), 149–160.
Nakai, Y., Plant, T., Hess, D., Keogh, E., Knobil, E., 1978. On the sites of the negative and positive feedback actions of estradiol in the control of gonadotropin secretion in the rhesus monkey. Endocrinology 102 (4), 1008–1014.
National Health Service (NHS), Periods and fertility in the menstrual cycle, https://www.nhs.uk/conditions/periods/fertility-in-the-menstrual-cycle/, 2021..
Pritchard, J.K., Seielstad, M.T., Perez-Lezaun, A., Feldman, M.W., 1999. Population growth of human Y chromosomes: a study of Y chromosome microsatellites. Mol. Biology Evol. 16 (12), 1791–1798.
Reinecke, I., Deuflhard, P., 2007. A complex mathematical model of the human menstrual cycle. J. Theor. Biol. 247 (2), 303–330.
Riccobene, T.A., Omann, G.M., Linderman, J.J., 1999. Modeling activation and desensitization of G-protein coupled receptors provides insight into ligand efficacy. J. Theor. Biol. 200 (2), 207–222.
Röblitz, S., Weber, M., 2013. Fuzzy spectral clustering by PCCA+: application to Markov state models and data classification. Adv. Data Anal. Classif. 7 (2), 147–179.
Röblitz, S., Stötzel, C., Deuflhard, P., Jones, H.M., Azulay, D.-O., van der Graaf, P.H., Martin, S.W., 2013. A mathematical model of the human menstrual cycle for the administration of GnRH analogues. J. Theor. Biol. 321, 8–27.

Rosenfield, R.L., 2013. Adolescent anovulation: maturational mechanisms and implications. J. Clinical Endocrinol. Metabolism 98 (9), 3572–3583.
Schipper, I., Hop, W.C., Fauser, B.C., 1998. The follicle-stimulating hormone (FSH) threshold/window concept examined by different interventions with exogenous FSH during the follicular phase of the normal menstrual cycle: duration, rather than magnitude, of FSH increase affects follicle development. J. Clinical Endocrinol. Metabolism 83 (4), 1292–1298.
Schlosser, P.M., Selgrade, J.F., 2000. A model of gonadotropin regulation during the menstrual cycle in women: Qualitative features. Environ. Health Perspectives, 873–881.
Selgrade, J.F., 2001. Modeling hormonal control of the menstrual cycle. Comments Theor. Biol. 6 (1), 79–101.
Shankaran, H., Wiley, H.S., Resat, H., 2007. Receptor downregulation and desensitization enhance the information processing ability of signalling receptors. BMC Systems Biol. 1 (1), 1–15.
Shaw, N., Histed, S., Srouji, S., Yang, J., Lee, H., Hall, J., 2010. Estrogen negative feedback on gonadotropin secretion: evidence for a direct pituitary effect in women. J. Clinical Endocrinology Metabolism 95 (4), 1955–1961.
Sinisi, S., Alimguzhin, V., Mancini, T., Tronci, E., Mari, F., Leeners, B., 2020. Optimal personalised treatment computation through in silico clinical trials on patient digital twins. Fundamenta Informaticae 174 (3–4), 283–310.
Sinisi, S., Alimguzhin, V., Mancini, T., Tronci, E., Leeners, B., 2020. Complete populations of virtual patients for in silico clinical trials, Bioinformatics..
Sirotkin, A.V., Florkovičová, I., Schaeffer, H.-J., Laurincik, J., Harrath, A.H., 2017. Interrelationships between ovarian follicles grown in culture and possible mediators. Reprod. Biol. 17 (1), 97–104.
Toni, T., Welch, D., Strelkowa, N., Ipsen, A., Stumpf, M.P., 2009. Approximate Bayesian computation scheme for parameter inference and model selection in dynamical systems. J. R. Soc. Interface 6 (31), 187–202.

Paper B

Mathematical Modeling and Simulation Provides Evidence for New Strategies of Ovarian Stimulation

Sophie Fischer, Rainald Ehrig, Stefan Schäfer, Enrico Tronci, Toni Mancini, Marcel Egli, Fabian Ille, Tillmann H. C. Krüger, Brigitte Leeners and Susanna Röblitz

Frontiers in Endocrinology 12 (2021): 117

frontiers in Endocrinology

ORIGINAL RESEARCH
published: 11 March 2021
doi: 10.3389/fendo.2021.613048

Mathematical Modeling and Simulation Provides Evidence for New Strategies of Ovarian Stimulation

Sophie Fischer[1], Rainald Ehrig[2], Stefan Schäfer[3], Enrico Tronci[4], Toni Mancini[4], Marcel Egli[5], Fabian Ille[5], Tillmann H. C. Krüger[6], Brigitte Leeners[7†] and Susanna Röblitz[1†]*

[1] Computational Biology Unit, Department of Informatics, University of Bergen, Bergen, Norway, [2] Computational Systems Biology Group, Zuse Institute Berlin (ZIB), Berlin, Germany, [3] Department of Microstructure and Residual Stress Analysis, Helmholtz Centre Berlin for Materials and Energy, Berlin, Germany, [4] Department of Computer Science, University of Rome "La Sapienza", Rome, Italy, [5] Centre of Competence in Aerospace Biomedical Science & Technology, Lucerne University of Applied Sciences and Arts, Lucerne, Switzerland, [6] Department of Psychiatry, Social Psychiatry and Psychotherapy, Hannover Medical School, Hannover, Germany, [7] Department of Reproductive Medicine, University Hospital Zurich, Zurich, Switzerland

OPEN ACCESS

Edited by:
Ray Boston, University of Pennsylvania, United States

Reviewed by:
Duncan MacGregor, University of Edinburgh, United Kingdom
Chiara Dalla Man, University of Padua, Italy

***Correspondence:**
Susanna Röblitz
susanna.roblitz@uib.no

[†]*These authors share senior authorship*

Specialty section:
This article was submitted to Systems Endocrinology, a section of the journal Frontiers in Endocrinology

Received: *01 October 2020*
Accepted: *26 January 2021*
Published: *11 March 2021*

Citation:
Fischer S, Ehrig R, Schäfer S, Tronci E, Mancini T, Egli M, Ille F, Krüger THC, Leeners B and Röblitz S (2021) Mathematical Modeling and Simulation Provides Evidence for New Strategies of Ovarian Stimulation. Front. Endocrinol. 12:613048. doi: 10.3389/fendo.2021.613048

New approaches to ovarian stimulation protocols, such as luteal start, random start or double stimulation, allow for flexibility in ovarian stimulation at different phases of the menstrual cycle. It has been proposed that the success of these methods is based on the continuous growth of multiple cohorts ("waves") of follicles throughout the menstrual cycle which leads to the availability of ovarian follicles for ovarian controlled stimulation at several time points. Though several preliminary studies have been published, their scientific evidence has not been considered as being strong enough to integrate these results into routine clinical practice. This work aims at adding further scientific evidence about the efficiency of variable-start protocols and underpinning the theory of follicular waves by using mathematical modeling and numerical simulations. For this purpose, we have modified and coupled two previously published models, one describing the time course of hormones and one describing competitive follicular growth in a normal menstrual cycle. The coupled model is used to test ovarian stimulation protocols *in silico*. Simulation results show the occurrence of follicles in a wave-like manner during a normal menstrual cycle and qualitatively predict the outcome of ovarian stimulation initiated at different time points of the menstrual cycle.

Keywords: endocrinological networks, systems biology, follicular dynamics, ordinary differential equations, assisted reproductive technologies

INTRODUCTION

Infertility is a worldwide problem. According to the World Health Organization, about 48.5 million couples worldwide were affected by unwanted childlessness in 2010, and the number continues to grow (1). Men and women are just as likely to contribute to the couple's infertility (2). Infertility as a disease of the female reproductive system affects approximately 10% of women of reproductive age

worldwide (3). Unbalanced hormone levels are one cause, in a wide range of conditions, leading to infertility. For many couples, unwanted childlessness is a burden. Assisted reproductive technologies (ART) provide strategies to deal with infertility. Both unwanted childlessness and ART increase the risk for negative psycho-social functioning, such as depression and anxiety disorders (4–6), whereby the treatment burden has fallen mainly on women (2). Therefore, new ART approaches deserve to be highlighted. We want to add further scientific evidence for the efficiency of those new approaches by using mathematical modeling and numerical simulations.

Female reproduction is essentially enabled by a feedback mechanism between ovarian hormones, mainly progesterone (P4) and estradiol (E2), and the pituitary hormones luteinizing hormone (LH) and follicular stimulating hormone (FSH), see **Figure 1**. The hormone interaction network is important for regulating folliculogenesis. While the initial recruitment of follicles does not depend on gonadotropins (7, 8), the growth of cohorts of larger follicles relies on a stimulatory effect of FSH. FSH signaling is mediated by the expression of FSH receptors on granulosa cells (9, 10). The gonadodropins LH and FSH are responsible for follicular estradiol production. LH stimulates androstenedione production, which is the substrate for the FSH stimulated aromatase reaction producing estradiol (8, 11, 12). Around mid-cycle, usually one dominant follicle ovulates and releases an oocyte. The remaining parts of the dominant follicle transform into the corpus luteum, which has a key role in preparing the body for a possible pregnancy. If the oocyte is not fertilized, the corpus luteum decays and a new cycle starts (13–15). Interruptions in the feedback system are one reason for infertility.

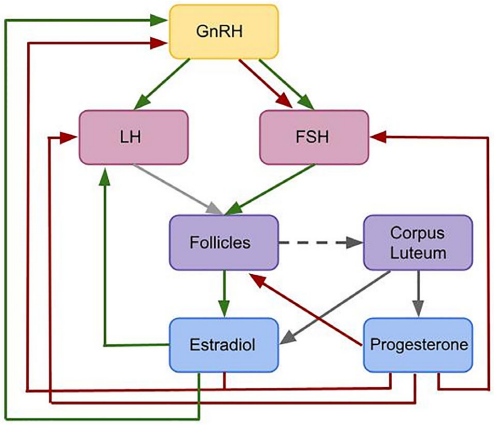

FIGURE 1 | Flowchart illustrating the interactions included in the given model. This is a simplified feedback interactions network for the hormonal control of the female menstrual cycle. Green arrows indicate positive feedback effects, while red arrows express negative feedback interactions. Gray arrows show other types of interactions. The pulsatile release of GnRH stimulates the release of the pituitary hormones LH and FSH. These hormones effect follicular maturation. Growing follicles produce E2 which has a positive feedback effect on the LH concentration. A high LH concentration triggers the ovulation of one selected follicle (light gray arrow) followed by the formation of the corpus luteum (dark gray dashed arrow). The simultaneous release of E2 and P4 by the corpus luteum (dark gray arrows) inhibits the release of GnRH. Additionally, P4 has an inhibitory effect on LH and FSH. While P4 only has an inhibitory effect on GnRH, E2 has either a stimulatory or an inhibitory effect on GnRH, depending on the E2 level.

Modern assisted reproductive technologies like *in vitro* fertilization (IVF) or intracytoplasmic sperm injection (ICSI) have increased the chance for pregnancy. Ovarian stimulation, which aims at obtaining multiple fertilizable oocytes, is a critical step in ART (16). Since the 1980s, the long gonadotropin-releasing hormone (GnRH) agonist protocol has been commonly used to prepare for oocyte retrieval and in-vitro fertilization (17, 18). This protocol starts around mid-luteal phase with GnRH agonist administration for about 14 days. Right after the beginning of GnRH agonist administration, a short period of gonadotropin (FSH and LH) hypersecretion is observable. The treatment leads to GnRH-receptor down-regulation in the pituitary (19, 20). In the next step, the growth of multiple follicles is stimulated by FSH administration alone, e.g. with recombinant FSH (rFSH), or by a combination of FSH and LH, e.g. with human menopausal gonadotropin (hMG). Continuation of GnRH agonist administration during the stimulation phase prevents an LH surge and hence ovulation. In the final step, ovulation is induced by injecting human chorionic gonadotropin (hCG) (18). Patient-specific and clinic-dependent modifications of these general procedures are common. The two most common alternatives are the short GnRH agonist protocol and the antagonist protocol. Both protocols work without downregulation, though some clinics perform a pre-treatment phase for 10 to 25 days with a P4 antagonist that inhibits ovulation.

The stimulation phase in the short GnRH agonist protocol is the same as in the long protocol. It includes the stimulation with hMG or rFSH and the concurrent administration of a GnRH agonist. The antagonist protocol also includes the stimulation with hMG or rFSH but, in contrast to the agonist protocols, a GnRH antagonist is administered from day 5 of the stimulation period. The final step in all protocols is the induction of ovulation by hCG.

In general, infertility treatment is a long-term and expensive therapy with high dropout rates (21), mainly because it imposes physical, mental, and emotional burdens (22). Often, life has to be subordinated to medical procedures. Therefore, treatment alternatives are of interest. Both the short and the antagonist protocol are less time-consuming than the long protocol. However, the stimulation phase in these protocols conventionally starts in the early follicular phase. This constraint could cause too long waiting times, e.g. for women requiring emergency fertility preservation. Hence, the advancement of a new class of ovarian stimulation approaches called random - and luteal phase-start ovarian stimulation protocol (23) has progressed. In recent years, several studies investigating ovarian stimulation

protocols with various starting points have been published (24–26). Originally, these protocols were invented for fertility preservation in cancer patients, where time is a limiting factor (27). However, they might be beneficial for patients outside an oncological setting (23), though there is an ongoing debate whether the oocyte quality differs between protocols. Other approaches like the double ovarian stimulation, where two waves within one cycle are stimulated, might help to increase the number of accumulated oocytes within one treatment cycle (28). That strategy could be of particular interest for the therapy of poor ovarian response patients (29, 30).

One possible explanation for the success of stimulation initiated in different phases of the cycle is the "wave" theory. The use of high-resolution transvaginal ultrasonography has underpinned the hypothesis that, similar to ruminants, follicular growth and development in human is characterized by waves (31, 32), whereby each wave involves the recruitment of a cohort of follicles and the possible selection of a dominant follicle. Given that multiple waves of follicles appear each cycle, there are multiple time points during one cycle that are suitable to start ovarian stimulation.

The mathematical model underlying this study simulates the time-evolution of key hormones and growth behavior of multiple follicles. In particular, we test the hypothesis that random recruitment of follicles leads to the emergence of follicular waves. Based on the occurrence of follicular waves that we observe in our simulation results, we study variable-start ovarian stimulation protocols in silico. We demonstrate simulation results for two protocols, namely (i) stimulation initiated in the late follicular phase and (ii) stimulation initiated in the luteal phase. We analyze statistics of treatment duration and numbers of follicles in our simulation results and compare them with the literature.

MATERIALS AND METHODS

Mathematical Modeling of the Female Menstrual Cycle

Mathematical modeling is a useful tool to better understand the human menstrual cycle by validating or testing hypothesis in silico, and predicting possible dynamics. A first mathematical model for the human menstrual cycle was introduced in a series of articles by Schlosser, Selgrade, and Harris-Clark (33). Their model allows to simulate the time course of hormones and follicular maturation stages over several cycles and is able to display multiple follicular waves (34). This model was extended by pharmacokinetic sub-models to simulate the administration of drugs, including ovarian contraceptive pills (35, 36) and GnRH analogs (37). These pharmacokinetic-pharmacodynamic (PKPD) models allow to study the influence of dose and time point of administration of various drugs on the cycle dynamics.

All those models are based on ordinary or delay differential equations since they allow to simulate the time evolution of hormone concentrations and follicles. Hill functions have been used to characterize stimulatory and inhibitory effects, as it is common practice for modeling regulatory networks. The model by Röblitz et al. (37) consists of 33 ordinary differential equations that describe the feedback mechanisms between the hormones that are of particular importance for the female menstrual cycle (GnRH, FSH, LH, E2, P4, inhibin A, inhibin B) and the development of follicles and corpus luteum throughout consecutive cycles. Compared to previous models, it does not use delay differential equations and consists of fewer equations and parameters. However, all those models have in common that follicular growth is described in terms of activity levels of different follicular maturation stages, but not in terms of follicle numbers and sizes. Thus, the simulation results cannot be compared with ultrasound data.

A mathematical model that quantifies the time evolution of the sizes of multiple follicles comparable to observations by ultrasound measurements in mono-ovulatory species was presented by (38). This model contains a separate differential equation for each follicle, whereby the structure of this equation is the same for all follicles, but the initial follicle sizes are different. The equations are coupled *via* a term that accounts for competitive interactions between follicles. Together with the model by (37) a previous version of the model by (38) formed the basis for the development of computational tools to enable in silico clinical trials in reproductive endocrinology (39, 40). In particular, by introducing variability into model parameters (41–43), the authors could analyze inter-individual variability in the cycle and automatically synthesize, by means of artificial intelligence guided by patient digital twins, optimal personalized treatments for the patients at hand (44). However, the tools could only be applied to the downregulation phase before follicular stimulation, because the feedback mechanisms from the ovaries to the pituitary were not implemented in the modified model. This drawback motivated the development of the fully coupled model as presented in this work. To our knowledge, this is the first mathematical model that allows for the simulation of stimulation protocols that start at different time points in the cycle.

Model Construction and Assumptions

The mathematical model underlying this work is the result of modifying and coupling the two previously published models by Röblitz et al. (37) and Lange et al. (38). In a first step, the model by Röblitz et al. (37) was reduced by removing the equations for the development of follicles and the corpus luteum and the hormones produced by them (inhibin A, inhibin B, E2, P4). In addition, we removed the equations for LH receptor binding mechanisms, since they were not needed for our purpose. The remaining equations were kept exactly as in (37), except for the FSH synthesis rate. In the new model, this rate is inhibited by P4 instead of inhibin A and B [**Eq. (S5) in the Supplement**], since P4 reaches its peak in the mid-luteal phase exactly as inhibin A. The influence of inhibin B could be neglected without any consequences for the qualitative behavior of the model. In addition, we have introduced a new equation for the amount of FSH that reaches the follicles [**Eq. (S9) in the Supplement**] to account for delays caused by transportation and for changes in concentration caused by different volumes. In contrast to (37), the equations for FSH receptor binding now take into account

FSH in the ovaries instead of the FSH blood concentration [**Eqs. (S10)–(S12) in the Supplement**].

Instead of re-introducing a corpus luteum into the model equations, we decided to use algebraic equations to directly model the amounts of E2 and P4 produced in the luteal phase of the cycle [**Eqs. (S23) and (S25) in Supplement S1**]. The model describes E2 and P4 levels in the luteal phase by Gaussian-shaped curves with fixed parameters based on fits to experimental data (for P4 see **Figure S1 in Supplement S3**). This simplification is based on the observation that the variability in the length of the luteal phase is significantly lower than the variability in the length of the follicular phase (45).

We modified the follicle equation introduced by (38) in a way that the hormone dynamics in the system have a direct effect on the follicular growth behavior [**Eqs. (S20)-(S22) in Supplement S1**]. The maturation of each follicle is modeled by a separate ODE. All ODEs have the same structure and include both shared and follicle specific parameters. Each follicle carries two random properties that are follicle specific, hence there are two follicle specific parameters: the time point at which a follicle is recruited, and its FSH sensitivity. The following assumptions are made about these two parameters:

- The time point at which a follicle is recruited and starts growing is follicle-specific and follows a Poisson process. The overall number of follicles that are recruited within a specific time interval is a Poisson random variable. The parameter of this distribution, in the following named Poisson parameter, corresponds to the probability that a given number of follicles is recruited in a fixed time interval. In the model, the Poisson parameter is modulated by the FSH concentration: if the FSH concentration is above a certain threshold, more follicles are recruited.
- The second property is a follicle specific FSH value, referred to as FSH sensitivity threshold value, which has to be exceeded in order to stimulate the follicle's growth. This refers to the biological finding that follicle growth does not occur below a certain level of FSH (46), and that any two follicles might respond differently to FSH, even if the two have the same size, because they differ in the FSH receptor density. The distribution of the FSH sensitivity threshold values in the population of follicles is assumed to follow a normal distribution. Follicles that are more sensitive to FSH, i.e. which require less FSH to start growing, have a competitive advantage for being selected as the dominant follicle. Whether a follicle becomes dominant, however, depends on both its FSH sensitivity and its recruitment time point.

The competition between follicles, which is represented by a common parameter [**Eq. (S22) in Supplement S1**], is inhibited by FSH concentrations above a certain threshold, taking into account the "FSH window concept" (47–49). This concept is based on the observation that the period of time during which FSH is above a certain threshold effects the number of follicles reaching the dominant follicle's size (50, 51). Moreover, we assume that the follicular growth rate is inhibited by P4 and stimulated by the FSH receptor complex level in a threshold dependent way [**Eq. (S21) in Supplement S1**] (52).

Growing follicles are the main source of E2 in the female body and the dominant follicle produces the most E2 (12, 53, 54). Estradiol is produced by granulosa cells, which proliferate and form a multilayered structure. This is included in the model by an additional term in E2 production which is dependent on the follicular size [**Eqs. (S24) and (S25) in Supplement S1**].

To sum up, the coupling between the hormone dynamics model and the follicular growth model is realized as follows (compare **Figure 1**). The levels of FSH in the blood and of the FSH receptor complex enter into the equations for the follicles in a threshold dependent way. In addition, the LH level plays a role in determining the time point of ovulation. Ovulation of a follicle that exceeds the size threshold occurs 12 h after the LH level is higher than a certain threshold. The levels of E2 and P4 in the luteal phase depend on the time point of the last ovulation. E2 and P4 levels enter into the equations for LH and FSH synthesis and for the frequency and mass of GnRH, in the same way as in (37). The coupled model contains in total 72 parameters, i.e. less than the two original models taken together (114 parameters in (37) and 5 parameters in (38). We adopted 44 parameters from (37) and only changed the values of three of them. A detailed parameter list can be found in the Supplement. The model has been implemented in MATLAB and numerical simulations were performed using the ODE solver *ode15s*. The code is available at https://github.com/SoFiwork/GynCycle.

Ovarian Stimulation Protocols

Stimulation protocols are introduced to the model by a pharmacokinetic approach. The dosing concentrations of the administered drug, as used in the ovarian stimulation protocols, are calculated during the simulation based on three drug specific pharmacokinetic parameters using the information given by (55) [**Eq. (S26) in Supplement S1**]. In order to study treatment outcomes, two different stimulation protocols were implemented. The two studies were selected based on the accessibility of results, the size of study cohorts and the physiological stage of patients. Each study includes data from more than 100 women. Patients were at the age of 18 to 40 years with a body mass index of 18 to 30 kg/m^3. All women showed spontaneous ovulation.

Stimulation Initiated in the Late Follicular Phase

Our simulated treatment protocol for ovarian stimulation during the late follicular phase follows the description in Zhu and Fu (24). As a simplification, we did not vary the administered hMG dose during the first days of stimulation. The stimulation starts with a daily administration of 150 IU hMG when at least one follicle measures 14 mm in diameter. After 6 days, the daily dose is increased to 225 IU per day. We chose day 6 to change the hMG concentration because re-examination and dose adjustment in the clinical trial took place after 5 - 7 days. The stimulation stops whenever at least 3 follicles reach a diameter of at least 18 mm. The ovulation of a dominant follicle during the stimulation phase is characteristic for this protocol.

Stimulation Initiated in the Luteal Phase

The protocol described in (26) served as a reference to simulate the stimulation of multiple follicular growth during the luteal phase. In this clinical trial, the drug administration in the simulation starts between day 1 and 3 after ovulation under the condition that there exist follicles smaller than 8 mm. Follicular growth is stimulated by the daily administration of 225 IU hMG. The stimulation terminates if at least three follicles have reached a diameter of 18 mm.

RESULTS

Unstimulated Cycle

As indicated in **Figure 2**, the model generates quasi-periodic solutions for all four hormones. Due to the individual growth behavior of follicles implemented in the model, variations in cycle length and number of follicles per cycle occur. Simulations for a normal cycle were performed for more than 1000 time steps in order to get an idea of the variability in the model outcome. In total, 42 simulated menstrual cycles (here, one menstrual cycle is defined from one ovulation to the next one) were used for a statistical analysis. In the simulations, the average cycle length was 30.56 days, with a standard deviation of 7.00 days (**Figure S2 in Supplement**). On average, 16.19 follicles greater than 4 mm were detected during one cycle, with a standard deviation of 3.08 follicles. The results were tested for normality using the Shapiro-Wilk test with a 95 confidence interval. A correlation between the cycle length and the follicular count was not observed.

The simulated hormone curves are supposed to be comparable to serum hormone concentration profiles in terms of shape and peak values. **Figures 2A–E** display consecutive menstrual cycles in the time period between day 50 and day 130 from one simulation run. The time evolution of all four hormone profiles is illustrated, and the described interplay between hormones and follicles is apparent.

The wave-like growth behavior of the follicles (**Figure 2E**) is generated by the model itself and is not enforced by the implementation. **Figure 2G** shows an example of the ovulation of a dominant follicle that occurs 12 h after LH reached its peak concentration. This 12-h gap is accomplished by the way the ovulation event is defined in our model (see *Discussion*). Once ovulation is detected during the run time of the simulation, the ovulated follicle is taken out from the cohort of follicles

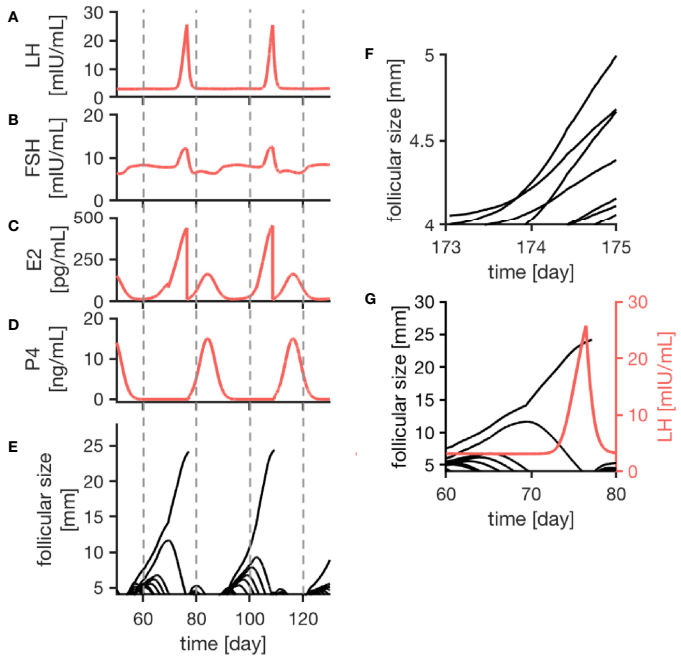

FIGURE 2 | Simulation results of the female menstrual cycle model are displayed. The left column illustrates the simulation outcome for two menstrual cycles and the right column zooms into details. Here, one cycle is defined from one ovulation to the next one. Sub-figures **(A–D)** represent the simulated hormone concentration profiles for LH, FSH, E2 and P4. **(E)** portrays growth trajectories of follicles >4 mm. The ovulation of a dominant follicle is indicated by terminating trajectories, as seen for example around day 80 of the simulation. **(F)** illustrates competition between follicles indicated by crossing growth trajectories. **(G)** Points out that the ovulation of a dominant follicle occurs 12 h after the LH peak concentration as a result of the way the ovulation process is implemented in the model.

(indicated by the terminating trajectory in **Figure 2G**). This follicle no longer contributes to steroid production. Keeping it in the simulation would needlessly increase computational time. The growth behavior of follicles causes variation in the length of the follicular phase. In contrast to that, the luteal phase has a constant length of 14 days due to its implementation.

The follicular growth equation, as introduced by (38) and modified for the given model, includes a term addressing the competition for dominance between follicles. In the simulation results, its effect is visible by crossing growth trajectories (**Figure 2F**). This crossing only is possible because each follicle has its specific parameters. As it can be seen in **Figure 2**, competition is stronger during the early follicular phase before a dominant follicle emerges.

Ovarian Stimulation

The simulations of ovarian stimulation initiated in the luteal phase or the late follicular phase are characterized by the growth of multiple follicles. Additionally, the ovulation of a dominant follicle during a stimulation protocol occurs only during stimulation in the late follicular phase. In the model, the competition term is inhibited by high FSH concentrations, enabling the growth of multiple follicles under stimulatory treatment.

Figure 3 exemplarily displays hormone concentration profiles and follicle development for one simulation of each treatment approach. Additionally, error bars at four characteristic time points (one day before treatment, one day after first drug administration, six days after first drug administration, last day of drug administration) indicate the variability in the hormone levels between 20 simulations using the same treatment conditions. The characteristic time points where chosen in a way that the results are easily comparable to the clinical data. In both cases, the FSH concentration rises with each day of the treatment. Due to the growth of multiple large follicles, which are the main source of E2, the E2 level increases significantly during ovarian stimulation. The levels are almost ten times higher compared to the normal cycle (**Figure 2C**).

Simulations of an ovarian stimulation during the luteal phase are dominated by high P4 levels during the stimulation with hMG. The high P4 concentration prevents the ovulation of

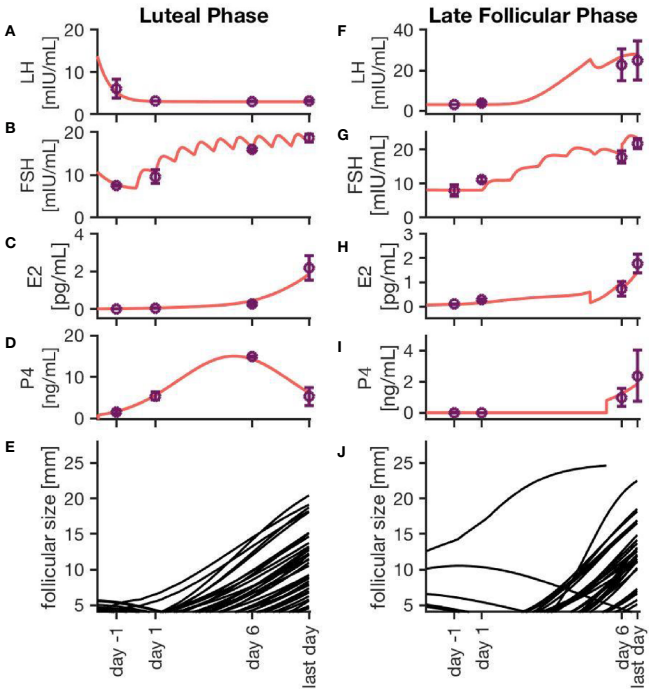

FIGURE 3 | Simulation results for two different ovarian stimulation protocols. The growth of multiple large follicles, caused by the stimulation treatment, is characteristic for both strategies. The left column represents simulation results from a luteal phase stimulation protocol, while the right column shows the effect of a stimulation during the late follicular phase. Sub-figures **(A–D, F–I)** exemplary represent hormone profiles originating from one simulation in red. Purple dots and error bars represent mean values and variances, respectively, from 20 simulations at four characteristic time points: 1 day before the stimulation treatment starts, 1 day after starting the treatment, 6 days after starting the treatment, and the last day of treatment. Sub-figures **(E, J)** illustrate the growth trajectories of the follicles.

follicles (through the negative feedback mechanisms of P4 on LH). The concentrations of LH, FSH, P4 and E2 in **Figures 3A–D** are comparable to observations by (26).

Figure 3J illustrates the follicular growth behavior under stimulation in the late follicular phase, initiated after the occurrence of a dominant follicle. The ovulation of the dominant follicle is followed by an increase in P4 concentration comparable to non-treated conditions. The E2 level decreases after the ovulation of the dominant follicle but starts to increase again. This increase is caused by multiple large follicles as a result of the stimulation.

Figure 4 represents the individual outcomes (treatment duration and follicular count) of 20 simulations per treatment protocol. The mean and standard deviation of these results are given in **Table 1**. The simulation results for ovarian stimulation initiated in the luteal phase match the observations from Kuang et al. (26). The simulated treatment duration for the late follicular phase stimulation approach is noticeably lower than the clinical observations, which goes along with comparably low counts of follicles >14 mm. **Figure 4** convincingly shows that simulations differ among each other even if non-follicular parameters are the same in all simulations. Hence, the individual growth behaviors of the follicles have a major effect on treatment simulations and outcomes.

DISCUSSION

The mathematical model developed in this work addresses the interplay between pituitary hormones, ovarian hormones and follicular growth. Simulation results for the unstimulated cycle agree qualitatively and quantitatively with observations reported in literature. In particular:

- The time evolution of the four hormone profiles for LH, FSH, P4 and E2 is consistent with the scientific literature (56).
- An average cycle length of around 29 days, ranging from cycles with a duration of 22–25 up to 36 days, is reported in experimental studies (56–58). The simulation results are in line with these observations.
- In the literature, it is described that the variability in the length of the follicular phase is significantly higher than for the luteal phase (58, 59). The given simulation results fulfill the same property.
- The observed intra-cycle variability of 7 days is comparable to experimental results by (58).
- (32) observed the emergence of two to three waves carrying 4 to 14 follicles greater than 4 mm. The given simulation results of 16.19 ± 3.08 follicles in two waves per cycle match their experimental investigations.

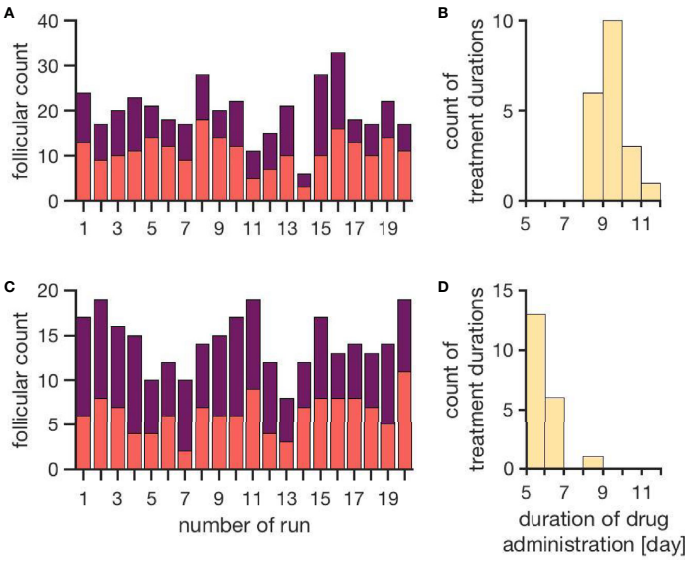

FIGURE 4 | Simulation outcomes of 20 independent cycles for each treatment: ovarian stimulation induced either during the luteal phase (top, **A, B**) or the late follicular phase (bottom, **C, D**). In the upper row **(A, B)**, follicular counts and treatment duration for the luteal phase stimulation approach are displayed (red: follicles 10–14 mm; purple: follicles >14 mm). On average, 11.1 ± 3.5 follicles with a diameter of 10 to 14 mm and 8.9 ± 3.7 follicles with a diameter >14 mm are observed. The average treatment duration is 9.4 ± 0.7 days. The lower row **(C, D)** shows follicular counts and treatment durations for simulated stimulations in the late follicular phase. A treatment cycle takes about 6.0 ± 0.7 days. The average count of follicles with diameters 10 - 14 mm is 6.3 ± 2.2 and the one for follicles >14 mm is 8.0 ± 2.2. (Numbers refer to mean ± standard deviation.)

TABLE 1 | Comparison between simulation results and clinical observations.

	Luteal phase ovarian stimulation		Late follicular phase ovarian stimulation	
	Kuang et al. (26)	Simulation	Zhu and Fu (24)	Simulation
Num. of follicles with diameter 10 - 14 mm	13.9 ± 7.8	11.1 ± 3.5		6.3 ± 2.2
Num. of follicles with diameter > 14 mm	11.1 ± 5.5	8.9 ± 3.7	11.7 ± 6.2	8.0 ± 2.2
Duration of treatment with hMG	10.2 ± 1.6	9.4 ± 0.7	10.93 ± 1.66	6.0 ± 0.7

Ovarian stimulation is induced either during the luteal phase or the late follicular phase. Each of the two studies includes data from more than 100 woman. Patients were at the age of 18 – 40 years with a body mass index of 18 – 30 kg/m^3. All woman showed spontaneous ovulation.

The discontinuity in the profile of the E2 curve (**Figure 2** at day 85 of the simulation) is related to the growth behavior of the follicles and is caused by atresia of larger sub-dominant follicles.

By comparing the results in Table 4, it is visible that variations in the experimental data are higher than in the simulation results. That indicates the fact that the inter-individual variability in human is higher than the variability between simulations sharing one set of non-follicular parameters. The stochastic growth behavior of follicles is the only source of variability between simulations. According to (24), the LH concentration under stimulatory treatment in the late follicular phase is not supposed to increase after the ovulation of the dominant follicle due to the inhibitory effect of P4. However, this effect is not visible in the simulation results (**Figures 3F–J**). This might be due to the comparably lower P4 concentrations in the simulation results. Here, the P4 concentration at day 6 is about 0.99 ± 0.6 ng/mL, whereas the figures published by (24) indicate P4 concentrations up to more than five times as high. In the present model, the P4 concentration is linked to the formation of the corpus luteum as the only source of P4. Minor P4 sources such as the adrenal cortex are neglected. However, the equations for the P4 concentration matches experimental measurements quite well (**Figure S1 in Supplementary Material**). A relation between the high LH concentrations, the low P4 concentrations and the follicular growth behavior are conceivable as well. Since the simulated treatment duration is several days shorter than those in the clinical observations, it appears that follicles are growing too fast during the simulation of ovarian stimulation. If this is the reason for the mismatch between the simulation results and the observations by (24), two explanations are credible: (i) the model parameters should have other values, or (ii) at least one mechanism is missing. However, at this point it was not possible to compare the simulated follicular growth under treatment to detailed experimental investigations since ultrasound measurement data were not available from literature.

Another reason for the mismatch could be that we could not simulate the clinical treatment procedures in full detail. In a clinical setting the dose is adjusted according to the treatment response, which is based on an evaluation of follicular growth during the stimulation procedure. Since the criteria for dose adjustment were not described in the available publications, we did not implement adjustments in our model.

We have not yet simulated double ovarian stimulation due to technical difficulties with the model implementation. However, we will do this in future work in order to address some of the problems that are still unsolved (60), for example the choice of the best day to start the second stimulation or the necessity of using a GnRH antagonist during the second stimulation.

Finally, we want to point out that clinical data are mainly reported as summary statistics, usually in terms of means and standard deviations, and for very few indicators, e.g. treatment duration or number and sizes of follicles on certain treatment days. However, with our model-based approach we could go beyond a simple comparison of moments. Since the model simulations generate distributions, we could compare them with data from literature if the publications about clinical trial outcomes reported the complete data distributions.

CONCLUSION

This study demonstrates how mathematical modeling and simulations can contribute to enhance our mechanistic understanding of ovarian stimulation protocols. In particular, our approach allows to study the extend of variability in both treated and untreated cycles. The model simulations confirm that follicular size is not a reliable parameter for determining treatment outcome since the receptor status of each individual follicle (modeled by the FSH sensitivity threshold) and the timing of growth matter. However, we cannot (yet) make use of that knowledge in a clinical setting as long as the receptor status cannot be inferred from measurements. Making predictions on the level of individuals, either in-vivo or in-silico, will therefore remain notoriously difficult. However, models that include random effects can be used to quantify uncertainties in the predictions. Even though these uncertainties might be large, being aware of what could happen as well as identifying outliers can assist in making decisions. Moreover, the model presented here could be used to compare the outcome of different treatment strategies in terms of specific success criteria (e.g. average number of follicles larger than a threshold size at the end of the stimulation), similar to the approach in (39). This requires to first validate the model with data from other stimulation protocols. For example, in order to compare the two protocols simulated here with the three currently most often used protocols (long, short, and antagonist), we would need data on each protocol from cohorts that are comparable in terms of size and physiological stage (e.g. race, age, BMI). We therefore invite clinicians to share their data and to join interdisciplinary research projects with the ultimate goal to develop model-based clinical decision support systems.

DATA AVAILABILITY STATEMENT

The original contributions presented in the study are included in the article/**Supplementary Material**. Further inquiries can be directed to the corresponding author.

AUTHOR CONTRIBUTIONS

SF and SR conceived the study. ET, TM, ME, FI, TK, BL, and SR obtained the funding. BL collected the data. SF, RE, SS, BL, and SR analyzed and interpreted the data. SF, RE, SS, and SR developed the mathematical model. SF and SS implemented the model and performed the simulations. All authors contributed to the article and approved the submitted version.

FUNDING

The work of SF and SR was supported by the Trond Mohn Foundation (BSF, https://www.mohnfoundation.no/), grant no. BFS2017TMT01. The funder had no role in study design, data collection and analysis, decision to publish, or preparation of the manuscript.

SUPPLEMENTARY MATERIAL

The Supplementary Material for this article can be found online at: https://www.frontiersin.org/articles/10.3389/fendo.2021.613048/full#supplementary-material

REFERENCES

1. Mascarenhas M, Flaxman S, Boerma T, Vanderpoel S, Stevens G. National, regional, and global trends in infertility prevalence since 1990: a systematic analysis of 277 health surveys. *PloS Med* (2012) 9:e1001356. doi: 10.1371/journal.pmed.1001356
2. Turner KA, Rambhatla A, Schon S, Agarwal A, Krawetz SA, Dupree JM, et al. Male infertility is a women's health issue – Research and clinical evaluation of male infertility is needed. *Cells* (2020) 9:990. doi: 10.3390/cells9040990
3. Yatsenko SA, Rajkovic A. Genetics of human female infertility. *Biol Reprod* (2019) 101:549–66. doi: 10.1093/biolre/ioz084
4. Wischmann T, Stammer H, Scherg H, Gerhard I, Verres R. Psychosocial characteristics of infertile couples: a study by the 'Heidelberg Fertility Consultation Service'. *Hum Reprod* (2001) 16:1753–61. doi: 10.1093/humrep/16.8.1753
5. Quesnel-Vallée A, Maximova K. Mental health consequences of unintended childlessness and unplanned births: Gender differences and life course dynamics. *Soc Sci Med* (2009) 68:850–7. doi: 10.1016/j.socscimed.2008.11.012
6. Suthersan D, Kennedy S, Chapman M. Physical symptoms throughout ivf cycles. *Hum Fertil* (2011) 14:122–8. doi: 10.3109/14647273.2011.571748
7. Oktay K, Briggs D, Gosden RG. Ontogeny of follicle-stimulating hormone receptor gene expression in isolated human ovarian follicles. *J Clin Endocrinol Metab* (1997) 82:3748–51. doi: 10.1210/jc.82.11.3748
8. McGee EA, Hsueh AJ. Initial and cyclic recruitment of ovarian follicles. *Endocr Rev* (2000) 21:200–14. doi: 10.1210/edrv.21.2.0394
9. Gougeon A. Regulation of ovarian follicular development in primates: facts and hypotheses. *Endocr Rev* (1996) 17:121–55. doi: 10.1210/edrv-17-2-121
10. Filicori M. The role of luteinizing hormone in folliculogenesis and ovulation induction. *Fertil Steril* (1999) 71:405–14. doi: 10.1016/S0015-0282(98)00482-8
11. Erickson GF, Shimasaki S. The physiology of folliculogenesis: the role of novel growth factors. *Fertil Steril* (2001) 76:943–9. doi: 10.1016/S0015-0282(01)02859-X
12. Hiller SG, Reichert JR LE, Van Hall EV. Control of preovulatory follicular estrogen biosynthesis in the human ovary. *J Clin Endocrinol Metab* (1981) 52:847–56. doi: 10.1210/jcem-52-5-847
13. Henzl M, Segre E. Physiology of human menstrual cycle and early pregnancy. A review of recent investigations. *Contraception* (1970) 1:315–38. doi: 10.1016/0010-7824(70)90017-X
14. Odell W. The reproductive system in women. In: DeGroot LJ, ed. *Endocrinology Vol 3*. New York: Grune & Stratton (1979). 3:1383–400.
15. Franz W3rd. Basic review: Endocrinology of the normal menstrual cycle. *Prim Care* (1988) 15:607.
16. Arslan M, Bocca S, Mirkin S, Barroso G, Stadtmauer L, Oehninger S. Controlled ovarian hyperstimulation protocols for in vitro fertilization: two decades of experience after the birth of Elizabeth Carr. *Fertil Steril* (2005) 84:555–69. doi: 10.1016/j.fertnstert.2005.02.053
17. Shrestha D, La X, Feng HL. Comparison of different stimulation protocols used in in vitro fertilization: A review. *Ann Trans Med* (2015) 3:137. doi: 10.3978/j.issn.2305-5839.2015.04.09
18. Lai Q, Zhang H, Zhu G, Li Y, Jin L, He L, et al. Comparison of the GnRH agonist and antagonist protocol on the same patients in assisted reproduction during controlled ovarian stimulation cycles. *Int J Clin Exp Pathol* (2013) 6:1903–10.
19. Huirne J, Homburg R, Lambalk C. Are GnRH antagonists comparable to agonists for use in IVF? *Hum Reprod* (2007) 22:2805–13. doi: 10.1093/humrep/dem270
20. Khalaf M, Mittre H, Levallet J, Hanoux V, Denoual C, Herlicoviez M, et al. GnRH agonist and GnRH antagonist protocols in ovarian stimulation: differential regulation pathway of aromatase expression in human granulosa cells. *Reprod Biomed Online* (2010) 21:56–65. doi: 10.1016/j.rbmo.2010.03.017
21. Domar A. Impact of psychological factors on dropout rates in insured infertility patients. *Fertil Steril* (2004) 81:271–3. doi: 10.1016/j.fertnstert.2003.08.013
22. Pasch LA, Holley SR, Bleil ME, Shehab D, Katz PP, Adler NE. Addressing the needs of fertility treatment patients and their partners: are they informed of and do they receive mental health services? *Fertil Steril* (2016) 106:209–15.e2. doi: 10.1016/j.fertnstert.2016.03.006
23. Sighinolfi G, Grisendi V, La Marca A. How to personalize ovarian stimulation in clinical practice. *J Turk Ger Gynecol Assoc* (2017) 18:148. doi: 10.4274/jtgga.2017.0058
24. Zhu X, Fu Y. Evaluation of ovarian stimulation initiated from the late follicular phase using human menopausal gonadotropin alone in normo-ovulatory women for treatment of infertility: A retrospective cohort study. *Front Endocrinol* (2019) 10:448. doi: 10.3389/fendo.2019.00448
25. Kim JH, Kim SK, Lee HJ, Lee JR, Jee BC, Suh CS, et al. Efficacy of random-start controlled ovarian stimulation in cancer patients. *J Korean Med Sci* (2015) 30:290–5. doi: 10.3346/jkms.2015.30.3.290
26. Kuang Y, Hong Q, Chen Q, Lyu Q, Ai A, Fu Y, et al. Luteal-phase ovarian stimulation is feasible for producing competent oocytes in women undergoing in vitro fertilization/intracytoplasmic sperm injection treatment, with optimal pregnancy outcomes in frozen-thawed embryo transfer cycles. *Fertil Steril* (2014b) 101:105–11. doi: 10.1016/j.fertnstert.2013.09.007
27. Cakmak H, Rosen M. Ovarian stimulation in cancer patients. *Fertil Steril* (2013) 99:1476–84. doi: 10.1016/j.fertnstert.2013.03.029
28. Moffat R, Pirtea P, Gayet V, Wolf JP, Chapron C, de Ziegler D. Dual ovarian stimulation is a new viable option for enhancing the oocyte yield when the time for assisted reproductive technnology is limited. *Reprod Biomed Online* (2014) 29:659–61. doi: 10.1016/j.rbmo.2014.08.010
29. Kuang Y, Chen Q, Hong Q, Lyu Q, Ai A, Fu Y, et al. Double stimulations during the follicular and luteal phases of poor responders in IVF/ICSI programmes (Shanghai Protocol). *Reprod Biomed Online* (2014a) 29:684–91. doi: 10.1016/j.rbmo.2014.08.009
30. de Almeida Cardoso MC, Evangelista A, Sartório C, Vaz G, Werneck CLV, Guimarães FM, et al. Can ovarian double-stimulation in the same menstrual cycle improve IVF outcomes? *JBRA Assist Reprod* (2017) 21:217. doi: 10.5935/1518-0557.20170042
31. Baerwald A, Adams G, Pierson R. Characterization of ovarian follicular wave dynamics in women. *Biol Reprod* (2003a) 69:1023–31. doi: 10.1095/biolreprod.103.017772

32. Baerwald A, Adams G, Pierson R. A new model for ovarian follicular development during the human menstrual cycle. *Fertil Steril* (2003b) 80:116–22. doi: 10.1016/S0015-0282(03)00544-2
33. Harris-Clark L, Schlosser P, Selgrade J. Multiple stable periodic solutions in a model for hormonal control of the menstrual cycle. *Bull Math Biol* (2003) 65:157–73. doi: 10.1006/bulm.2002.0326
34. Panza N, Wright A, Selgrade J. A delay differential equation model of follicle waves in women. *J Biol Dyn* (2016) 10:200–21. doi: 10.1080/17513758.2015.1115564
35. Reinecke I, Deuflhard P. A complex mathematical model of the human menstrual cycle. *J Theor Biol* (2007) 247:303–30. doi: 10.1016/j.jtbi.2007.03.011
36. Reinecke I. *Mathematical modeling and simulation of the female menstrual cycle. Ph.D. thesis, PhD thesis*. Freie Universität Berlin (2009).
37. Röblitz S, Stötzel C, Deuflhard P, Jones HM, Azulay D-O, van der Graaf PH, et al. A mathematical model of the human menstrual cycle for the administration of GnRH analogues. *J Theor Biol* (2013) 321:8–27. doi: 10.1016/j.jtbi.2012.11.020
38. Lange A, Schwieger R, Plöntzke J, Schäfer S, Röblitz S. Follicular competition in cows: the selection of dominant follicles as a synergistic effect. *J Math Biol* (2018) 78(3):579–606. doi: 10.1007/s00285-018-1284-0
39. Ehrig R, Dierkes T, Schäfer S, Röblitz S, Tronci E, Mancini T, et al. *An Integrative Approach for Model Driven Computation of Treatments in Reproductive Medicine*. ZIB report 16-04, Berlin: Zuse Institute (2016). Available at: https://opus4.kobv.de/opus4-zib/frontdoor/index/index/docId/5710.
40. Mancini T, Mari F, Massini A, Melatti I, Salvo I, Sinisi S, et al. Computing personalised treatments through in silico clinical trials. A case study on downregulation in assisted reproduction. In: *Proceedings of 25th RCRA International Workshop on Experimental Evaluation of Algorithms for Solving Problems with Combinatorial Explosion. EasyChair* (2018). doi: 10.29007/g864
41. Tronci E, Mancini T, Salvo I, Sinisi S, Mari F, Melatti I, et al. Patient-specific models from inter-patient biological models and clinical records. In: *Proceedings of 14th Conference in Formal Methods in Computer-Aided Design (FMCAD 2014)*. IEEE (2014). p. 207–14. doi: 10.1109/FMCAD.2014.6987615
42. Mancini T, Tronci E, Salvo I, Mari F, Massini A, Melatti I. Computing biological model parameters by parallel statistical model checking. In: *Proceedings of the 3rd International Conference on Bioinformatics and Biomedical Engineering (IWBBIO 2015) (Springer), vol. 9044 of Lecture Notes in Computer Science*. Springer (2015). p. 542–54. doi: 10.1007/978-3-319-16480-9_52
43. Sinisi S, Alimguzhin V, Mancini T, Tronci E, Leeners B. Complete populations of virtual patients for in silico clinical trials. *Bioinformatics* (2020a). doi: 10.1093/bioinformatics/btaa1026
44. Sinisi S, Alimguzhin V, Mancini T, Tronci E, Mari F, Leeners B. Optimal personalised treatment computation through in silico clinical trials on patient digital twins. *Fundam Inform* (2020b) 174:283–310. doi: 10.3233/FI-2020-1943
45. Waller K, Swan SH, Windham GC, Fenster L, Elkin EP, Lasley BL. Use of urine biomarkers to evaluate menstrual function in healthy premenopausal women. *Am J Epidemiol* (1998) 147:1071–80. doi: 10.1093/oxfordjournals.aje.a009401
46. Brown J. Pituitary control of ovarian function—concepts derived from gonadotrophin therapy. *Aust New Z J Obstet Gynaecol* (1978) 18:47–54. doi: 10.1111/j.1479-828X.1978.tb00011.x
47. Baerwald A, Adams G, Pierson R. Ovarian antral folliculogenesis during the human menstrual cycle: A review. *Hum Reprod Update* (2011) 18:73–91. doi: 10.1093/humupd/dmr039
48. Fauser BB, van Heusden AM. Manipulation of human ovarian function: physiological concepts and clinical consequences. *Endocr Rev* (1997) 18 (1):71–106. doi: 10.1210/edrv.18.1.0290
49. Adams G, Kot K, Smith C, Ginther O. Selection of a dominant follicle and suppression of follicular growth in heifers. *Anim Reprod Sci* (1993) 30:259–71. doi: 10.1016/0378-4320(93)90076-4
50. Schipper I, Hop WC, Fauser BC. The follicle-stimulating hormone (FSH) threshold/window concept examined by different interventions with exogenous FSH during the follicular phase of the normal menstrual cycle: duration, rather than magnitude, of fsh increase affects follicle development. *J Clin Endocrinol Metab* (1998) 83:1292–8. doi: 10.1210/jc.83.4.1292
51. Baird D. The selection of the follicle of the month. In: *From Ovulation to Implantation Proceedings of the VII Regnier de Graaf Symposium*. Maastricht, the Netherlands: Excerpta Medica (1990).
52. Baird DT, Bäckström T, McNeilly AS, Smith SK, Wathen CG. Effect of enucleation of the corpus luteum at different stages of the luteal phase of the human menstrual cycle on subsequent follicular development. *J Reprod Fertil* (1984) 70:615–24. doi: 10.1530/jrf.0.0700615
53. Baird D, Fraser I. Concentration of oestrone and oestradiol in follicular fluid and ovarian venous blood of women. *Clin Endocrinol* (1975) 4:259–66. doi: 10.1111/j.1365-2265.1975.tb01533.x
54. McNatty K, Baird D, Bolton A, Chambers P, Corker C, McLean H. Concentration of oestrogens and androgens in human ovarian venous plasma and follicular fluid throughout the menstrual cycle. *J Endocrinol* (1976) 71:77–85. doi: 10.1677/joe.0.0710077
55. Dataset Kompendium. *Arzneimittelkompendium der Schweiz* (2020). Available at: https://compendium.ch/ (Accessed 10 June 2020).
56. Landgren B-M, Unden A-L, Diczfalusy E. Hormonal profile of the cycle in 68 normally menstruating women. *Eur J Endocrinol* (1980) 94:89–98. doi: 10.1530/acta.0.0940089
57. Cole L, Ladner D, Byrn F. The normal variabilities of the menstrual cycle. *Fertil Steril* (2009) 91:522–7. doi: 10.1016/j.fertnstert.2007.11.073
58. Fehring RJ, Schneider M, Raviele K. Variability in the phases of the menstrual cycle. *J Obstet Gynecol Neonatal Nurs* (2006) 35:376–84. doi: 10.1111/j.1552-6909.2006.00051.x
59. Lenton EA, Landgren B-M, Sexton L. Normal variation in the length of the luteal phase of the menstrual cycle: identification of the short luteal phase. *BJOG* (1984) 91:685–9. doi: 10.1111/j.1471-0528.1984.tb04831.x
60. Sighinolfi G, Sunkara SK, La Marca A. New strategies of ovarian stimulation based on the concept of ovarian follicular waves: from conventional to random and double stimulation. *Reprod Biomed Online* (2018) 37:489–97. doi: 10.1016/j.rbmo.2018.07.006

Conflict of Interest: The authors declare that the research was conducted in the absence of any commercial or financial relationships that could be construed as a potential conflict of interest.

Paper C

A workflow for incorporating cross-sectional data into the calibration of dynamic models

Sophie Fischer-Holzhausen and Susanna Röblitz

bioRxiv (2023): 523407

A WORKFLOW FOR INCORPORATING CROSS-SECTIONAL DATA INTO THE CALIBRATION OF DYNAMIC MODELS

A PREPRINT

Sophie Fischer-Holzhausen
Computational Biology Unit
Department of Informatics
University of Bergen
Norway
sophie.fischer@uib.no

Susanna Röblitz
Computational Biology Unit
Department of Informatics
University of Bergen
Norway
susanna.roblitz@uib.no

January 10, 2023

ABSTRACT

Mathematical modelling and dynamic simulations are commonly used in systems medicine to investigate the interactions between various biological entities in time. The level of model complexity is mainly restricted by the number of model parameters that can be estimated from available experimental data and prior knowledge. The calibration of dynamic models usually requires longitudinal data from multiple individuals, which is challenging to obtain and, consequently, not always available. On the contrary, the collection of cross-sectional data is often more feasible. Here, we demonstrate how the parameters of individual dynamic models can be estimated from such cross-sectional data using a Bayesian updating method. We illustrate this approach on a model for puberty in girls with cross-sectional hormone measurement data.

Keywords systems biology · parameter estimation · female puberty · Bayesian updating

1 Introduction

Mechanistic models formulated as systems of ordinary differential equations (ODE) are widely used to study the dynamic behaviour of biological systems (Motta and Pappalardo, 2013). Often, only a limited number of model parameters are known, and at least a subset of the model parameters must be estimated to construct a useful model. The model calibration (parameter estimation) is typically done by fitting the model to experimental data, which poses several challenges (Gábor and Banga, 2015). In systems biology, we often encounter parameter landscapes with multiple local optima, complicating the parameter optimization. Additionally, there are different sources of uncertainty, such as a lack of prior knowledge, noisy data, ambiguities in the model structure and a mismatch between model complexity and available data. Despite those challenges, model calibration and analysis are central to creating a meaningful model (Villaverde et al., 2022). For the calibration of a dynamic model, one needs information about the system's time evolution (longitudinal data/time-series data). In general, data collection is time and resource-consuming, and the collection of time-series data comes with additional challenges (Udtha et al., 2015). Especially in clinical studies, the acquisition of longitudinal data requires a long-term commitment of study participants (Robinson et al., 2007), and the number of samples that can be taken is limited. Consequently, the data sets are sparse in the number of time points, and the sample size tends to be small (Greenland et al., 2016). In addition, populations often show a high inter- and inter-individual variability (Sebastian-Gambaro et al., 1997; Friedman et al., 2015). Consequently, performing model calibration with clinical data is challenging, and the resulting model uncertainty can limit the model's applicability, e.g., the prediction of an individual dose-response or disease progression (Briggs et al., 2012).

With this work, we aim to address the problem of small and sparse individual time-series data that often poses a bottleneck for calibrating dynamic models with clinical applications. We suggest a Bayesian approach incorporating data sets with observations from many individuals at one sampling time point (cross-sectional data) into the model

calibration. The workflow we propose is similar to the method explained in (Tariq et al., 2016). The authors in (Tariq et al., 2016) aim to predict the individual patient outcome by (1.) calibrating a population-average model using the pooled longitudinal data of patients and (2.) "personalizing" the population-average model for a given individual using a Bayesian parameter estimation method. In contrast to (Tariq et al., 2016), we use a cross-sectional population sample to calibrate the population-average model. The advantage of using a cross-sectional population sample is that the data collection is less challenging and time-consuming than time-series data. However, cross-sectional population data does not contain information about individual dynamics. The question we want to address with this work is whether a cross-sectional population data set can be used to construct individual dynamic models.

We demonstrate our approach using a mechanistic model describing the time evolution of three reproductive hormones over the time course of puberty in girls. The model describes a simplified feedback network between these three hormones. The population-average model is calibrated using cross-sectional data of 601 healthy Norwegian girls from the Bergen Growth Study (BGS, 2006; Madsen et al., 2020, 2022). Subsequently, the model analysis guides a reduction of the parameter space and the re-estimation of model parameters in a Bayesian setting (Bayesian updating) to personalize the population-average model.

2 Materials and methods

In the following sections, we introduce the mechanistic model used to demonstrate our method, the calibration and analysis steps of the population-average model, and the translation of the population-average model into individual-specific models.

Mathematical model

During childhood, reproductive hormones such as follicle-stimulating hormone (FSH), luteinizing hormone (LH), and estradiol (E2) are not secreted at concentrations that trigger reproductive function. This lack of reproductive function during childhood is primarily caused by the suppression of the gonadotropin-releasing hormone (GnRH) pulse generator – a functional unit in the brain that regulates the synthesis and release of GnRH (Krsmanovic et al., 2009; Herbison, 2018). The reactivation of the GnRH pulse generator during puberty is key for developing the reproductive system and activating the hypothalamic–pituitary–gonadal axis (HPG axis) (Naulé et al., 2021; Uenoyama et al., 2019; Terasawa, 2022).

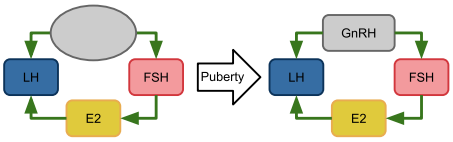

Figure 1: **Schematic representation of hormone interactions and re-activation of the HPG axis**. With the onset of puberty, the release of GnRH gets enabled. As a result, the signalling along the HPG axis starts working. GnRH stimulates the release of FSH and LH. FSH has a positive feedback effect on E2. E2 again stimulates the release of LH. Additional interactions between those hormones are not represented, because the model neglects them.

The model we introduce describes regulatory feedback loops between GnRH, FSH, LH and E2 (Fig. 1). All are critical elements of the HPG axis and the reproductive system. We encode the reactivation process of the GnRH pulse generator in a semi-mechanistic way by using a sigmoidal input curve for the increase of GnRH release over time,

$$f(t) = \frac{1}{1 + (e^{-f_s(t-f_m)})}. \tag{1}$$

The parameter f_s determines the steepness of the curve, i.e., how rapidly the activity increases and the parameter f_m determines the time point at which $f(t)$ reaches half of its maximum, i.e., the time at which the pulse generator reaches half of its total activity. This formulation is motivated by the observation that GnRH increases gradually and independently of gonadal activity (Terasawa, 2022).

Experimental studies have shown that ovaries can be stimulated before puberty (Wildt et al., 1980; Plant, 2015) and that the HPG axis begins to function when GnRH levels become high enough (Ellison et al., 2012). Those observations motivated us to base the mathematical model formulation of the hormone interactions during pubertal development on a previously developed model for the human menstrual cycle (Fischer-Holzhausen and Röblitz, 2022).

Compared to the menstrual cycle model, the model of the hormone dynamics during female puberty can be drastically reduced in the number and complexity of the ordinary differential equations and parameters. This significant model reduction is possible because the hormone concentrations during puberty do not reach the same peak concentrations as in menstrual cycles. Consequently, we removed all processes from the original model that remained inactive during puberty due to high thresholds of the regulating hormones. Note that the reduced model can, therefore, not be used to simulate late puberty or the first menstrual bleeding (menarche).

A synthesis-clearance relationship describes the dynamics of each hormone. The regulatory interactions (illustrated in Fig. 1) are approximated using Hill functions – a common way to encode feedback interactions as threshold-dependent processes without mechanistic details. Positive Hill functions describe positive feedback actions as sigmoidal curves and are denoted as $H^+(S,T,n) = S^n/(T^n + S^n)$. The regulator species S regulates another species in a threshold-dependant manner with threshold $T > 0$. The Hill exponent $n > 0$ influences the sigmoidal curve's steepness and thereby the regulatory process's rapidity (Santillán, 2008). The proposed model reads as follows:

$$\frac{dFSH(t)}{dt} = k_{syn}^{FSH} \cdot f(t) - k_{cl}^{FSH} \cdot FSH(t), \tag{2a}$$

$$\frac{dE2(t)}{dt} = k_{syn}^{E2} \cdot H^+(FSH(t), T_{FSH}^{E2}, n_{FSH}^{E2}) - k_{cl}^{E2} \cdot E2(t), \tag{2b}$$

$$\frac{dLH(t)}{dt} = k_{syn}^{LH} \cdot f(t) \cdot H^+(E2(t), T_{E2}^{LH}, n_{E2}^{LH}) - k_{cl}^{LH} \cdot LH(t). \tag{2c}$$

Modulation of the synthesis rate constants k_{syn}^{FSH} and k_{syn}^{LH} by the function $f(t)$ in Eqs. (2a) and (2c), respectively, represents the stimulatory action of GnRH on the release of the pituitary hormones FSH and LH (Marques et al., 2022). FSH stimulates the growth of ovarian follicles, hence the release of E2 (Brown, 1978) included in Eq. (2b) via a positive Hill function with FSH concentration threshold T_{FSH}^{E2} and Hill exponent n_{FSH}^{E2}. The ovarian hormone E2 has a positive effect on LH (Reed and Carr, 2015), modelled using a positive Hill function with threshold T_{E2}^{LH} and Hill exponent n_{E2}^{LH}.

The model is implemented in Python3 (Van Rossum and Drake Jr, 1995), and numerical simulations were performed using SciPy (Virtanen et al., 2020). A model and workflow demonstration is available at https://github.com/SoFiwork/CrossSectional2Individual.

Experimental data and pre-processing

We use the cross-sectional data set from the Bergen Growth Study 2 (BGS2) (BGS, 2006) to calibrate a population-average model. The BGS2 study includes hormone blood concentrations with chronological age for E2 (No. = 547), LH (No. = 600), and FSH (No. = 599). (Madsen et al., 2020) and (Bruserud et al., 2020) describe the data collection and the cohort composition in detail.

To make the data usable for the calibration of the population-average model, we estimate the continuous mean and standard deviation using the rolling window calculation function provided by the pandas package (Wes McKinney, 2010; The pandas development team, 2020) with a window size of 50 observations.

For the model adaptation to individual time-series data, we use simulated data, because clinical time-series data was unavailable for this work. We simulate time-series data by performing a forward simulation using a parameter set from the stationary parameter distribution of the population-average model, which we obtain from an uncertainty analysis. We add Gaussian noise to the simulated data points and time points to account for noise.

Population-average model calibration

Figure 2 illustrates our workflow to calibrate and analyse the population-average model. Our routine consists of three main steps:

1. Model calibration using maximum likelihood (ML) estimation
2. Identifiability analysis using profile likelihoods (PL)
3. Uncertainty quantification using the Metropolis-Hastings (MH) sampling algorithm and Sobol sensitivity analysis

In the first step, we estimate model parameters θ by fitting the model to the processed population-average data y using maximum likelihood estimation. The aim is to find a set of parameters $\hat{\theta}_{ML}(y)$ that minimizes the negative log-likelihood. When assuming additive Gaussian measurement noise, this optimisation problem corresponds to

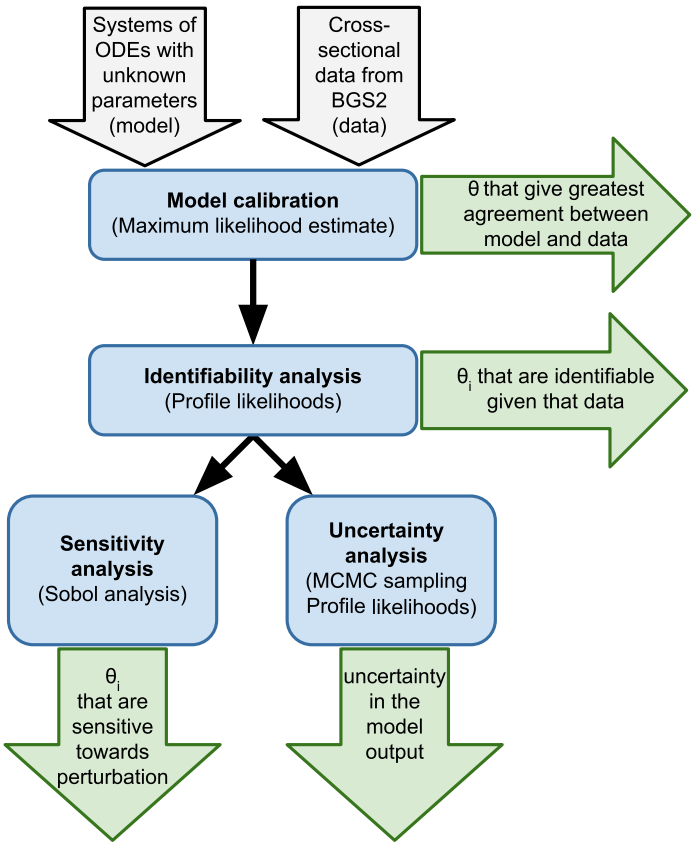

Figure 2: **Workflow for calibrating and analysing the population-average model.** The pipeline inputs are the mechanistic model and the cross-sectional data set (grey arrows). In the first step, a set of model parameters θ that minimizes the distance between the model and the moving average of the cross-sectional data is estimated using ML estimation. In a second step, the likelihood is profiled for each parameter θ_i to identify parameters that can/can not be estimated within bounded confidence intervals. In the third step, the sensitivity and uncertainty of the model are quantified. Sensitivity analysis is performed using the Sobol method. A Markov chain Monte Carlo simulation reveals information about the model uncertainty.

minimizing the least squares error between simulated trajectories $x(\theta)$ and associated measurement data y, weighted by the estimated standard deviation (Cox and Hinkley, 1979; Eliason, 1993). We use the open-source Python Parameter EStimation TOolbox (pyPESTO) (Schälte et al., 2022) to solve the ML estimation with a multi-start optimization (500 runs). We apply a quasi-Newton method (L-BFGS-B) provided by SciPy (Virtanen et al., 2020) as an optimization algorithm and calculate the gradients numerically with a 3-point finite difference schema provided by the SciPy optimization library (Virtanen et al., 2020). Tab. 1 contains the parameter search regions.

In the second step, an identifiability analysis is performed by calculating the profile likelihoods (Murphy and Van der Vaart, 2000; Raue et al., 2009) for each model parameter numerically. In doing so, we gain information about ambiguities in the model structure and whether the available data is sufficient to estimate parameter values with finite confidence intervals. In this context, parameters that can not be determined with finite confidence intervals are called non-identifiable. There exist two types of non-identifiable parameters. Structurally non-identifiable parameters are the consequence of redundancies in the model formulation. Practically non-identifiable parameters lack precision

because the data do not provide enough information (Wieland et al., 2021; Raue et al., 2009; Kreutz et al., 2013). With a step-wise optimization routine, we obtain a PL for each parameter. Hereby, the parameter θ_i is varied around its optimal value, and for each value of θ_i, all remaining parameters $\theta_{j\neq i}$ are re-optimized using, for example, the ML estimation method. In this work, we use the routine implemented in the pyPESTO package (Schälte et al., 2022) to calculate the profile likelihoods around the optimized model parameters from step one.

In the third step, the model uncertainty is quantified using the Metropolis-Hastings algorithm (Metropolis et al., 1953; Hastings, 1970), to obtain random samples of model parameters according to the likelihood function constructed in step one (Valderrama-Bahamóndez and Fröhlich, 2019). We use an adaptive parallel tempering sampler available in pyPESTO (Schälte et al., 2022) for the MH sampling. Geweke test (Geweke, 1992) is applied to the sampling chain to determine the burn-in period, i.e., the early proportion of the sampling chain that may not converge to the target distribution.

Sensitivity analysis allows studying model output uncertainty resulting from perturbations in the model input (Saltelli et al., 2004). Here we use the Sobol method (Sobol, 1993), which is a variance-based global sensitivity analysis technique. This method quantifies the contribution to the uncertainty in the model output by each parameter individually and by parameter interactions. We use the implementation of Sobol's sensitivity analysis provided by the SALib package (Herman and Usher, 2017). We decided to allow for parameter perturbations of up to 20% around the estimated parameter value $\hat{\theta}_{ML}(y)$.

The results of the model calibration and analysis steps are:

- a parameter point estimate
- identification of identifiable parameters
- identification of sensitive parameters
- distribution and confidence interval of each parameter

We use this information to enable the translation from a population-average model to an individual-specific model, as outlined in the following.

Individual-specific model calibration

We use a Bayesian parameter estimation framework (Wakefield, 1996; Tariq et al., 2016) to transform the population-average model into an individual-specific model that can be used to predict the individual time-evolution of hormones (Fig. 3). In a Bayesian framework, the posterior distribution $p(\theta|y)$ is proportional to the product of the likelihood function $L(\theta|y)$, which describes the probability of observing the data y given a parameter set θ, and the prior distribution $p(\theta)$. Here we use this idea to update our population parameter set (prior parameter distributions $p(\theta)$) using individual time-series data y in the likelihood function to obtain an individual parameter set $p(\theta|y)$ as posterior parameter distribution.

In our approach, the prior parameter distribution $p(\theta)$ originates from the uncertainty quantification of the population-average model, where we sampled from the likelihood function using MCMC sampling. Hereby, we obtain histograms of all marginal parameter distributions, to which we then fit continuous log-normal distributions. For the Bayesian parameter estimation, we use the product of these one-dimensional continuous distributions as prior distribution $p(\theta)$. In doing so, we lose information about the correlation between the parameters, but we gain an analytical representation of the priors, from which it is easy to sample.

The likelihood $L(\theta|y)$ is based on calculating the mean squared error between the individual time-series data y and the simulated model trajectories for a given parameter set θ. We solve the Bayesian parameter estimation problem by sampling from the posterior $p(\theta|y)$ using the MH algorithm provided by pyPESTO package(Schälte et al., 2022). Hereby, we obtain individual-specific parameter sets. To reduce the complexity of the parameter estimation problem, we do not perform this approach in the full 12-dimensional parameter space but only on those parameters that were identified as sensitive in the Sobol analysis.

Results and Discussion

We now present the results for calibrating the population-average model, following the workflow in Fig. 2, and its translation into an individual-specific model according to the Bayesian adaptation workflow described in Fig. 3. The data from the Bergen Growth Study 2 is used to calibrate the population-average model, whereas the individual-specific model is calibrated with simulated data. We present the population-average model's results, followed by the individual-specific model.

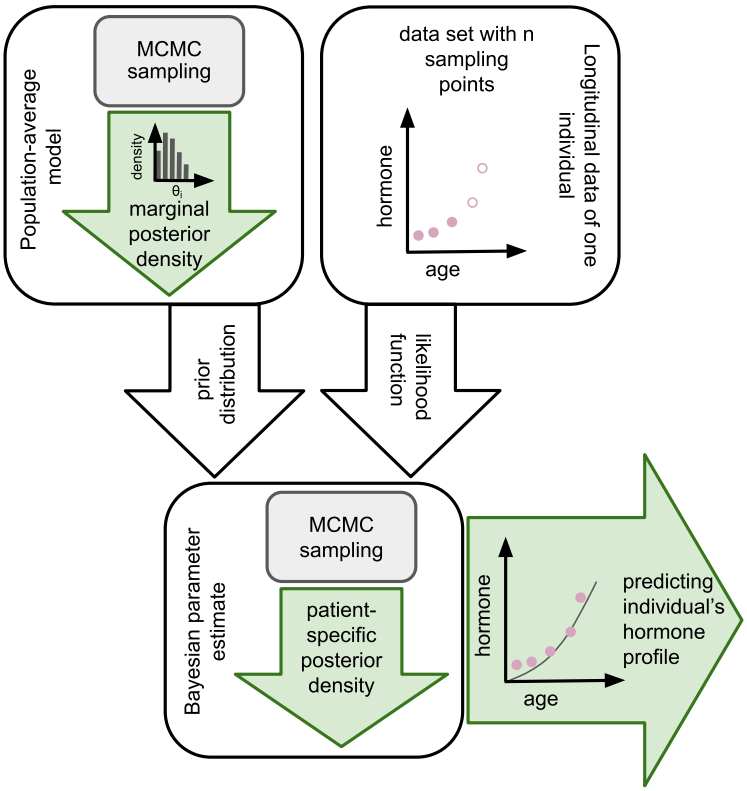

Figure 3: **Workflow for Bayesian updating to generate an individual-specific model fit.** Individual-specific parameter sets are obtained from a Bayesian parameter estimation approach. The parameter distribution generated with MCMC sampling applied to the population-average model with the cross-sectional data is employed as prior knowledge. For calculating an individual-specific likelihood, only the first 75% of the data points of an individual's longitudinal data set are used. An individual-specific posterior distribution of the parameters is approximated with MCMC sampling. This parameter distribution can be used for predicting the individual's hormone dynamics.

Population-average model

The 12 model parameters were first estimated using ML estimation to find the parameter set that minimizes the error between simulated hormone time-evolution and the averaged hormone concentrations from the BGS2 data. From the multi-start optimization, we selected the parameter set that resulted in the smallest least-squares error between simulated trajectories and data, see Tab. 1. Fig. 4 shows the simulated trajectory with this optimal parameter set. However, the plot of the optimisation history (Fig. A.1 in the Appendix) indicates the existence of several alternative parameter sets which fit the data comparably well.

Figure 5 represents the PL for each model parameter. The shape of the profile discloses the type of identifiability. Confidence intervals for each parameter (Tab. 1) were derived from the intersection between the profile and the line indicating 95 % confidence interval (Fig. 5). Because all profiles are bounded either towards plus or minus infinity, we can conclude that the model does not have structurally non-identifiable parameters. The parameter profiles presented in Fig. 5(a, c, e, f, j, k) indicate identifiablilty showing finite confidence intervals (Tab. 1). The remaining six parameters are practically non-identifiable. Their confidence intervals miss either lower or upper bounds.

Table 1: **Summary of population-average model parameters.** Model parameters are estimated using ML estimation with a search space restricted by the parameter intervals given in the column "Search region". Confidence intervals result from the analysis of the profiled likelihoods for each parameter.

Parameter and unit	**ML Search region**	**Estimated parameter value** $\hat{\theta}_{ML}(y)$	**Profile likelihood-based confidence interval**	**MCMC sampling region**
k_{syn}^{FSH} $\left[\frac{mIU}{a \cdot mL}\right]$	$[10^{-3}, 150.0]$	126.77	$[102.80, 137.98]$	$[10^{-9}, 150.0]$
k_{cl}^{FSH} $\left[\frac{1}{a}\right]$	$[10^{-7}, 150.0]$	10^{-7}	$[-\infty, 0.24]$	$[10^{-9}, 10.0]$
k_{syn}^{E2} $\left[\frac{mIU}{a \cdot mL}\right]$	$[10^{-3}, 150.0]$	26.82	$[7.98, 43.79]$	$[10^{-9}, 150.0]$
k_{cl}^{E2} $\left[\frac{1}{a}\right]$	$[10^{-7}, 150.0]$	0.43	$[-\infty, 0.62]$	$[10^{-9}, 10.0]$
T_{FSH}^{E2} $\left[\frac{mIU}{mL}\right]$	$[10^{-3}, 20.0]$	3.50	$[2.39, 6.16]$	$[10^{-9}, 50.0]$
n_{FSH}^{E2} [1]	$[1.0, 5.0]$	4.05	$[2.72, 5.00]$	$[10^{-9}, 10.0]$
k_{syn}^{LH} $\left[\frac{ng}{a \cdot mL}\right]$	$[10^{-3}, 150.0]$	149.87	$[133.03, +\infty]$	$[10^{-9}, 150.0]$
k_{cl}^{LH} $\left[\frac{1}{a}\right]$	$[10^{-3}, 150.0]$	10^{-3}	$[-\infty, 0.47]$	$[10^{-9}, 10.0]$
T_{E2}^{LH} $\left[\frac{ng}{mL}\right]$	$[10^{-3}, 10.0]$	8.85	$[3.39, +\infty]$	$[10^{-9}, 50.0]$
n_{E2}^{LH} [1]	$[1.0, 5.0]$	2.00	$[1.01, 2.20]$	$[10^{-9}, 10.0]$
f_s $\left[\frac{1}{a}\right]$	$[10^{-3}, 10.0]$	0.39	$[0.29, 0.45]$	$[10^{-9}, 10.0]$
f_m $[a]$	$[5.0, 25.0]$	22.53	$[18.53, +\infty]$	$[10^{-9}, 50.0]$

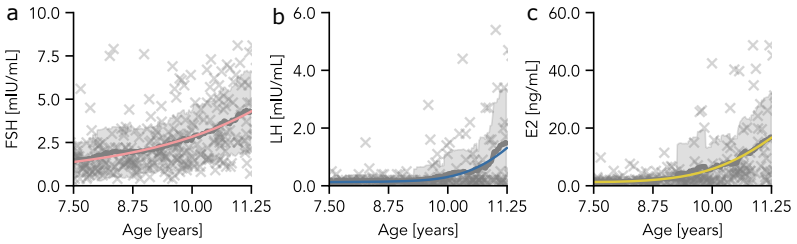

Figure 4: **Population-average model simulation results.** Representation of the model trajectories of the three sex hormones (FSH, LH, E2) resulting from numerical simulations with the parameter set given in Tab. 1. The moving average is marked as grey lines, and grey areas are the moving standard deviation of the data. The individual measurement points are marked as grey crosses.

One way to handle practical non-identifiable parameters is model reduction. The authors in (Tönsing et al., 2018) suggest that parameters with likelihood profiles that flatten out towards minus infinity can be set to zero. We deliberately decided not to apply this approach to our model, because we would remove all clearance terms. The presence of the clearance terms in our model represents the prior biological knowledge, that hormones have a finite lifetime. However, that is not visible in the cross-sectional data. Consequently, we have a model that is not fully identifiable, increasing the uncertainty in the model output.

We performed uncertainty quantification in terms of a full MCMC sampling of the likelihood function (see Tab. 1 for search regions). The marginals of the resulting parameter distribution are illustrated as violin plots in Fig. 6. The ML estimates (Tab. 1) lie within the sampled range (marked as green x) but do not agree with the median or mean of the sampled parameter densities. This is not unexpected because the model is not fully identifiable, and there exist multiple local optima (Raue et al., 2013).

The Sobol analysis (Fig. 7) reveals that the parameters of the sigmoidal input curve are the most sensitive ones. Additionally, their effect on the uncertainty in the simulation outcome increases with time. Initial values are sensitive during earlier time steps and lose their effect over the simulation time. Other sensitive parameters are T_{FSH}^{E2} and n_{FSH}^{E2}, which are both among the identifiable parameters. Perturbations in all other model parameters did not show notable effects on the simulation outcome. Note that sensitivity and practical identifiability are two different concepts because

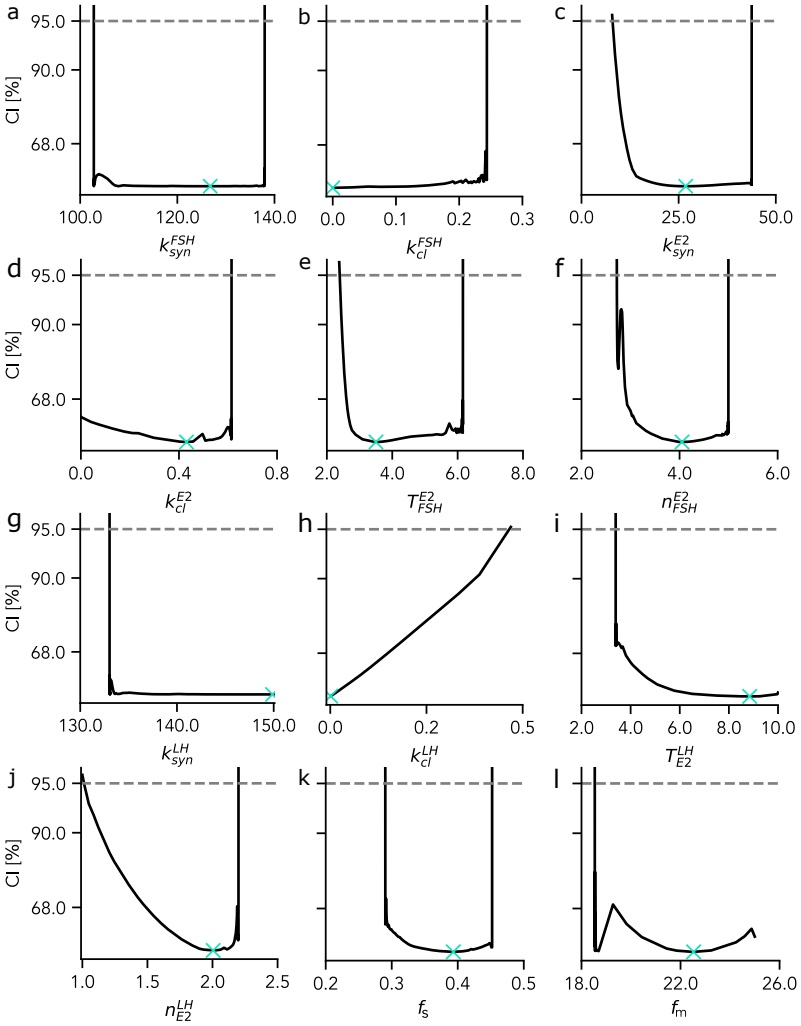

Figure 5: **Profile likelihood for each model parameter θ_i.** The likelihood profile and the ML estimate (marked as a cross) are shown for each parameter separately. The analysis reveals that k_{syn}^{FSH} (panel a), k_{syn}^{E2} (panel c), T_{FSH}^{E2} (panel e), n_{FSH}^{E2} (panel e) n_{E2}^{LH} (panel j), and f_s (panel k) are identifiable. In contrast, parameters k_{cl}^{FSH} (panel b), k_{cl0}^{E2} (panel d), k_{syn}^{LH} (panel g), k_{cl}^{LH} (panel h) T_{E2}^{LH} (panel j), and f_m (panel l) are practically non-identifiable.

sensitivity does not consider any experimental data. Hence sensitive parameters can be practically non-identifiable (e.g. f_m), and practically identifiable parameters do not necessarily need to be sensitive (e.g. n_{E2}^{LH}).

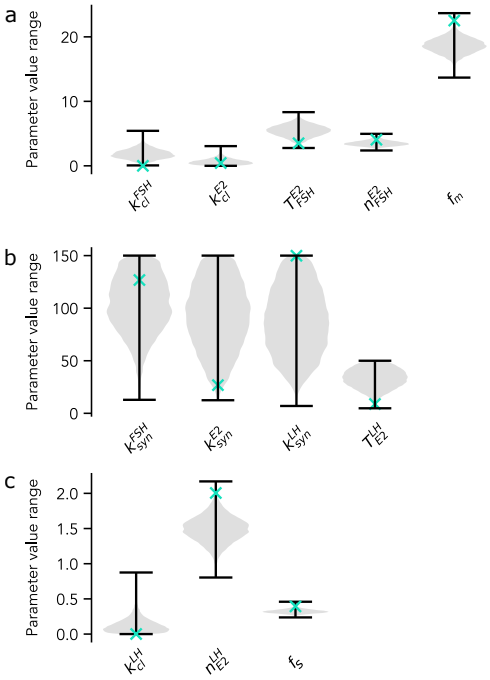

Figure 6: **Representation of stationary parameter distributions from MCMC sampling as violin plots.** Each violin (grey area) represents a kernel density estimate for each marginal parameter distribution derived from its histogram. Horizontal black lines mark the minimum and maximum of the distributions. Green crosses mark ML estimates.

Individual-specific model

Translating the population-average model to an individual-specific model requires re-estimating model parameters. Based on the Sobol sensitivity analysis (Fig. 7), we selected f_s, f_m, T^{E2}_{FSH}, and n^{E2}_{FSH} for re-estimation. All other eight parameters remained at the values given in Tab. 1. Reducing the parameter space to sensitive parameters avoids re-estimating parameters that do not affect the model output and thereby increases the efficiency of the MCMC sampling. The initial values of the three hormones were inferred directly from the data as the first data point of the time-series.

For the Bayesian parameter estimation of individual parameter distributions, we not only utilize the results from the sensitivity analysis but also the results from the uncertainty analysis of the population-average model. The insights about the model parameters are used to construct prior parameter distributions. Those prior distributions are updated, resulting in individual posterior distributions with a likelihood solely based on the individual data. By construction, parameter correlations (Fig. A.3 in the Appendix) are neglected by the prior but rediscovered after updating the parameter distributions (Fig. 8).

We used a set of simulated data, generated by a forward simulation with a parameter set from the stationary distribution of the MCMC sampling performed for the population-average model, as an individual data set to demonstrate our adaptation approach. Only one simulated individual is displayed because the range of variability covered by the stationary distribution is not large (see Fig. A.2). The simulation results of the individual-specific model are summarized in Fig. 9. Figs. 9 (a-c) allow for a comparison between the cross-sectional data and the simulated time-series. As expected, the individual data set generated with parameters from the stationary distribution of the population-average model lies within the cross-sectional data set. Figs. 9 (d-f) show simulated trajectories for the individual-specific model. Note that we only used the first three measurement points of the simulated time-series to estimate the individual parameter distributions. The remaining data points can be used to evaluate the model's predictive performance. All

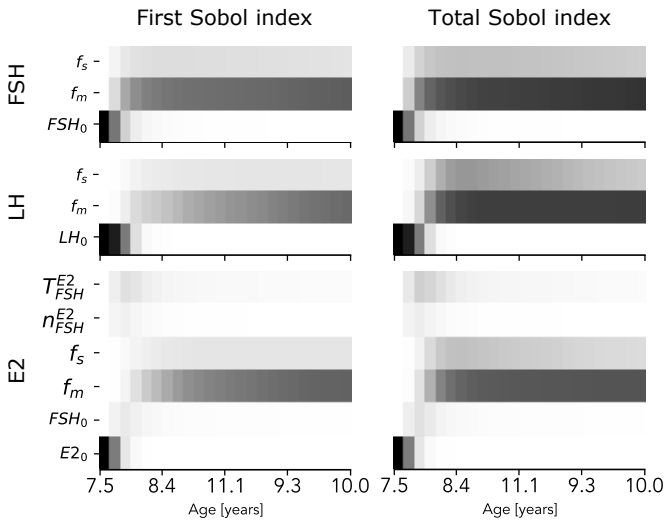

Figure 7: **Representation of parameters' first and total Sobol index over the simulation time.** Sensitivity values are encoded as grey scale values (black = highly sensitive and white = not sensitive). For clarity, this figure only represents parameters that are sensitive.

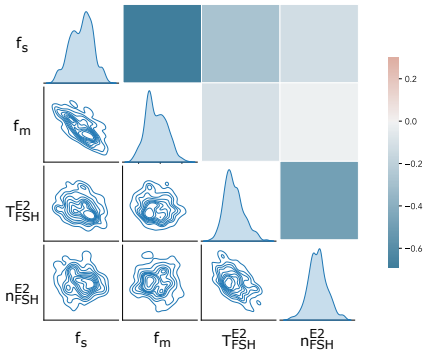

Figure 8: **Parameter correlation in the individual-specific model.** The upper right half of the matrix contains the pairwise Pearson correlation coefficients. The lower left half shows the corresponding bi-variate densities resulting from marginalization. The marginal parameter distributions are given diagonal.

data points, except the last data point of the LH time-series, are within the 99 % confidence interval, generated based on 100000 solutions with parameter sets from the stationary distribution. Figs. 9 (g-j) demonstrate that the population-parameter distributions have been updated for the individual-specific model. For a quantitative comparison between the distributions, the value of the Jensen-Shannon divergence (JSD) between the prior and each posterior is plotted in Fig. 9 (k). It is visible that the posterior distributions of the two parameters from the input curve, f_m and f_s, differ more from the prior than the distributions of the Hill function's parameters T^{E2}_{FSH} and n^{E2}_{FSH}. So far, this is only an observation, and further investigations are needed to draw any biological conclusions.

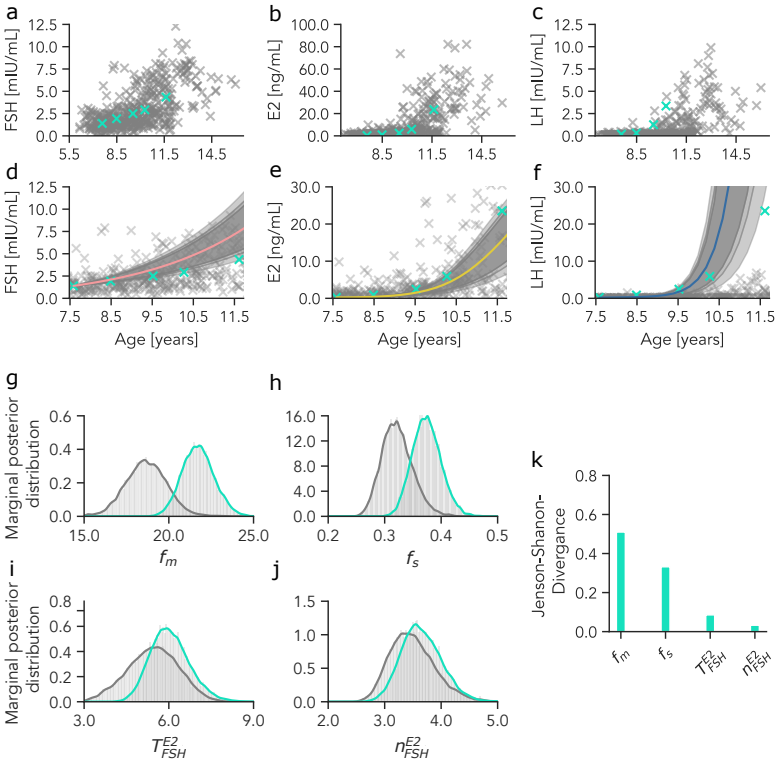

Figure 9: **Individual-specific model simulation.** Figures (a-c) illustrate the location of simulated time-series data in the cross-sectional data set. Figures (d-f) show the simulated result of the individual-specific model. The presented percentiles (99.0% - light grey, 95.0% - grey, 90.0% - dark grey) are derived from 100000 model simulations with parameter sets from the stationary posterior distribution. Figures (g-j) show the four updated parameters' marginal distributions (grey - population parameters, green - individual parameters). Those figures indicate that all distributions are updated. Figure k represents the JSD, quantifying the difference between the two distributions for each parameter.

3 Conclusion

In this work, we propose a workflow incorporating cross-sectional clinical data into calibration of an individual-specific dynamic model. We demonstrate that a population-average model calibrated with a cross-section data set can be translated into an individual-specific model using Bayesian updating. However, the presented study has some limitations, which we would like to point out in the following.

Using a well-established benchmark model would better underline the value of the proposed workflow. However, we did not have access to a cross-sectional data set for a well-established mechanistic model. We, therefore, decided to construct a mechanistic model for the time evolution of sex hormones during puberty in girls to be able to demonstrate our model calibration pipeline.

The model formulation itself is motivated by biological knowledge (bottom-up approach). Therefore, it would be interesting to compare it to alternative model formulations that fit the data, especially statistical models derived from a top-down approach. One could argue that machine learning (ML) models are expected to have a better predictive performance than mechanistic models. However, ML models are known to be data-hungry and would need training data of high quality and quantity, which are usually not available in a clinical context (Baker et al., 2018). In conclusion, the model formulation was not the central objective of this work, and therefore, we did not investigate alternatives.

From an algorithmic perspective, the construction of the prior distributions for the individual-specific model calibration, as performed in this work, is a subject for discussion. Some kernel density estimation could be applied to the full-dimensional parameter space sample as an alternative to marginalisation. This also results in an analytical representation of the prior from which one can sample, but this representation will depend on the selected bandwidth. Another alternative would be sampling importance re-sampling (SIR), which is based on re-weighting the prior samples. However, this approach assumes that the individual under consideration is sufficiently well-represented by the population-average model given by the prior, which might not always be true. Finally, in a continuous clinical monitoring context, particle filters that allow for sequential data processing are usually more efficient than MCMC methods (Maier et al., 2020).

Another limitation of this work is using simulated longitudinal data instead of clinical data for individual-specific model calibration. Such clinical longitudinal data have been collected, as part of the Copenhagen Puberty Study[1]. In future, we aim to work with these clinical data to systematically assess the predictive performance of individual-specific dynamic models.

Overall, finding individual-specific dynamic models is of interest because they form a basis for further analysis. For example, clustering individual models in the parameter space can help identify phenotypes. We hope that our work advocates the use of Bayesian methods as a means to integrate different data sources into mathematical models.

Acknowledgment

The authors like to thank Pétur Benedikt Júlíusson and Andre Madsen for providing access to the Bergen Growth Study data.

Funding

The work of SF and SR was supported by the Trond Mohn Foundation (BSF, https://www.mohnfoundation.no/), Grant no. BFS2017TMT01. The funder had no role in study design, data collection and analysis, decision to publish, or manuscript preparation.

A Appendix

A.1 Optimisation history

Fig. A.1 shows the waterfall plot from the multi-start optimisation to demonstrate the convergence of the optimization runs.

A.2 Simulation of the population-average model

Fig. A.2 displays percentiles resulting from simulations with sampled parameter sets from the stationary solution of the Metropolis-Hastings sampling routine. It gives an impression of the model uncertainty. For the interpretation of Fig. A.2, one has to keep in mind that the moving average of the data is used for model calibration and sampling and not the cross-sectional data set itself (grey marks in Fig. A.2). As a result, it is not surprising that the percentiles do not cover the entire spread of the BGS 2 data set.

A.3 Parameter correlations

Fig. A.3 shows the pairwise Pearson correlation coefficients between model parameters together with the bivariate distributions resulting from the MCMC sampling of the likelihood for the population-avarage model.

References

Baker, R. E., Pena, J.-M., Jayamohan, J., and Jérusalem, A. (2018). Mechanistic models versus machine learning, a fight worth fighting for the biological community? *Biology Letters*, 14(5):20170660.

BGS (2003-2006). The Bergen Growth Study 1 and 2. `https://www.vekststudien.no/en/`. Accessed: 06-Oct-2022.

[1] `https://www.clinicaltrials.gov/ct2/show/NCT01411527`

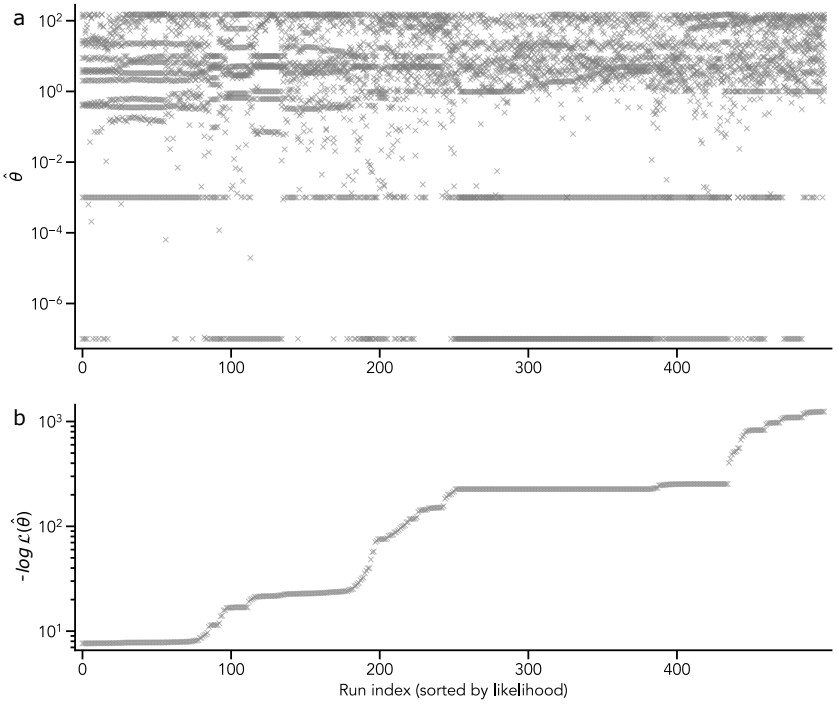

Figure A.1: **Optimization history** a) Parameter set at the endpoint of each optimisation run. It can be seen that many parameters keep their value in different local optima. b) Values of the negative log-likelihood function at the end of each optimization run.

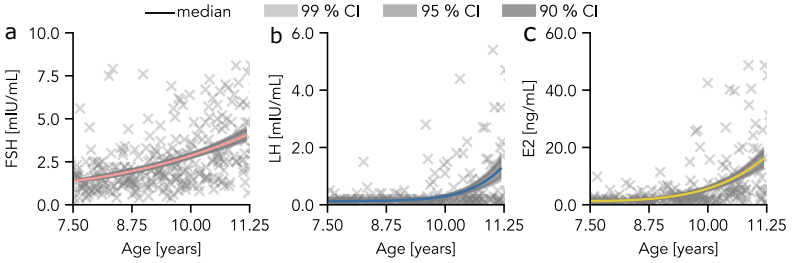

Figure A.2: **MCMC Sampling based confidence intervals.** Illustrated percentiles are derived from model simulations with 150000 parameter sets drawn from the stationary distribution. Confidence intervals (99%, 95%, 90%) are represented as grey areas. The median of the sampling based simulation trajectories is gives as a colored line.

Briggs, A. H., Weinstein, M. C., Fenwick, E. A., Karnon, J., Sculpher, M. J., Paltiel, A. D., Force, I.-S. M. G. R. P. T., et al. (2012). Model parameter estimation and uncertainty: a report of the ISPOR-SMDM modeling good research practices task force-6. *Value in Health*, 15(6):835–842.

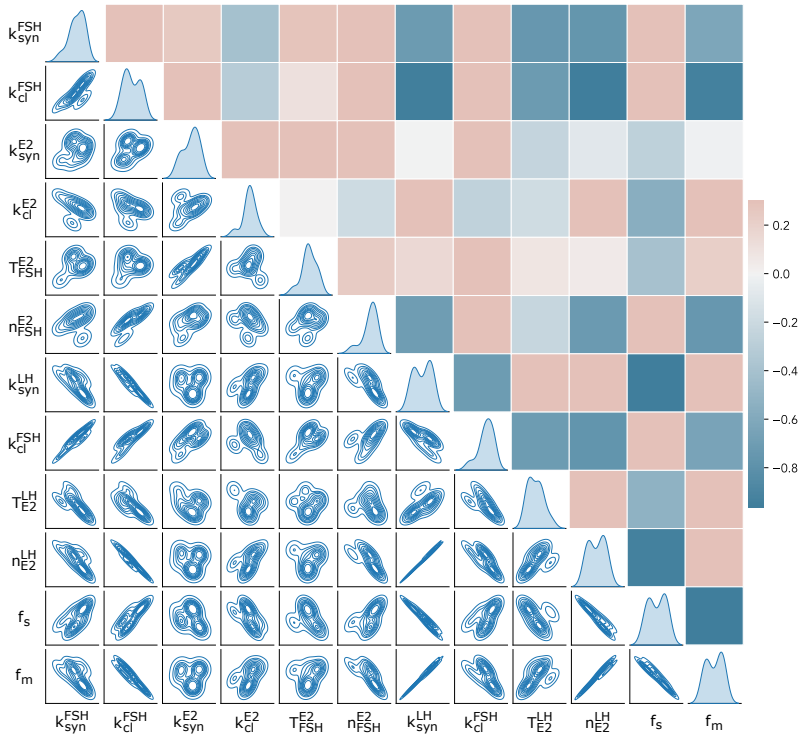

Figure A.3: **Parameter correlation in the population-average model.** The upper right half of the matrix contains the pairwise Pearson correlation coefficients. The lower left half shows the corresponding bi-variate densities resulting from marginalization.

Brown, J. (1978). Pituitary control of ovarian function—concepts derived from gonadotrophin therapy. *Australian and New Zealand Journal of Obstetrics and Gynaecology*, 18(1):47–54.

Bruserud, I. S., Roelants, M., Oehme, N. H. B., Madsen, A., Eide, G. E., Bjerknes, R., Rosendahl, K., and Juliusson, P. B. (2020). References for ultrasound staging of breast maturation, Tanner breast staging, pubic hair, and menarche in Norwegian girls. *The Journal of Clinical Endocrinology & Metabolism*, 105(5):1599–1607.

Cox, D. R. and Hinkley, D. V. (1979). *Theoretical Statistics*. CRC Press.

Eliason, S. R. (1993). *Maximum likelihood estimation: Logic and practice*, volume 96 of *Quantitative Applications in the Social Sciences*. Sage.

Ellison, P. T., Reiches, M. W., Shattuck-Faegre, H., Breakey, A., Konecna, M., Urlacher, S., and Wobber, V. (2012). Puberty as a life history transition. *Annals of Human Biology*, 39(5):352–360.

Fischer-Holzhausen, S. and Röblitz, S. (2022). Hormonal regulation of ovarian follicle growth in humans: Model-based exploration of cycle variability and parameter sensitivities. *Journal of Theoretical Biology*, page 111150.

Friedman, L. M., Furberg, C. D., DeMets, D. L., Reboussin, D. M., and Granger, C. B. (2015). *Fundamentals of Clinical Trials*. Springer.

Gábor, A. and Banga, J. R. (2015). Robust and efficient parameter estimation in dynamic models of biological systems. *BMC Systems Biology*, 9(1):1–25.

Geweke, J. (1992). Evaluating the accuracy of sampling-based approaches to the calculations of posterior moments. *Bayesian Statistics*, 4:641–649.

Greenland, S., Mansournia, M. A., and Altman, D. G. (2016). Sparse data bias: a problem hiding in plain sight. *BMJ*, 352.

Hastings, W. K. (1970). Monte Carlo sampling methods using Markov chains and their applications. *Biometrika*, 57(1):97–109.

Herbison, A. E. (2018). The gonadotropin-releasing hormone pulse generator. *Endocrinology*, 159(11):3723–3736.

Herman, J. and Usher, W. (2017). SALib: An open-source python library for sensitivity analysis. *The Journal of Open Source Software*, 2(9).

Kreutz, C., Raue, A., Kaschek, D., and Timmer, J. (2013). Profile likelihood in systems biology. *The FEBS journal*, 280(11):2564–2571.

Krsmanovic, L. Z., Hu, L., Leung, P.-K., Feng, H., and Catt, K. J. (2009). The hypothalamic GnRH pulse generator: multiple regulatory mechanisms. *Trends in Endocrinology & Metabolism*, 20(8):402–408.

Madsen, A., Almås, B., Bruserud, I. S., Oehme, N. H. B., Nielsen, C. S., Roelants, M., Hundhausen, T., Ljubicic, M. L., Bjerknes, R., Mellgren, G., et al. (2022). Reference curves for pediatric endocrinology: leveraging biomarker Z-scores for clinical classifications. *The Journal of Clinical Endocrinology & Metabolism*, 107(7):2004–2015.

Madsen, A., Bruserud, I. S., Bertelsen, B.-E., Roelants, M., Oehme, N. H. B., Viste, K., Bjerknes, R., Almås, B., Rosendahl, K., Mellgren, G., et al. (2020). Hormone references for ultrasound breast staging and endocrine profiling to detect female onset of puberty. *The Journal of Clinical Endocrinology & Metabolism*, 105(12):e4886–e4895.

Maier, C., Hartung, N., de Wiljes, J., Kloft, C., and Huisinga, W. (2020). Bayesian data assimilation to support informed decision making in individualized chemotherapy. *CPT: Pharmacometrics & Systems Pharmacology*, 9(3):153–164.

Marques, P., Skorupskaite, K., Rozario, K. S., Anderson, R. A., and George, J. T. (2022). Physiology of GnRH and gonadotropin secretion. *Endotext [Internet]*.

Metropolis, N., Rosenbluth, A. W., Rosenbluth, M. N., Teller, A. H., and Teller, E. (1953). Equation of state calculations by fast computing machines. *The Journal of Chemical Physics*, 21(6):1087–1092.

Motta, S. and Pappalardo, F. (2013). Mathematical modeling of biological systems. *Briefings in Bioinformatics*, 14(4):411–422.

Murphy, S. A. and Van der Vaart, A. W. (2000). On profile likelihood. *Journal of the American Statistical Association*, 95(450):449–465.

Naulé, L., Maione, L., and Kaiser, U. B. (2021). Puberty, a sensitive window of hypothalamic development and plasticity. *Endocrinology*, 162(1):bqaa209.

Plant, T. M. (2015). 60 years of neuroendocrinology: The hypothalamo-pituitary–gonadal axis. *Journal of Endocrinology*, 226(2):T41–T54.

Raue, A., Kreutz, C., Maiwald, T., Bachmann, J., Schilling, M., Klingmüller, U., and Timmer, J. (2009). Structural and practical identifiability analysis of partially observed dynamical models by exploiting the profile likelihood. *Bioinformatics*, 25(15):1923–1929.

Raue, A., Kreutz, C., Theis, F. J., and Timmer, J. (2013). Joining forces of Bayesian and frequentist methodology: a study for inference in the presence of non-identifiability. *Philosophical Transactions of the Royal Society A: Mathematical, Physical and Engineering Sciences*, 371(1984):20110544.

Reed, B. G. and Carr, B. R. (2015). The normal menstrual cycle and the control of ovulation. *Endotext [Internet]*. Available from: `https://www.ncbi.nlm.nih.gov/books/NBK279054/`.

Robinson, K. A., Dennison, C. R., Wayman, D. M., Pronovost, P. J., and Needham, D. M. (2007). Systematic review identifies number of strategies important for retaining study participants. *Journal of Clinical Epidemiology*, 60(8):757–e1.

Saltelli, A., Tarantola, S., Campolongo, F., Ratto, M., et al. (2004). Sensitivity analysis in practice: a guide to assessing scientific models. *Chichester, England*.

Santillán, M. (2008). On the use of the Hill functions in mathematical models of gene regulatory networks. *Mathematical Modelling of Natural Phenomena*, 3(2):85–97.

Schälte, Y., Fröhlich, F., Stapor, P., Vanhoefer, J., Weindl, D., Jost, P. J., Wang, D., Lakrisenko, P., Raimúndez, E., Pathirana, D., Schmiester, L., Städter, P., Contento, L., Merkt, S., Dudkin, E., Grein, S., and Hasenauer, J. (2022). pyPESTO - Parameter EStimation TOolbox for python, version v0.2.14. Zenodo. `https://doi.org/10.5281/zenodo.7248648`.

Sebastian-Gambaro, M. A., Liron-Hernandez, F. J., and Fuentes-Arderiu, X. (1997). Intra-and inter-individual biological variability data bank. *European Journal of Clinical Chemistry and Clinical Biochemistry*, 35:845–852.

Sobol, I. M. (1993). Sensitivity analysis for non-linear mathematical models. *Mathematical Modelling and Computational Experiment*, 1:407–414.

Tariq, I., Chen, T., Kirkby, N. F., and Jena, R. (2016). Modelling and Bayesian adaptive prediction of individual patients' tumour volume change during radiotherapy. *Physics in Medicine & Biology*, 61(5):2145.

Terasawa, E. (2022). The mechanism underlying the pubertal increase in pulsatile GnRH release in primates. *Journal of Neuroendocrinology*, page e13119.

The pandas development team (2020). pandas-dev/pandas: Pandas. Zenodo. `https://doi.org/10.5281/zenodo.3509134`.

Tönsing, C., Timmer, J., and Kreutz, C. (2018). Profile likelihood-based analyses of infectious disease models. *Statistical methods in medical research*, 27(7):1979–1998.

Udtha, M., Nomie, K., Yu, E., and Sanner, J. (2015). Novel and emerging strategies for longitudinal data collection. *Journal of Nursing Scholarship*, 47(2):152–160.

Uenoyama, Y., Inoue, N., Nakamura, S., and Tsukamura, H. (2019). Central mechanism controlling pubertal onset in mammals: A triggering role of kisspeptin. *Frontiers in Endocrinology*, 10:312.

Valderrama-Bahamóndez, G. I. and Fröhlich, H. (2019). MCMC techniques for parameter estimation of ODE based models in systems biology. *Frontiers in Applied Mathematics and Statistics*, 5:55.

Van Rossum, G. and Drake Jr, F. L. (1995). *Python reference manual*. Centrum voor Wiskunde en Informatica Amsterdam.

Villaverde, A. F., Pathirana, D., Fröhlich, F., Hasenauer, J., and Banga, J. R. (2022). A protocol for dynamic model calibration. *Briefings in Bioinformatics*, 23(1):bbab387.

Virtanen, P., Gommers, R., Oliphant, T. E., Haberland, M., Reddy, T., Cournapeau, D., Burovski, E., Peterson, P., Weckesser, W., Bright, J., van der Walt, S. J., Brett, M., Wilson, J., Millman, K. J., Mayorov, N., Nelson, A. R. J., Jones, E., Kern, R., Larson, E., Carey, C. J., Polat, İ., Feng, Y., Moore, E. W., VanderPlas, J., Laxalde, D., Perktold, J., Cimrman, R., Henriksen, I., Quintero, E. A., Harris, C. R., Archibald, A. M., Ribeiro, A. H., Pedregosa, F., van Mulbregt, P., and SciPy 1.0 Contributors (2020). SciPy 1.0: Fundamental Algorithms for Scientific Computing in Python. *Nature Methods*, 17:261–272.

Wakefield, J. (1996). Bayesian individualization via sampling-based methods. *Journal of Pharmacokinetics and Biopharmaceutics*, 24(1):103–131.

Wes McKinney (2010). Data Structures for Statistical Computing in Python. In Stéfan van der Walt and Jarrod Millman, editors, *Proceedings of the 9th Python in Science Conference*, pages 56 – 61.

Wieland, F.-G., Hauber, A. L., Rosenblatt, M., Tönsing, C., and Timmer, J. (2021). On structural and practical identifiability. *Current Opinion in Systems Biology*, 25:60–69.

Wildt, L., Marshall, G., and Knobil, E. (1980). Experimental induction of puberty in the infantile female rhesus monkey. *Science*, 207(4437):1373–1375.

Review

Mathematical modelling of follicular growth and ovarian stimulation

Sophie Fischer-Holzhausen and Susanna Röblitz

Current Opinion in Endocrine and Metabolic Research (2022): 100385

Available online at www.sciencedirect.com

ScienceDirect

Current Opinion in
Endocrine and Metabolic Research

ELSEVIER

Reviews

Mathematical modelling of follicular growth and ovarian stimulation

Sophie Fischer-Holzhausen and Susanna Röblitz

Abstract

The aim of ovarian stimulation in fertility treatment is to increase the number of large follicles and hence the number of eggs that can be retrieved for in vitro fertilisation (IVF). However, large inter- and intra-individual variability in the menstrual cycle and ovarian response to stimulation drugs complicate treatment planning and prediction. Hence, many mathematical models have been developed to support treatment decisions. In this article, we give an overview of mechanistic models that cover different aspects of the processes involved in normal menstrual cycles and ovarian stimulation, including hormonal regulation and follicular maturation. We also review statistical models that have been designed to predict different IVF outcome criteria. Finally, we outline the use of mathematical models for in-silico clinical trials in reproductive endocrinology.

Addresses

University of Bergen, Computational Biology Unit, Department of Informatics, Thormøhlensgate 55, Bergen, 5008, Norway

Corresponding author: Röblitz, Susanna (Susanna.Roblitz@uib.no)

Current Opinion in Endocrine and Metabolic Research 2022, **26:**100385

This review comes from a themed issue on **Mathematical Modelling of Endocrine Systems**

Edited by **Craig McArdle**, **Krasimira Tsaneva-Atanasova** and **Margaritis Voliotis**

For a complete overview see the Issue and the Editorial

Available online 6 August 2022

https://doi.org/10.1016/j.coemr.2022.100385

Keywords

Hypothalamic-pituitary-gonadal (HPG) axis, Hormone dynamics, Follicular competition, Assisted reproductive technology (ART).

Introduction

Approximately 15% of people of reproductive age are affected by infertility [67], and unwanted childlessness puts a psychological and psycho-social burden on many of them [27,41,14]. This makes infertility and its consequences a global health issue. In 85% of all cases of infertility, the underlying causes are dysfunctions in the female or/and male reproductive system [13]. Female factors, such as ovulatory disorders, endometriosis and tubal abnormalities, are responsible for approximately one-third of all cases [62].

The hypothalamic-pituitary-gonadal (HPG) axis is central to enable reproduction in both sexes. In females, the HPG axis regulates the menstrual cycle, including the maturation and release of oocytes, the periodic release of reproductive hormones, as well as the preparation of the female body for a possible pregnancy. This is enabled through the feedback interactions between ovarian hormones, mainly progesterone (P4) and oestradiol (E2), the pituitary hormones luteinising hormone (LH) and follicle-stimulating hormone (FSH), and the hypothalamic hormone gonadotropin-releasing hormone (GnRH), see Fig. 1. GnRH stimulates the release of FSH and LH. Both regulate follicular maturation [15]. However, the initial recruitment of follicles from the ovarian reservoir is independent of LH and FSH [44]. Within each menstrual cycle cohorts of follicles, called waves, start growing as a result of increasing FSH levels, see Fig. 2 [4–6]. Growing follicles produce E2, which enables a feedback loop back to the hypothalamus. Usually one follicle of the cohort, rarely multiple follicles, ovulates around mid-cycle. During ovulation, the follicle releases its oocyte, and the sac forms the corpus luteum, which produces ovarian hormones in the luteal phase. If the oocyte is not fertilised and pregnancy does not occur, the corpus luteum decays and a new cycle begins [15]. Failure in this endocrine network is one cause of infertility.

Treatment options for infertility depend on its cause and the patient itself. In vitro fertilisation (IVF) is a form of assisted reproductive technology (ART) that can result in a successful pregnancy for patients suffering from different causes of infertility. IVF can not only be used to overcome female infertility but also assist in cases of male infertility. Intracytoplasmic sperm injection (ICSI), a technique where a sperm cell is injected directly into the egg cell, may be used for patients with low sperm quality or number. IVF treatment proceeds in three steps: (i) egg retrieval through controlled ovarian stimulation (COS), (ii) fertilisation of oocytes in the laboratory and (iii) embryo transfer into the uterus [2]. COS aims to stimulate the growth of multiple ovarian follicles synchronously by the administration of

Figure 1

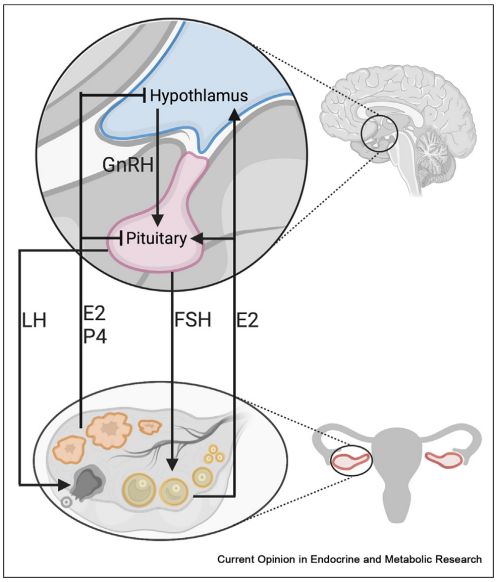

Schematic representation of the hypothalamic-pituitary-gonadal (HPG) axis. Gonadotropin-releasing hormone (GnRH) is synthesised in the hypothalamus and released into the hypophyseal portal circulation system in a pulsatile manner. In the pituitary, GnRH stimulates the synthesis of luteinising hormone (LH) and follicle-stimulating hormone (FSH) and their release into the blood. LH and FSH regulate follicular maturation in the ovaries. FSH stimulates follicular growth, whereas LH triggers the ovulation of a dominant follicle. Growing follicles (yellow) produce oestradiol (E2). After ovulation (dark grey), the corpus luteum (orange) produces both E2 and progesterone (P4). E2 and P4 exhibit feedback mechanisms on the hypothalamus and the pituitary, which closes the loop (created with BioRender.com).

Figure 2

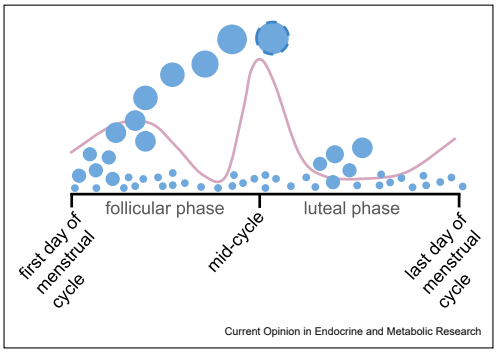

Illustration of the follicular wave theory. Small follicles are available throughout the menstrual cycle. With the beginning of a new menstrual cycle, the follicle-stimulating hormone level (FSH, pink line) starts rising and stimulates the growth of a cohort of follicles. Until mid-cycle, one follicle will be selected for ovulation. During the luteal phase, another cohort of follicles starts growing. However, none of those follicles will ovulate due to the low level of FSH.

gonadotrophins [40]. Several COS protocols are available. The conventional GnRH agonist protocol and the GnRH antagonist protocol are well established [30]. Newer protocols are based on the follicular wave theory [6], which motivates ovarian stimulation at different time points within a menstrual cycle [54]. Protocols which start ovarian stimulation at a random time point are of particular interest in the context of fertility preservation in cancer patients, where time is a determining factor [64,12]. Stimulation treatments that start during the luteal phase have been used to treat patients who did not respond to conventional protocols [50,29] as well as women with normal ovarian response [33]. Double stimulation protocols comprise two consecutive treatment cycles and offer more opportunities for oocyte retrieval in a shorter time interval [32,63]. Overall, it is challenging to find the best therapy for an individual patient in order to achieve the best treatment outcome in terms of pregnancy and live birth rates while simultaneously decreasing treatment-related risks like ovarian hyperstimulation syndrome [53].

Mathematical modelling can improve our understanding of complex regulatory networks involving multiple levels of organisation, such as endocrine systems [73,37]. Computational models can also be helpful to answer scientific questions in cases where appropriate model organisms are not available, and experimental investigations are challenging. Until recently, a menstrual cycle was only observed in primates. Evidence of a menstruating rodent was provided [9]. Since every model is a simplification and based on assumptions, it is important to find a model that is appropriate for the research question [66,65]. Mathematical models can be divided into two main groups: (i) empirical models and (ii) mechanistic models [7,51]. Empirical models are statistical models and therefore data driven. They are tailored towards prediction and are widely used in medical research [26]. An example in the scope of this review is the prediction of menstrual cycle length [47,39]. Mechanistic models are process-based and consider the elements forming a system and their interactions [11]. Their strength lies in generating, testing, and refining hypotheses [20]. An example is the model by Ref. [31] that provides evidence for the follicular wave theory.

In the following, we give an overview of statistical models (Sec. 2) and mechanistic models (Sec. 3) that

have been developed to simulate and predict IVF treatment outcomes, including the number of mature oocytes after ovarian stimulation and pregnancy rates. In addition, we briefly review the use of mathematical models in in-silico clinical trials (ISCT) related to IVF treatment (Sec. 4).

Prediction of IVF outcomes

A review by Ref. [56] summarises the statistical methods and available software tools for scoring embryo quality and predicting pregnancy rates. The review emphasises the role of these models as a clinical decision support tool, and that the final decisions need to be made by the practitioners and laboratory staff. Another publication from the same group [55] gives an overview of statistical models based on patient and/or embryo characteristics for predicting pregnancy and/or live birth rates. The authors suggest that the way forward would be in enriching, improving and strengthening the reproducibility and prognostic value of current models instead of suggesting new ones. However, both the definition of new success criteria as well the advancement of computational methods and tools, particularly in the fields of machine learning (ML) and artificial intelligence (AI), has led to the development of new models over the past years, which we briefly review in the following.

An intermediate marker of successful outcome in IVF/ICSI cycles, which has been introduced by the POSEIDON group,[1] is the ability to retrieve the number of oocytes needed to achieve at least one euploid embryo for transfer, i.e., an embryo that contains a normal number of chromosomes. In Ref. [21], members of the POSEIDON group developed a statistical model to estimate the minimum number of mature oocytes required to obtain at least one euploid blastocyst (based on pretreatment information, including female age and sperm source used for ICSI) and to estimate the individualised probability of blastocyst euploidy per mature retrieved oocyte. External multicentre validation is currently ongoing using suitable ART datasets from different countries.

There are also studies that focus on predicting the total number of oocytes. Ref. [1] demonstrated that results from random forest analysis were consistent with a generalised linear regression model suggesting that follicle sizes of 12–19 mm (but not the total number of follicles) on the day of trigger had the greatest predictive importance for the number of oocytes and number of mature oocytes retrieved. This knowledge enables the accurate determination of trigger efficacy and could potentially also be used to determine the optimal day of trigger administration.

[1] https://www.groupposeidon.com/.

Ref. [60] introduced a logistic regression model based on seven predictors for estimating the assisted fecundity of women before starting the first IVF/ICSI cycle, which translates into the probability of live birth in the first treatment cycle. This kind of prediction complements the approach of estimating cumulative and cycle-specific probabilities of live birth over multiple treatment cycles.

A great challenge for ART is a poor ovarian response, which refers to an unexpected low number of oocytes upon stimulation treatment. Using univariate and multivariate logistic regression analyses, Ref. [69] developed a statistical model based on four predictors (anti-Müllerian hormone, antral follicle counts, basal FSH, and age, in order of their significance) in order to estimate the probability of poor ovarian response and to assess the true ovarian reserve. Similarly, Ref. [38] developed a statistical model that can predict the probability of clinical pregnancy failure in poor ovarian responders before embryo transfer in IVF/ICSI procedure.

ML models allow for including an increased number of features and to untangle their complex relationships. Ref. [8] compared two widely used ML methods (support vector machines with different kernel functions and artificial neural networks) with logistic regression models for the prediction of different IVF outcome criteria. They demonstrated that the ML methods are superior to the standard statistical models. The authors argue that ML algorithms, as opposed to classical statistical models, can take into consideration complex associations between different parameters and can consequently better utilise the synergism between these associated parameters. In the same direction, Ref. [25] used 25 attributes in combination with a feature selection algorithm to assess the prediction ability of IVF pregnancy success for five different ML models. Two features, namely indication of infertility factor and the number of mature eggs, were selected by all classifiers, and antral follicle count (AFC) was selected by four methods. Moreover, age was ranked highest by three of the classifiers, which is consistent with other studies. The authors demonstrated that the prediction performance of all five classifiers improved with the selected features compared to using all features. Their article also includes a summary of studies that applied ML techniques for the classification of IVF outcomes. Those techniques differ in the ML technique used, the attribute/feature selection technique used, the list of selected features, the validation (training/test procedure), and the performance measure reported. These differences make it difficult to compare the methods with each other and also limit their transferability to other clinics due to variations in the amount and quality of data. The publication of codes as well as the availability of benchmark datasets would be preferable in order to increase the reproducibility and reusability of ML methods and results.

Modelling follicular maturation on a systems level

Both classical statistical models as well as ML models are based on predefined input and output variables. They do not explicitly include time as a variable and can therefore not be used to predict system behaviour over time, e.g., the growth of ovarian follicles. For this purpose, process-based models have been developed, which will be summarised in the following.

Moment models that describe the response of follicles in IVF

Ref. [72] developed a mathematical model that describes how the discrete follicle size distribution evolves over time, whereby it is assumed that the number of follicles activated during an IVF cycle is constant, i.e., that no new follicles start growing during stimulation. The kinetics of follicle growth is modelled as a function of injected FSH, and the follicle properties are represented in terms of the moments of the (unknown) statistical size distribution. Initial data from two treatment days (follicle sizes and prescribed FSH dose on days 2 and 5) of an individual patient are used to obtain patient-specific model parameters and predict the follicle size distribution for the remaining treatment days, whereby the dose is not adjusted but constant throughout treatment. The authors demonstrate that the follicle size distribution predicted by the moment model is in good agreement with the actual size distribution seen in the IVF cycle data for five patients.

In [71], the authors extended their model by an optimal control approach in order to predict the optimum FSH dosage for the desired treatment outcome, which is to have as many follicles as possible in the largest size class. A proof of concept based on data from five patients was presented in Ref. [71], before the model was tested in a double-blinded trial involving 10 patients [45]. Even though the cohort size was small, the results from Ref. [45] demonstrate that model-based treatment planning can lead to lower doses and fewer tests and monitoring requirements along with higher numbers of mature follicles and a similar percentage of good quality eggs compared to standard treatment routines.

Since the model does not include hormone dynamics and does not consider outcomes other than follicle number and sizes, the risk of ovarian hyperstimulation syndrome still needs to be checked by the physician, which might overrule the model-based treatment suggestions in many cases.

Cellular population models

Ovarian follicles carry two types of hormone-sensitive cells: (i) LH-responsive theca cells and FSH-responsive granulosa cells. Both cell types are crucial for the development of ovarian follicles and ovarian hormone production. Proliferation and cellular signalling processes of these cells have been investigated experimentally and by mathematical modelling [16]. Recently, Ref. [18] introduced a continuous-time Markov chain model for cell population dynamics to identify events in follicle maturation. Modelling follicular maturation on different levels of organisation, for example, by incorporating cell dynamics in follicle population dynamic models, can be valuable to characterise the pool of follicles over the lifetime of individuals [17,10].

Models based on follicular maturation stages and masses

A number of models have been developed [24,48,49,46] in which discrete stages of follicular maturation are defined as a state variables to describe follicular growth dynamics. Thereby, each maturation stage encodes a specific capability to produce ovarian hormones, but the variables do not refer to the size or number of follicles in that stage of maturation. However, this heuristic approach is useful to study different aspects of the female menstrual cycle. For example, Refs. [49,68] used this approach to model drug administrations, while Ref. [46] investigated follicular wave dynamics. Ref. [23] used the model to investigate the effect of testosterone on normal menstrual cycles and ovulatory function. The model provides a framework to investigate polycystic ovary syndrome and ovulatory dysfunctions.

Follicle population models

A mathematical formulation for ovarian follicle maturation dynamics in terms of number and sizes of follicles was first introduced to the literature by Refs. [34,35]. Ref. [52] used this model to predict ovarian response in stimulation treatments. Ref. [59] modified the Lacker's model in order to simulate higher ovulations rates, i.e., double and multiple ovulations, in sheep and cattle. Based on these previous modelling attempts for follicular maturation on the level on individual follicles, Ref. [36] introduced a follicular growth equation that includes competition between follicles, with the follicular size as state variable. All these models, however, can only be used to simulate one follicular wave. Ref. [22] coupled the Lange model with the hormone dynamics along the HGP axes. The coupled model allows us to study the interplay between hormone dynamics and follicular maturation throughout consecutive menstrual cycles and can be used to simulate ovarian stimulation protocols with random start times.

Treatment computations and in-silico clinical trials

Mechanistic models can be used as a safe and efficient tool to predict patient-specific treatment outcomes as part of ISCT. Those approaches promise to decrease experimental efforts, including animal and human

Figure 3

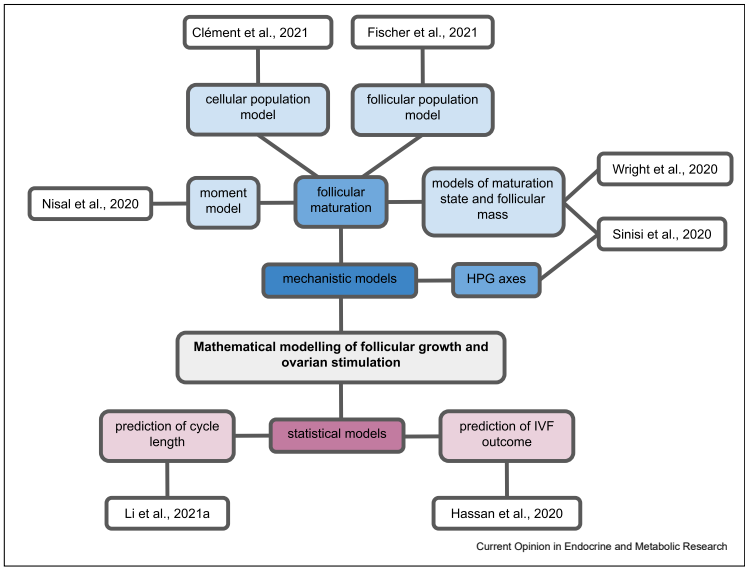

This review gives an overview of different mathematical modelling approaches focusing on ovarian follicle maturation and female health. There are two main model types, namely statistical models and mechanistic models, both branching into sub-classes depending on the application. Each sub-class links to one of its most recent references, which are also cited in this review.

testing, and optimise the individual treatment outcome. The group of E. Tronci developed methods and software based on intelligent search strategies, and statistical model checking to find sets of model parameters that result in physiologically meaningful model behaviours [61,43]. In Ref. [57], they applied these methods to compute huge populations of virtual patients (VPs) for a non-identifiable quantitative virtual physiological human (VPH) model of the human menstrual cycle, including drug treatments [49]. Using the same VPH model, Refs. [42,58] showcased how VPs can be used to support precision medicine. Their work demonstrates how to compute a personalised down-regulation treatment protocol (a protocol used for assisted reproduction) that maximises the aimed outcome while simultaneously minimising the risk for severe side effects.

These methods and software tools have reached a high level of technological readiness, and the indispensable next step would be to test their performance in clinical trials. In particular, ethical and legal issues need to be considered carefully before such tools can become part of clinical practice [19].

Conclusion

This review summarises different mathematical approaches to model follicular maturation and ovarian stimulation in humans, see Fig. 3. It demonstrates how medical research in the context of female health already has or might in the future benefit from computational work, such as statistical and mechanistic modelling. Statistical models are a powerful tool to predict different outcome criteria of IVF treatment based on both patient and embryo characteristics. In particular, ML models help determine which phenotype and cycle factors are the most useful in making predictions.

Mechanistic modelling, with its way of thinking about complex dynamical systems in biology, can provide valuable insights on its own [20]. In particular, mechanistic models can be used to test the hypothesis about the underlying processes and identify parameters on which measurement efforts should be focused on. Moreover, they can be combined with pharmacokinetic models to study drug administration schemes, which is not possible with statistical models. Recent publications have demonstrated how mechanistic and ML models can be combined to infer hidden dynamics in biological networks and enable robust predictions, e.g., Ref. [70]. This is certainly a promising avenue for future research.

The review here focuses on follicular dynamics, and there are several ongoing modelling efforts in closely related areas, for example, on the endometrial cycle

[3]. Also, we did not discuss modelling approaches based on images, as this would be out of the scope for this review. The reader interested in the application of ML methods to predict embryo ploidy from images is referred to Ref. [28] and references therein. It is likely that in future, different models and model types will be combined in order to achieve an even more holistic picture of the processes that are involved in female fertility.

Declaration of competing interest

Nothing declared

Acknowledgement

The work of SF and SR was supported by the Trond Mohn Foundation (BSF, https://www.mohnfoundation.no/), Grant no. BFS2017TMT01. The funder had no role in study design, data collection and analysis, decision to publish, or preparation of the manuscript.

References

Papers of particular interest, published within the period of review, have been highlighted as:

* of special interest

1. Abbara A, Vuong LN, Ho VNA, Clarke SA, Jeffers L, Comninos AN, Salim R, Ho TM, Kelsey TW, Trew GH, Humaidan P, Dhillo WS: **Follicle size on day of trigger most likely to yield a mature oocyte**. *Front Endocrinol* 2018, **9**:193.
2. Anwar S, Anwar A: **Infertility: a review on causes, treatment and management**. *Women's Health Gynecol* 2016, **5**:2.
3. Arbeláez-Gómez D, Benavides-López S, Giraldo-Agudelo MP, Guzmán-Álvarez JP, Ramirez-Mazo C, Gómez-Echavarría LM: **A phenomenological-based model of the endometrial growth and shedding during the menstrual cycle**. *J Theor Biol* 2022, **532**, 110922.
4. Baerwald A, Adams G, Pierson R: **Characterization of ovarian follicular wave dynamics in women**. *Biol Reprod* 2003a, **69**: 1023–1031.
5. Baerwald A, Adams G, Pierson R: **A new model for ovarian follicular development during the human menstrual cycle**. *Fertil Steril* 2003b, **80**:116–122.
6. Baerwald A, Adams G, Pierson R: **Ovarian antral folliculogenesis during the human menstrual cycle: a review**. *Hum Reprod Update* 2011, **18**:73–91.
7. Baker RE, Peña JM, Jayamohan J, Jérusalem A: **Mechanistic models versus machine learning, a fight worth fighting for the biological community?** *Biol Lett* 2018, **14**, 20170660, https://doi.org/10.1098/rsbl.2017.0660.
8. Barnett-Itzhaki Z, Elbaz M, Butterman R, Amar D, Amitay M, Racowsky C, Orvieto R, Hauser R, Baccarelli AA, Machtinger R: **Machine learning vs. classic statistics for the prediction of IVF outcomes**. *J Assist Reprod Genet* 2020, **37**:2405–2412.
9. Bellofiore N, Ellery SJ, Mamrot J, Walker DW, Temple-Smith P, Dickinson H: **First evidence of a menstruating rodent: the spiny mouse (acomys cahirinus)**. *Am J Obstet Gynecol* 2017, **216**:40. e1.
10. Bonnet C, Chahour K, Clément F, Postel M, Yvinec R: **Multiscale population dynamics in reproductive biology: singular perturbation reduction in deterministic and stochastic models**. *ESAIM: Proceedings and Surveys* 2020, **67**: 72–99.
11. Brigandt I: **Systems biology and the integration of mechanistic explanation and mathematical explanation**. *Stud Hist Philos Sci C Stud Hist Philos Biol Biomed Sci* 2013, **44**:477–492, https://doi.org/10.1016/j.shpsc.2013.06.002.
12. Cakmak H, Katz A, Cedars MI, Rosen MP: **Effective method for emergency fertility preservation: random-start controlled ovarian stimulation**. *Fertil Steril* 2013, **100**:1673. 1618.
13. Carson SA, Kallen AN: **Diagnosis and management of infertility: a review**. *JAMA* 2021, **326**:65–76.
14. Chow KM, Cheung MC, Cheung IK: **Psychosocial interventions for infertile couples: a critical review**. *J Clin Nurs* 2016, **25**: 2101–2113.
15. Christensen A, Bentley G, Cabrera R, Ortega HH, Perfito N, Wu T, Micevych P: **Hormonal regulation of female reproduction**. *Horm Metab Res* 2012, **44**:587–591.
16. Clément F, Crépieux P, Yvinec R, Monniaux D: **Mathematical modeling approaches of cellular endocrinology within the hypothalamo-pituitary-gonadal axis**. *Mol Cell Endocrinol* 2020, **518**, 110877.
17. * Clément F, Monniaux D: **Mathematical modeling of ovarian follicle development: a population dynamics viewpoint**. *Current Opinion in Endocrine and Metabolic Research* 2021.
This review article gives an overview of modelling follicle population dynamics on different levels of organisation and highlights the modelling of cell population dynamics in the context of folliculogenesis.
18. Clément F, Robin F, Yvinec R: **Stochastic nonlinear model for somatic cell population dynamics during ovarian follicle activation**. *J Math Biol* 2021, **82**:1–52.
19. Cohen IG, Amarasingham R, Shah A, Xie B, Lo B: **The legal and ethical concerns that arise from using complex predictive analytics in health care**. *Health Aff* 2014, **33**:1139–1147, https://doi.org/10.1377/hlthaff.2014.0048.
20. Enderling H, Wolkenhauer O: **Are all models wrong?** *Computational and Systems Oncology* 2021, **1**, e1008.
21. Esteves SC, Carvalho JF, Bento FC, Santos J: **A novel predictive model to estimate the number of mature oocytes required for obtaining at least one euploid blastocyst for transfer in couples undergoing in vitro fertilization/intracytoplasmic sperm injection: the art calculator**. *Front Endocrinol* 2019, **10**:99.
22. * Fischer S, Ehrig R, Schäfer S, Tronci E, Mancini T, Egli M, Ille F, Krüger TH, Leeners B, Röblitz S: **Mathematical modeling and simulation provides evidence for new strategies of ovarian stimulation**. *Front Endocrinol* 2021, **12**:117.
This work introduces a mathematical model that combines hormone dynamics along the HPG-axis with follicle growth dynamics on a follicle population level in order to simulate ovarian stimulation protocols with different start times in the cycle.
23. Graham EJ, Selgrade JF: **A model of ovulatory regulation examining the effects of insulin-mediated testosterone production on ovulatory function**. *J Theor Biol* 2017, **416**: 149–160.
24. Harris-Clark L, Schlosser P, Selgrade J: **Multiple stable periodic solutions in a model for hormonal control of the menstrual cycle**. *Bull Math Biol* 2003, **65**:157–173.
25. * Hassan MR, Al-Insaif S, Hossain MI, Kamruzzama J: **A machine learning approach for prediction of pregnancy outcome following IVF treatment**. *Neural Comput Appl* 2020, **32**: 2283–2297.
The authors demonstrate that automatic feature selection combined with ML classifiers improves the prediction performance for IVF pregnancy rates. The article also contains an overview of studies that applied machine learning techniques for classification of IVF outcome.
26. Henley SS, Golden RM, Kashner TM: **Statistical modeling methods: challenges and strategies**. *Biostatistics & Epidemiology* 2020, **4**:105–139, https://doi.org/10.1080/24709360.2019.1618653.
27. Ho TTT, Le MT, Truong QV, Nguyen VQH, Cao NT: **Psychological burden in couples with infertility and its association with sexual dysfunction**. *Sex Disabil* 2020, **38**:123–133.
28. Huang B, Tan W, Li Z, Jin L: **An artificial intelligence model (euploid prediction algorithm) can predict embryo ploidy status based on time-lapse data**. *BMC Reproductive Biology and Endocrinology* 2021, **19**:185.

29. Kalra SK, Ratcliffe S, Gracia1 CR, Martino L, Coutifaris C, Barnhart KT: **Randomized controlled pilot trial of luteal phase recombinant fsh stimulation in poor responders**. *Reprod Biomed Online* 2008, **17**:745–750.

30. Karimzadeh MA, Ahmadi S, Oskouian H, Rahmani E: **Comparison of mild stimulation and conventional stimulation in art outcome**. *Arch Gynecol Obstet* 2010, **281**:741–746.

31. Kirillova A, Martazanova B, Mishieva N, Semenova M: **Follicular waves in ontogenesis and female fertility**. *Biosystems* 2021: 104558.

32. Kuang Y, Chen Q, Hong Q, Lyu Q, Ai A, Fu Y, Shoham Z: **Double stimulations during the follicular and luteal phases of poor responders in IVF/ICSI programmes (Shanghai Protocol)**. *Reprod Biomed Online* 2014a, **29**:684–691.

33. Kuang Y, Hong Q, Chen Q, Lyu Q, Ai A, Fu Y, Shoham Z: **Luteal-phase ovarian stimulation is feasible for producing competent oocytes in women undergoing in vitro fertilization/intracytoplasmic sperm injection treatment, with optimal pregnancy outcomes in frozen-thawed embryo transfer cycles**. *Fertil Steril* 2014b, **101**:105–111.

34. Lacker H: **Regulation of ovulation number in mammals. a follicle interaction law that controls maturation**. *Biophys J* 1981, **35**:433–454.

35. Lacker HM, Akin E: **How do the ovaries count?** *Math Biosci* 1988, **90**:305–332.

36. Lange A, Schwieger R, Plöntzke J, Schäfer S, Röblitz S: **Follicular competition in cows: the selection of dominant follicles as a synergistic effect**. *J Math Biol* 2019, **78**:579–606.

37. Leng G, MacGregor DJ: **Mathematical modelling in neuroendocrinology**. *J Neuroendocrinol* 2008, **20**:713–718.

38. Li F, Lu R, Zeng C, Li X, Xue Q: **Development and validation of a clinical pregnancy failure prediction model for poor ovarian responders during IVF/ICSI**. *Front Endocrinol* 2021a, **12**.

39. Li K, Urteaga In, Shea A, Vitzthum VJ, Wiggins CH, Elhadad N: **A predictive model for next cycle start date that accounts for adherence in menstrual self-tracking**. *J Am Med Inf Assoc* 2021b, **29**:3–11.

40. Macklon NS, Stouffer RL, Giudice LC, Fauser BC: **The science behind 25 years of ovarian stimulation for in vitro fertilization**. *Endocr Rev* 2006, **27**:170–207.

41. Malina A, Pooley JA: **Psychological consequences of ivf fertilization–review of research**. *Ann Agric Environ Med* 2017, **24**:554–558.

42. Mancini T, Mari F, Massini A, Melatti I, Salvo I, Sinisi S, Tronci E, Ehrig R, Röblitz S, Leeners B: **Computing personalised treatments through in silico clinical trials. A case study on downregulation in assisted reproduction**. In *Proceedings of 25th RCRA international Workshop on experimental Evaluation of algorithms for Solving Problems with Combinatorial Explosion*; 2018:16.

43. Mancini T, Tronci E, Salvo I, Mari F, Massini A, Melatti I: **Computing biological model parameters by parallel statistical model checking**. In *Proceedings of the 3rd international Conference on Bioinformatics and Biomedical Engineering (IWBBIO 2015)*. Springer; 2015:542–554.

44. McGee EA, Hsueh AJ: **Initial and cyclic recruitment of ovarian follicles**. *Endocr Rev* 2000, **21**:200–214.

45. * Nisal A, Diwekar U, Bhalerao V: **Personalized medicine for in vitro fertilization procedure using modeling and optimal control**. *J Theor Biol* 2020, **487**, 110105.
Based on a moment model of follicular size distributions, the authors introduce an optimal control approach to compute patient-specific drug doses needed to achieve an optimal ovarian stimulation outcome.

46. Panza NM, Wright AA, Selgrade JF: **A delay differential equation model of follicle waves in women**. *J Biol Dynam* 2016, **10**: 200–221.

47. de Paula Oliveira T, Bruinvels G, Pedlar C, Moore B, Newell J: **Modelling menstrual cycle length in athletes using state-space models**. *Sci Rep* 2021, **11**, 16972.

48. Reinecke I, Deuflhard P: **A complex mathematical model of the human menstrual cycle**. *J Theor Biol* 2007, **247**: 303–330.

49. Röblitz S, Stötzel C, Deuflhard P, Jones HM, Azulay DO, van der Graaf PH, Martin SW: **A mathematical model of the human menstrual cycle for the administration of GnRH analogues**. *J Theor Biol* 2013, **321**:8–27.

50. Rombauts L, Anne-MariaSuikkari, MacLachlan V, Trounson AO, Healy DL: **Recruitment of follicles by recombinant human follicle-stimulating hormone commencing in the luteal phase of the ovarian cycle**. *Fertil Steril* 1998, **69**:665–669.

51. Saltelli A: **A short comment on statistical versus mathematical modelling**. *Nat Commun* 2019, **10**:1–3.

52. Sarty GE, Pierson RA: **An application of Lacker's mathematical model for the prediction of ovarian response to superstimulation**. *Math Biosci* 2005, **198**:80–96.

53. Sighinolfi G, Grisendi V, La Marca A: **How to personalize ovarian stimulation in clinical practice**. *J Turk Ger Gynecol Assoc* 2017, **18**:148.

54. Sighinolfi G, Sunkara SK, La Marca A: **New strategies of ovarian stimulation based on the concept of ovarian follicular waves: from conventional to random and double stimulation**. *Reprod Biomed Online* 2018, **37**:489–497.

55. Simopoulou M, Sfakianoudis K, Antoniou N, Maziotis E, Rapani A, Bakas P, Anifandis G, Kalampokas T, Bolaris S, Pantou A, *et al.*: **Making IVF more effective through the evolution of prediction models: is prognosis the missing piece of the puzzle?** *Syst Biol Reprod Med* 2018a, **64**:305–323.

56. Simopoulou M, Sfakianoudis K, Maziotis E, Antoniou N, Rapani A, Anifandis G, Bakas P, Bolaris S, Pantou A, Pantos K, *et al.*: **Are computational applications the "crystal ball" in the IVF laboratory? the evolution from mathematics to artificial intelligence**. *J Assist Reprod Genet* 2018b, **35**: 1545–1557.

57. * Sinisi S, Alimguzhin V, Mancini T, Tronci E, Leeners B: **Complete populations of virtual patients for in silico clinical trials**. *Bioinformatics* 2020a, **36**:5465–5472.
In this article, the authors compute a population of almost five million virtual patients for a non-identifiable quantitative virtual physiological human model of the HPG axis. They demonstrate that the computed parameters are physiologically meaningful, pairwise distinguishable, and complete, i.e., representative of the entire spectrum of behaviours defined by the given model.

58. Sinisi S, Alimguzhin V, Mancini T, Tronci E, Mari F, Leeners B: **Optimal personalised treatment computation through in silico clinical trials on patient digital twins**. *Fundam Inf* 2020b, **174**:283–310.

59. Soboleva T, Peterson A, Pleasants A, McNatty K, Rhodes F: **A model of follicular development and ovulation in sheep and cattle**. *Anim Reprod Sci* 2000, **58**:45–57.

60. Tarín JJ, Pascual E, García-Pérez MA, Gómez R, Hidalgo-Mora JJ, Cano A: **A predictive model for women's assisted fecundity before starting the first IVF/ICSI treatment cycle**. *J Assist Reprod Genet* 2020, **37**:171–180.

61. Tronci E, Mancini T, Salvo I, Sinisi S, Mari F, Melatti I, Massini A, Davi F, Dierkes T, Ehrig R, Röblitz S, Leeners B, Krüger T, Egli M, Ille F: **Patient-specific models from inter-patient biological models and clinical records**. In *Proceedings of 14th Conference in formal methods in Computer-Aided design*. FMCAD 2014); 2014:207–214.

62. Unuane D, Tournaye H, Velkeniers B, Poppe K: **Endocrine disorders & female infertility**. *Best Pract Res Clin Endocrinol Metabol* 2011, **25**:861–873.

63. Vaiarelli A, Cimadomo D, Trabucco E, Vallefuoco R, Buffo L, Dusi L, Fiorini F, Barnocchi N, Bulletti FM, Rienzi L, Ubaldi FM: **Double stimulation in the same ovarian cycle (DuoStim) to maximize the number of oocytes retrieved from poor prognosis patients: a multicenter experience and swot analysis**. *Front Endocrinol* 2018, **9**:317.

64. von Wolff M, Thaler CJ, Frambach T, Zeeb C, Lawrenz B, Popovici RM, Strowitzki T: **Ovarian stimulation to cryopreserve**

fertilized oocytes in cancer patients can be started in the luteal phase. *Fertil Steril* 2009, **92**:1360–1365.

65. Wolkenhauer O: **Why model?** *Front Physiol* 2014, **5**:21.

66. Wolkenhauer O, Mesarović M: **Feedback dynamics and cell function: why systems biology is called systems biology**. *Mol Biosyst* 2005, **1**:14–16.

67. World Health Organization: *Infertility*. 2022. https://www.who.int/health-topics/infertility#tab=tab_1. Accessed 4 February 2022.

68. * Wright AA, Fayad GN, Selgrade JF, Olufsen MS: **Mechanistic model of hormonal contraception**. *PLoS Comput Biol* 2020, **16**, e1007848.
This work demonstrates how a model based on follicular maturation stages coupled to the HPG-axis hormone dynamics can be used to simulate hormonal contraception.

69. Xu H, Feng G, Wang H, Han Y, Yang R, Song Y, Chen L, Shi L, Zhang MQ, Li R, *et al.*: **A novel mathematical model of true ovarian reserve assessment based on predicted probability of poor ovarian response: a retrospective cohort study**. *J Assist Reprod Genet* 2020, **37**:963–972.

70. Yazdani A, Lu L, Raissi M, Karniadakis GE: **Systems biology informed deep learning for inferring parameters and hidden dynamics**. *PLoS Comput Biol* 2020, **16**, e1007575.

71. Yenkie KM, Diwekar UM: **Optimal control for predicting customized drug dosage for superovulation stage of in vitro fertilization**. *J Theor Biol* 2014, **335**:219–228.

72. Yenkie KM, Diwekar UM, Bhalerao V: **Modeling the superovulation stage in in vitro fertilization**. *IEEE (Inst Electr Electron Eng) Trans Biomed Eng* 2013, **60**:3003–3008.

73. Zavala E, Wedgwood KC, Voliotis M, Tabak J, Spiga F, Lightman SL, Tsaneva-Atanasova K: **Mathematical modelling of endocrine systems**. *TEM (Trends Endocrinol Metab)* 2019, **30**:244–257.

Errata for

A matter of timing

A modelling-based investigation of the dynamic behaviour of reproductive hormones in girls and women

Thesis for the degree philosophiae doctor (PhD)

at the University of Bergen

	17.04.2023
(date and sign. of candidate)	(date and sign. of faculty)

Errata

Page vii Misspelling: “modeller trengs” - corrected to “modell trenges”

Page vii Missing word: “tillegg det” - corrected to “tillegg til det”

Page xi Inconsistent spelling: “Luteinizing” - corrected to “Luteinising”

Page xiv Misspelling: “identifiablilty” - corrected to “identifiability”

Page xiv Misspelling: “pharmacodyanimics” - corrected to “pharmacodynamics”

Page 3 Wrong word choice: “holistic” is a term that has been appropriated in some pseudoscientific circles - corrected to “systemic”

Page 4 Grammatical error: “Kuepfer et al. [2016] claims” - corrected to “Kuepfer et al. [2016] claim”

Page 4 Wrong word choice: “holistic” is a term that has been appropriated in some pseudoscientific circles - corrected to “systemic”

Page 4 Grammatical error: “Jackson et al. [2015] utilises” - corrected to “Jackson et al. [2015] utilise”

Page 4 Wrong word choice: “holistically” is a term that has been appropriated in some pseudoscientific circles - corrected to “systemically”

Page 5 Grammatical errors: “**who** demonstrate the model’s applicability **to simulate** the effects of hormonal treatment on **the** hormone profiles.” - corrected to “**to** demonstrate the model’s applicability **in simulating** the effects of hormonal treatment on hormone profiles.”

Page 6 Grammatical error: “Wright et al. [2020] tests” - corrected to “Wright et al. [2020] test”

Page 6 Inconsistent spelling: “characterizing” - corrected to “characterising”

Page 6 Grammatical error: “Shilo et al. [2022] introduces” - corrected to “Shilo et al. [2022] introduce”

Page 7 Missing word: “an average menstrual cycle is 28 days” - corrected to “an average menstrual cycle length is 28 day”

Page 7 Typo: “computation approach” - corrected to “computational approach”

Page 8 Inconsistent spelling: “emphasize” - corrected to “emphasise”

Page 8 Inconsistent spelling: “personalized” - corrected to “personalised”

Page 8 Wrong word choice: “renewal” - corrected to “novelty”

Page 9 Inconsistent spelling: “summarized” - corrected to “summarised”

Page 9 Inconsistent spelling: “summarizing” - corrected to “summarising”

Page 11 Wrong word choice: “glands” - corrected to “units”

Page 11 Missing plural: “shrew” - corrected to “shrews”

Page 11 Missing plural: “mouse” - corrected to “mice”

Page 12 Grammatical error: “Supposedly” - corrected to “Supposed”

Page 12 Grammatical error: “phase then menstruation” - corrected to “phase, menstruation”

Page 13 Wrong word choice: “glands” - corrected to “units”

Page 13 Inconsistent spelling: “Luteinizing” - corrected to “Luteinising”

Page 13 Wrong preposition: “in” - corrected to “underneath”

Page 13 Missing word: “both reach” - corrected to “both hormones reach”

Page 14 Misspelling in Figure 2.2: “Hypothlamus” - corrected to “Hypothalamus”

Page 15 Typo: “that this maturation” - corrected to “that maturation”

Page 15 Typo: “section” - corrected to “secretion”

Page 16 Inconsistent spelling: “Luterizing” - corrected to “Luteinising”

Page 17 Wrong word choice: “symptoms” - corrected to “factors”

Page 18 Typo: “one-third” - corrected to “one third”

Page 19 Typo: “increase” - corrected to “decrease”

Page 19 Misspelling: “lifes” - corrected to “lives”

Page 19 Typo: “afford” - corrected to “effort”

Page 22 Inconsistent spelling: “scheme” - corrected to “schema”

Page 22 Wrong word use: “integrative” - corrected to “integral”

Page 22 Typo: “model-building” - corrected to “model building”

Page 23 Wrong parentheses: (model calibration)(Sec. 3.2) - corrected to (model calibration (Sec. 3.2))

Page 23 Typo: “model-building” - corrected to “model building”

Page 23 Inconsistent capitalisation: “uncertainty quantification and Sensitivity Analysis” - corrected to “uncertainty quantification and sensitivity analysis”

Page 23 Grammar error: “a ODE” - corrected to “an ODE”

Page 23 Misspelling: “hypothesises” - corrected to “hypotheses”

Page 26 Wrong word use: “distinctiveness” - corrected to “steepness”

Page 27 Typo: “model-building” - corrected to “model building”

Page 27 Inconsistent spelling: “minimizes” - corrected to “minimises”

Page 27 Inconsistent spelling: “summarizes” - corrected to “summarises”

Page 27 Inconsistent spelling: “minimizing” - corrected to “minimising”

Page 28 Missing word: “each of N_{obs}” - corrected to “each of the N_{obs}”

Page 29 Typo: “data set y” - corrected to “data set $y(t)$”

Page 29 Typo: “data set is” - corrected to “data set $y(t)$ is”

Page 29 Missing comma: “and therefore does” - corrected to “and, therefore, does”

Page 29 Typo: “denoted” - corrected to “denotes”

Page 30 Missing word: “data set y” - corrected to “data set $y(t)$”

Page 30 Inconsistent spelling: “utilized” - corrected to “utilised”

Page 30 Inconsistent spelling: “realized” - corrected to “realised”

Page 30 Typo: “Markow” - corrected to “Markov”

Page 31 Misspelling: “identifiablilty” - corrected to “identifiability”

Page 31 Grammatical error: “data is” - corrected to “data are”

Page 31 Inconsistent spelling: “parametrization” - corrected to “parametrisation”

Page 32 Inconsistent spelling: “characterize” - corrected to “characterise”

Page 32 Grammatical error: “Raue et al. [2013a] compares” - corrected to “Raue et al. [2013a] compare”

Page 32 Grammatical error: “Rateitschak et al. [2012] demonstrates” - corrected to “Rateitschak et al. [2012] demonstrate”

Page 32 Typo: “limitations of the data collection” - corrected to “limitations of data collection”

Page 32 Typo: “Profile likelihoods” - corrected to “Profile likelihood”

Page 33 Typo: “sub-figure” - corrected to “subfigure”

Page 33 Grammatical error: “practical non-identifiable” - corrected to “practically non-identifiable”

Page 33 Grammatical error: “structural non-identifiable” - corrected to “structurally non-identifiable”

Page 33 Grammatical error in Figure 3.3: “practical non-identifiable” - corrected to “practically non-identifiable”

Page 33 Grammatical error in Figure 3.3: “structural non-identifiable” - corrected to “structurally non-identifiable”

Page 33 Typo in caption of Figure 3.3: “shapes the profile” - corrected to “shapes of profile”

Page 33 Typo: “denoted” - corrected to “denotes”

Page 33 Inconsistent capitalisation: “profile likelihoods” - corrected to “PLs”

Page 34 Grammatical error: “Tönsing et al. [2018] … computes … and uses” - corrected to “Tönsing et al. [2018] … compute … and use”

Page 34 Inconsistent capitalisation: “Markov chain Monte Carlo” - corrected to “Markov Chain Monte Carlo”

Page 35 Grammatical error: “propagates into the model output” - corrected to “propagates to the model output”

Page 35 Grammatical error: “decompose … variance in outputs’ contributions“ - corrected to “decompose … variance into its outputs’ contributions“

Page 36 Missing subscript: “V_ij” - corrected to “$V_{i,j}$”

Page 36 Grammatical error: “Lebedeva et al [2012] emphasises” - corrected to “Lebedeva et al [2012] emphasise”

Page 36 Missing word: “SA helps better understand” - corrected to “SA helps to better understand”

Page 36 Misspelling: “pharmacodyanimics” - corrected to “pharmacodynamics”

Page 36 Inconsistent capitalisation in Figure 3.4: “drug” - corrected to “Drug”

Page 36 Typo: “administrated” - corrected to “administered”

Page 38 Typo: “sub-population” - corrected to “subpopulation”

Page 39 Grammatical error: “to understand better the” - corrected to “to understand the”

Page 40 Typo: “wet-lab” - corrected to “wet lab”

Page 40 Typo: “computation” - corrected to “computational”

Page 42 Wrong comma: “in the follicle growth, hinders” - corrected to “in the follicle growth hinders ”

Page 44 Typo: “semi-mechanically” - corrected to “semi-mechanistically”

Page 45 Missing word: “interdisciplinary increases” - corrected to “interdisciplinary nature increases”

Page 45: Typo: “health care” - corrected to “healthcare”

Page 45: Typo: “sub-population” - corrected to “subpopulation”

Page 45 Typo: “conditions” - corrected to “condition”

Page 46 Typo: “model-building” - corrected to “model building”

Page 46 Typo: “developmental” - corrected to “development”

Page 47 Typo: “could” - corrected to “would”

Page 47 Grammatical error: “valuable but is” - corrected to “valuable but are”

Page 47 Grammatical error: “Rateitschak et al. [2012] argues” - corrected to “Rateitschak et al. [2012] argue”

Page 48 Typo: ”well established” - corrected to “well-established”

Page 47 Grammatical error: “clinical data is” - corrected to “clinical data are”

Page 48 Typo: “symbolical” - corrected to “symbolic”

Graphic design: Communication Division, UiB / Print: Skipnes Kommunikasjon AS

uib.no

ISBN: 9788230866153 (print)
9788230862124 (PDF)